An integrated framework for trajectory optimisation, prediction and parameter estimation for advanced aircraft separation concepts

SANTI VILARDAGA GARCIA-CASCON

Aeronautical Engineer (MSc)
Computer Science Engineer

Advisor
DR. XAVIER PRATS I MENÉNDEZ

Doctorate program in Aerospace Science and Technology
Department of Physics – Aeronautics Division
Technical University of Catalonia – BarcelonaTech

A dissertation submitted for the degree of
Doctor of Philosophy
September 2019

An integrated framework for trajectory optimisation, prediction and parameter estimation for advanced aircraft separation concepts

Author
Santi Vilardaga Garcia-Cascon

Advisor
Dr. Xavier Prats i Menéndez

Thesis committee
Dr. Víctor Fernando Gómez Comendador
Dr. Tatiana Polishchuk
Dr. Alfonso Valenzuela Romero

Doctorate program in Aerospace Science and Technology
Technical University of Catalonia – BarcelonaTech
September 2019

PhD. Thesis made in:
Department of Physics – Aeronautics Division
Esteve Terradas, 5.
08860 Castelldefels
Catalonia (Spain)

Seguim.

Contents

List of Figures

List of Tables

List of Publications

The list of publications resulting from this PhD. work is given in inverse chronological order as follows:

Journal Papers

- VILARDAGA, SANTI, DUAN, PENGFEI (PHIL), PRATS, XAVIER & UIJT DE HAAG, MAARTEN. 2018. (May) Conflict-Free Trajectory Optimization with Target Tracking and Conformance Monitoring. *Journal of Aircraft*, 55(3), 1252 - 1260 D.O.I: https://doi.org/10.2514/1.C034251

- VILARDAGA, SANTI & PRATS, XAVIER. 2015. (Dec) Operating cost sensitivity to required time of arrival commands to ensure separation in optimal aircraft 4D trajectories. *Transportation Research - Part C: Emerging Technologies*, 61, 75-86. D.O.I: http://dx.doi.org/10.1016/j.trc.2015.10.014

Conference Proceedings

- DALMAU, RAMON, MELGOSA, MARC, VILARDAGA, SANTI & PRATS, XAVIER. 2018. A fast and flexible trajectory predictor and optimiser for ATM research applications. *In: Proceedings of the 7th International Conference on Research in Air Transportation (ICRAT)*. Castelldefels (Spain).

- VILARDAGA, SANTI & PRATS, XAVIER. 2015. Mass Estimation for an Adaptive Trajectory Predictor using Optimal Control. *In: Proceedings of the 5th International Conference on Application and Theory of Automation in Command and Control Systems (ATACCS)*. Toulouse (France).

- PRATS, XAVIER, VILARDAGA, SANTI, ISANTA, ROGER, BAS, ISIDRO & BIRLING, FLORENT. 2015. WEMSgen: A real-time weather modelling library for on-board trajectory optimisation and planning. *In: Proceedings of the 34th Digital Avionics Systems Conference (DASC)*. Prague (Czesch Republic). **Best paper in session award.**

- VILARDAGA, SANTI, DUAN, PENGFEI (PHIL), PRATS, XAVIER & UIJT DE HAAG, MAARTEN. 2014. Conflict Free Trajectory Optimisation with Target Tracking and Conformance Monitoring. *In: Proceedings of the 14th AIAA Aviation Technology, Integration, and Operations (ATIO) conference*. Atlanta, GA (USA). AIAA paper 2014-2022.

- PRATS, XAVIER, PÉREZ-BATLLE, MARC, BARRADO, CRISTINA, VILARDAGA, SANTI, BAS, ISIDRO, BIRLING, FLORENT, VERHOEVEN, RONALD P. M., & MARSMAN, ADRI. 2014. Enhancement of a time and energy management algorithm for continuous descent operations. *In: Proceedings of the 14th AIAA Aviation Technology, Integration, and Operations (ATIO) conference*. Atlanta, GA (USA). AIAA paper 2014-3151.

- VILARDAGA, SANTI & PRATS, XAVIER. 2014. Conflict free trajectory optimisation for complex departure procedures. *In: Proceedings of the 6th international congress on research in air transportation (ICRAT)*. Istanbul (Turkey).

- VILARDAGA, SANTI & PRATS, XAVIER. 2013. Effects in Fuel Consumption of Assigning RTAs into 4D Trajectory Optimisation upon Departures. *In: Proceedings of the 3rd International Conference on Application and Theory of Automation in Command and Control Systems (ATACCS)*. Naples (Italy). **Best doctoral paper award.**

Agraïments

Escriure una tesi doctoral no es fa cada dia. Així com moltes de nosaltres (les persones) tenim la sort de dedicar-nos a fer recerca (les que tenim la sort de poder-ho fer, i de divertir-nos fent-ho), no sempre som prou curoses com per documentar amb el rigor necessari els nostres resultats. Escriure aquesta memòria m'ha fet descobrir que es pot gaudir tant de l'escriptura tècnica (o científica) com gaudeixo de fa temps de l'escriptura matemàtica o de programació.

He tingut la sort de poder fer recerca amb grans persones del món científic i tecnològic, amb qui he compartit moments d'èxtasi gairebé entròpic en pissarres i esbossos de conceptes i gargots mal il·lustrats, però també moments de calma literària per dissertar aquest compendi de vivències.

Per un ordre que a priori no dono importancia (potser a risc d'ofendre algú) m'agradaria començar els agraïments per les persones que van veure concebre (fins i tot de manera còmplice) la proposta de tesi. Des de l'extint Centre de Tecnologia Aeroespacial (CTAE), continuant pel renombrament per absorció (metamorfosi a la partit polític d'actualitat) dins d'ASCAMM i, finalitzant per ídem a l'avui anomenat Eurecat, l'equip de la Pepa Sedó i del Daniel Serrano vau creure en la possibilitat real de cooperar amb la universitat no només a través de projectes, sinó portant la universitat a l'empresa a través del doctorat. A tu Pepa t'agraeixo moltíssim que hi creguéssis, que vulgués mantenir oberta la porta a la gestió de tràfic aeri i a la optimització de trajectòries. A tu Dani t'agraeixo immensament la teva amistat, totalment necessària en tots els projectes que hem fet junts, a part d'una professionalitat i d'un tarannà lluitador sense el qual no haguéssim aconseguit el que vam aconseguir en l'era ICARUS. Evidentment, aquí incloc a l'Ernesto Teniente, al Germán Moreno i al Jesús Romero (quins riures a la furgoneta, quina atenció al camp de vol).

Tot i la connivència de les persones esmentades, les veritables incitadores d'aquesta recerca vau ser dues: l'omnipresent Xavier Prats, i l'inconfusible Maarten Uijt de Haag. We wrote a proposal for the SESAR HALA! research network and we were selected. This very spur opened for me the door to two magnificent scientists and two even greater friends with whom I don't even have to plan for it if I want to meet them in a completely random place in Europe, say Brussels, on a random day.

A tu Xevi et dec la dedicació, l'organització i la paciència, però sobretot la perseverància. Sé que la nostra condició d'amics fa que hagis volgut creure en mi encara que fos pel desig de veure'm atènyer allò que perseguia, però la manera com t'hi has abocat em fa sentir molt privilegiat. La meva condició de doctorat a temps parcial, des de l'empresa, i a edat tardia, segur que t'ha fet viure la tesi des d'una perspectiva diferent. A mi m'ha aportat una vivència inoblidable, i una

amistat que ja s'extén a les nostres famílies.

Maarten, you have shown me that you can be one of the best at your field and still be loved by all your students, coworkers, friends and the soccer team members. My stage at Ohio University has been an experience that I will never forget. You and your family (Sunny, Saskia and Desmond) made me feel at home (thousands of kilometers from my actual home), spending weekends at Old Man's Cave and many other hikes, cooking the typical american barbecue (by a Dutchman) and helping me with all the paperwork and in finding a nice flat. Being at the Avionics Research Centre with Evan Dill and Phil Duan was a real pleasure.

Tornant a Catalunya, la col·laboració amb el Xevi ens va portar a una nova proposta guanyadora (com no havia de ser altrament): FASTOP (FAST OPtimiser for continuous descent approaches). FASTOP va marcar un camí profund dins la tesi, sobretot en dues vessants tècniques (la maduració de l'arquitectura C++ i GAMS, i la generació de condicions meteorològices realistes amb els fitxers GRIB). For this, I would like to thank Ronald Verhoeven for your kind and passionate love to trajectory optimisation. You were kind enough to share with Xevi and me incredibly productive afternoons at NLR with only a whiteboard and a pen. Also, at NLR, I appreciated very much the very interesting interaction with Michiel Valens and Frank Bussink. També dins l'equip de FASTOP, i per la part de prediccions i històrics meteorològiques, guardo amb molta estima les converses amb l'Isidro Bas i el Florent Birling de GTD. De vosaltres he après molt, tant tècnicament com de gestió de projectes i persones.

Dins l'equip de la UPC m'agradaria fer un reconeixement molt especial al Ramon Dalmau. Una de les persones més intel·ligents que conec i que a més ets capaç de mantenir (i compartir!) el teu amor inacabable pel teu llogaret (Tamariu), la teva passió marina i la teva incalculabe generositat. De tu (i les teves truites de patates envasades) he après moltíssim.

També vull agrair la meva mare Tere i el meu pare Josep la vostra companyia omnipresent. No només heu seguit els meus periples acadèmics i professionals per tot europa (meus i dels meus germans) sinó que els heu propiciat i certament habilitat. A la vostra paciència i generositat infinita, com a pares primer i com a avis després, atribució a què us heu abonat des del primer dia amb un afany gegantesc, entrenyable. Al Jordi, al Josep, a l'Anna, l'Oriana, el Gabriel (*Gabichou*), a la Blanca i als qui quedin per venir.

Finalment, tot i que he intentat amb vehemència que la tesi no abastés temps familiar (ni com a pare ni com a parella), sé que la Diana, la Neus i el Gil heu viscut també, segurament més del que em penso, aquesta lluita diària del procés latent (i candent) de la tesi no resolta. Amb la vostra inestimable ajuda m'heu fet mantenir viva l'esperança, que m'ha portat avui a aquesta última paraula, ni en llenguatge matemàtic, ni de programació. Sinó en català i en llibertat:

Gràcies.

Vallvidrera, Setembre de 2019
Santi Vilardaga Garcia-Cascon

Resum

Des del naixement de l'aviació comercial, les aplicacions i beneficis dels avions han crescut immensament. Això, en perfecta sincronia amb l'augment mitjà del poder adquisitiu de la societat, ha augmentat el nombre d'avions que volen pel cel. Aquest augment comporta, tanmateix, un cost, tant en aspectes mediambientals com en la capacitat de l'espai aeri. Aquesta tesi és concebuda per treballar en l'alleujament dels problemes que resulten de l'elevat nombre de vols, proposant nous conceptes i mecanismes per augmentar la capacitat de l'espai aeri amb seguretat i alhora minimitzar l'impacte ambiental de l'aviació.

Aquesta recerca, complexa però extremadament necessària, és la protagonista d'una gran quantitat de treballs científics publicats. Des de la propulsió, fins a les aerostructures i la gestió del trànsit aeri, avui en dia es dedica un gran esforç a la reducció de l'impacte ambiental, així com a l'augment de la seguretat i la capacitat de l'espai aeri. Un tema prometedor és la introducció de nous conceptes d'operació que aprofiten al màxim l'optimització de trajectòries en les quatre dimensions (4D) i nivells d'automatització més elevats, tant per a sistemes de bord com de terra.

Conceptes com ara operacions de perfil vertical continu són cada cop més utilitzats en el dia a dia. També, la reducció de la distància recorreguda dels avions mitjançant rutes més directes esdevé una realitat com més va més evident. Per tal d'abastar un àmbit més àmpli, els sistemes embarcats i de terra hauran d'ésser actualitzats. És per això que s'haurà d'explorar minuciosament la quantificació dels beneficis esperats per als nou conceptes que es proposin, abans d'introduir-los a escala local o global.

La investigació d'aquesta tesi doctoral proposa un sistema integrat per a l'optimització de trajectòries, la predicció, i l'estimació de paràmetres, amb el qual es poden avaluar nous conceptes de gestió del trànsit aeri. Aquest sistema té la flexibilitat d'optimitzar trajectòries que van des d'un vol lliure (*free-flight*) fins a una estructura de ruta molt estricta, des d'una llibertat completa al perfil vertical fins a una adhesió específica als nivells de vol, etc. La definició d'escenaris és prou genèrica com per permetre una àmplia varietat de tipologies de vol, fases de vol, fases de rendiment, restriccions al llarg de la trajectòria, entre molts altres aspectes. L'estratègia d'optimització 4D dóna com a resultat una trajectòria que no només compleix les característiques del vol (i de l'entorn configurat), sinó que també minimitza un objectiu funcional determinat, com ara el cost operatiu, el temps, el combustible, etc. I com ja s'ha mencionat breument, aquesta mateixa estratègia d'optimització s'adapta lleugerament per presentar una innovadora estratègia per realitzar prediccions de trajectòria adaptativa (amb monitoratge de conformitat) i per

estimar paràmetres crucials inicialment desconeguts d'un avió.

Per resoldre un problema tan complex, es formula un problema de control òptim i es converteix en un problema de programació no lineal (NLP) amb mètodes de col·locació directa. Aquest problema es resol numèricament mitjançant un programari de resolució de problemes NLP i se n'extreuen els resultats per a l'anàlisi. Es presenta una arquitectura de programari integral, aprofitant el millor de dos mons: un llenguatge de programació orientat a objectes (C++) i un llenguatge matemàtic algebric molt potent (GAMS). La interacció entre aquests dos mons permet la flexibilitat i la genericitat del sistema d'optimització desenvolupat.

A partir d'aquest sistema d'optimització, els diferents capítols de la tesi produeixen resultats operatius rellevants. Això no només demostra que el sistema pot fer front a una gran varietat de problemes, sinó que també contribueix a l'objectiu final d'augmentar de forma segura la capacitat de l'espai aeri i l'eficiència del trànsit aeri. Es presenten diferents casos d'ús i exemples il·lustratius centrats en enlairaments dins l'àrea de maniobra terminal (TMA). Concretament, quatre etapes formen aquesta part de la tesi. Primer, es presenta una avaluació de l'eficiència dels temps requerits d'arribada (RTA) com a forma d'augmentar la capacitat del trànsit aeri. Aquest estudi proporciona resultats sobre el cost en termes de combustible i temps d'imposar aquests requisits de temps dins d'una TMA (que pot arribar a xifres sorprenentment baixes). A més, mostra com d'efectiva pot ser aquesta estratègia per a la separació del trànsit. En segon lloc, es presenta la implementació d'una metodologia de separació d'avions mitjançant el sistema d'optimització. En ella, una aeronau (*l'aeronau*) genera una predicció de trajectòria d'un avió extern amb qui preveu tenir un conflicte proper (*l'intrús*). Seguidament, *l'aeronau* calcula la seva pròpia trajectòria òptima que es desvia d'aquella predita de *l'intrús*. S'implementa una estratègia de control de la conformitat per assegurar que la separació es mantingui durant tot el vol, reconeixent les desviacions i reaccionant en conseqüència. En tercer lloc, la predicció de la trajectòria intrusa es veu millorada per l'estimació d'una massa equivalent mitjançant estats passats coneguts (*el deixant*). Com era d'esperar, com més llarg sigui aquest deixant, millor serà l'estimació de la massa. Tanmateix, s'aconsegueix una precisió impressionant molt poc després de l'inici del vol. Finalment, es presenta la implementació d'una estratègia de separació de múltiples aeronaus. En aquesta formulació, s'optimitzen simultàniament les trajectòries de diversos avions dins el mateix problema d'optimització, mantenint la separació entre ells. La complexitat de l'alineació temporal de les coordenades d'avions per a una comparació justa s'aborda des d'una perspectiva innovadora.

En conclusió, es comparen les diferents estratègies de separació d'avions i, sorprenentment, els millors resultats de cada estratègia són força similars. De fet, l'augment del cost operatiu que presenten les diferents estratègies (en comparació amb la trajectòria òptima individual) és insignificant i sempre millor que el paradigma actual de separació del control de trànsit aeri.

Abstract

Since the birth of commercial aviation, the applications and benefits of aircraft have grown immensely. This, in perfect synchrony with the average increase of purchasing power of the society, has rocketed the number of aircraft flying in our skies. This increase, however, comes at a cost, both in environmental and airspace capacity aspects. This thesis works towards the alleviation of the issues that have appeared caused by the high number of flights, proposing concepts and mechanisms to safely increase the airspace capacity whilst minimising the environmental impact of aviation.

This incredibly complex and neverending (but extremely necessary) pursuit is the focus of a great amount of research in the literature. From propulsion, to aerostructures and air traffic management, a lot of effort is devoted nowadays into reducing the environmental impact, as well as increasing safety and airspace capacity. One promising topic is the introduction of new concepts of operation that take full advantage of four dimensional (4D) trajectory optimisation and higher levels of automation either for on-board or ground systems.

Concepts such as continuous vertical profile operations are more and more utilised in a daily basis. Furthermore, reducing the travelled distance by taking more direct routes is also becoming a reality. In order to extend such operations to a wider scope, it is expected that airborne and ground systems should be updated. Besides, the quantification of expected gains for new concepts must be thoroughly explored, before introducing them in a local or global scale.

The research in this PhD thesis proposes an integrated framework for trajectory optimisation, trajectory prediction and parameter estimation, with which new air traffic management concepts can be assessed. This framework has the flexibility to optimise trajectories ranging from a free-flight to a very strict route structure, from a complete freedom at the vertical profile to a specific adherence to flight levels, etc. The definition of scenarios is generic enough to allow a wide variety of flight typologies, flight legs, performance phases, constraints along the trajectory, among many other aspects. Besides, the 4D optimisation strategy results in a trajectory that not only complies with the flight (and configured environment) characteristics, but also the one that minimises a given functional objective, such as operational cost, time, fuel, etc. Furthermore, the same mathematical formulation is slightly adapted in a novel strategy to perform adaptive trajectory prediction (with conformance monitoring), and to estimate crucial initially unknown parameters of an aircraft.

To resolve such a complex problem, an optimal control problem is formulated and converted

into a non-linear programming (NLP) problem with direct collocation methods. This problem is then numerically resolved by an NLP solver and the results are extracted for analysis. A comprehensive software architecture is presented, taking benefit from the best of two worlds: an object-oriented software coding language (C++) and a very powerful algebraic modelling language (GAMS). The interaction between these two worlds allows the flexibility and genericity of the developed optimisation framework.

Based on this optimisation framework, the different chapters in the thesis produce operationally relevant results. This does not only demonstrate that the framework can cope with a great variety of problems, but also contributes to the ultimate goal of safely increasing airspace capacity and air traffic efficiency. Different illustrative examples are presented focussed in the departure phase within a terminal manoeuvring area. Specifically, four stages form this part of the thesis. First, an assessment of the efficiency of required times of arrival as a ways to increase air traffic capacity is presented. This study provides results on the cost in terms of fuel and time of imposing these time requirements within a TMA (which can get to surprisingly low figures). Besides, it shows how effective this strategy can be for traffic separation. Second, the implementation of an aircraft separation methodology using the optimisation framework is presented. In it, an intruder trajectory is predicted and the ownship calculates its own optimal trajectory that deviates from it. A conformance monitoring strategy is implemented to ensure that the separation is maintained throughout the flight, acknowledging deviations, and reacting accordingly. Third, the prediction of the intruder trajectory is enhanced by the estimation of an equivalent mass using known past states. As expected, the longer the trailing track, the better the mass estimation. However, an impressive accuracy is achieved early after the beginning of the flight. Finally, the implementation of a multi-aircraft separation strategy is presented. In this formulation, multiple aircraft are simultaneously optimised in the same optimisation problem, all whilst maintaining separation between them. The complexity of the alignment of aircraft coordinates for a fair comparison is tackled from a novel perspective.

Conclusively, the different strategies for aircraft separation are compared, and quite surprisingly the best results for each strategy are quite similar. Indeed, the increase in operational cost that the different strategies present (when compared to the individual optimal trajectory) is negligible and allegedly better than the current air traffic control separation paradigm.

Notation

Throughout this dissertation and as a general rule, scalars and vectors are denoted either with lower or upper case letters. Vectors are noted with the conventional overhead arrow, like for example $\vec{a}$ or $\vec{\psi}$. Matrices are denoted using caligraphic fonts in bold series, like $\boldsymbol{\mathcal{R}}$. The time derivative of magnitude $a(t)$ is expressed by $\frac{\mathrm{d}a(t)}{\mathrm{d}t}$. Finally, if not otherwise noted, all vectors are column vectors and a transposed vector is denoted by $[\cdot]^T$. Next, the principal symbols that are used throughout this dissertation are shown along with their meaning. The reader should note that this list is not exhaustive.

$\mathbb{R}$	set of real numbers
$\times$	Cartesian product
$\mathbb{R}^m$	$\underbrace{\mathrm{R} \times \mathrm{R} \times \cdots \times \mathrm{R}}_{m \text{ times}}$
a	index of aircraft a, generally used as subscript: $(\cdot)_a$
A	number of aircraft in the multi-aircraft problem
$\mathcal{A}$	set that contains all the combinations of two aircraft in the multi-aircraft problem
$c_{ij}^{(\cdot)}$	polynomial coefficients for the approximation of $(\cdot)$
C_f	fuel cost
C_t	time cost
C_D	drag coefficient
C_L	lift coefficient
CI	cost index
χ	aerodynamic heading angle
d_h	required horizontal separation between aircraft
d_v	required vertical separation between aircraft
D	aerodynamic drag force
δ	normalised magnitude of air pressure
$\Delta t'$	time interval between two time samples in $\vec{t}'$
e	eastward position coordinate
e_i	intruder's observed eastward position coordinate
$\hat{e}_\mathrm{i}$	intruder's estimated eastward position coordinate
e'	comparable eastward position coordinate
$\vec{e}$	functions defining the event constraints

$\vec{e}_L$	bounds for the lower event constraints
$\vec{e}_U$	bounds for the upper event constraints
$\vec{f}$	equations of the aircraft dynamics
FF	fuel flow
g	gravity vector module
g_h	horizontal separation contraint
g_v	vertical separation contraint
γ	aerodynamic flight path angle
γ_a	specific heat ratio of the air
$\Gamma_{(\cdot)}$	spline approximation of $(\cdot)$
h	altitude position coordinate
h_{i}	intruder's observed altitude position coordinate
$\hat{h}_{\mathrm{i}}$	intruder's estimated altitude position coordinate
h'	comparable altitude position coordinate
$\vec{h}$	functions defining the path constraints
$\vec{h}_L$	lower bounds for the path constraints
$\vec{h}_U$	upper bounds for the path constraints
i	optimisation control problem phase i, generally used as superscript: $(\cdot)^{(i)}$
i	intruder, generally used as subscript: $(\cdot)_{\mathrm{i}}$
J	objective optimisation function
k	steepness coefficient of the switching function Υ
K_t	standard temperature lapse rate
λ_h	continuous variable for the horizontal separation constraint
λ_v	continuous variable for the vertical separation constraint
L	number of equally spaced time instants in the multi-aircraft problem
m	mass of the aircraft
M	mach number
M_a	number of collocation points for aircraft a
M_{MO}	maximum aircraft operating mach number
n	northward position coordinate
n_{i}	intruder's observed northward position coordinate
$\hat{n}_{\mathrm{i}}$	intruder's estimated northward position coordinate
n'	comparable northward position coordinate
n_e	number of engines of the airplane
n_u	number of control variables
n_x	number of state variables
n_z	vertical load factor
N	number of phases
N_a	number of phases of aircraft a
$N1$	revolutions of the engine fan
$N1_{idle}$	revolutions of the engine fan at idle throttle setting
$N1_{max}$	maximum revolutions of the engine fan
p	air pressure
p_0	air pressure at sea level
π	throttle setting
ϕ	bank angle
φ	total number of flap/slats configurations
$\boldsymbol{\mathcal{P}}$	state transition matrix for a constant velocity model
q	steepness coefficient of the superegg
$\boldsymbol{\mathcal{Q}}$	linearised Kalman filter state transition covariance matrix
R	ideal gas constant for the atmosphere

$\boldsymbol{\mathcal{R}}$	linearised Kalman fiter measurement covariance matrix
ρ	air density
ρ_0	air density at sea level
ϱ	collocation index in $\vec{t}'$
s	along path distance
S	total wing surface
S_h	observed minimum aircraft horizontal separation
$\hat{S}_h$	estimated minimum aircraft horizontal separation
$S_v\|_{S_h<3\,\mathrm{NM}}$	observed minimum vertical separation when the horizontal separation is not granted
$\hat{S}_v\|_{\hat{S}_h<3\,\mathrm{NM}}$	estimated minimum vertical separation when the horizontal separation is not granted
σ	normalised magnitude of air density
ς	collocation index in $\vec{t}$
t	time
$\vec{t}$	vector of time samples
$\vec{t}'$	vector of comparable time samples in the multi-aircraft problem
t_0	initial time, generally superscripted by the aircraft phase: $t_0^{(i)}$
t_{0_L}	lower bounds for the initial time
t_{0_U}	upper bounds for the initial time
t'_0	initial time of potential conflict in the multi-aircraft problem
t_f	final time, generally superscripted by the aircraft phase: $t_f^{(i)}$
t_{f_L}	lower bounds for the final time
t_{f_U}	upper bounds for the final time
t'_f	final time of potential conflict in the multi-aircraft problem
T	total net thrust force
τ	air temperature
τ_0	air temperature at sea level
θ	normalised magnitude of air temperature
$\vec{u}$	control vector, generally superscripted by the aircraft phase: $\vec{u}^{(i)}$
$\vec{u}_L$	lower bounds for the control vector
$\vec{u}_U$	upper bounds for the control vector
Υ	piecewise switching function modelling the resampling of collocation points
Υ_i	switching function modelling the aerondynamic coefficients transition
v	true airspeed (TAS)
v_i	intruder's observed true airspeed
$\vec{v}$	linearised Kalman filter measurement noise
v_{CAS}	calibrated airspeed (CAS)
$v_{i\to j}$	airspeed for flap/slat transition from i-th to j-th configuration
V_{MCA}	minimum aircraft operating speed whilst on the air
V_{MO}	maximum aircraft operating speed
w	linearised Kalman filter process noise
W_e	eastward local wind component
W_n	northward local wind component
W_h	vertical local wind component
$\vec{x}$	state vector, generally superscripted by the aircraft phase: $\vec{x}^{(i)}$
$\vec{x}_L$	lower bounds for the state vector
$\vec{x}_U$	upper bounds for the state vector
$\vec{y}$	linearised Kalman filter state vector
$\vec{z}$	linearised Kalman filter measurements

List of Acronyms

2D	2-Dimensions: position
3D	3-Dimensions: position and altitude
4D	4-Dimensions: position, altitude and time
3DOF	3 Degrees Of Freedom
6DOF	6 Degrees Of Freedom
ADS-B	Automatic Dependent Surveillance - Broadcast
AIDL	Aircraft Intent Description Language
API	Application Programming Interface
ASAS	Airborne Separation Assurance System
ATC	Air Traffic Control
ATCo	Air Traffic Controller
ATM	Air Traffic Management
BADA	Eurocontrol's Base of Aircraft Data
CAS	Calibrated AirSpeed
CCO	Continuous Climb Operation
CCO	Continuous Climb Operation
CDO	Continuous Descent Operation
CoG	Centre of Gravity
CTA	Controlled Time of Arrival
DME	Distance Measurement Equipment
DYNAMO	DYNAMic Optimiser
EDA	En-route Descent Advisor
ERAT	Environmentally Responsible Air Transport
ETA	Estimated Time of Arrival
FL	Flight Level
FMS	Flight Management System
FTE	Flight Technical Error
GAMS	General Algebraic Modelling System
GDX	GAMS Data eXchange protocol
GRIB	General Regularly-distributed Information in Binary form
IAP	Instrument Approach Procedure
ICAO	International Civil Aviation Organisation

IFR	Instrumental Flight Rules
IPOPT	Interior Point OPTimizer
ISA	International Standard Atmosphere
NACp	Navigation Accuracy Category for Position
NACv	Navigation Accuracy Cat- egory for Velocity
NADP	Noise Abatement Departure Procedure
NASA	National Aeronautics and Space Administration
NDB	Non Directional Beacon
NOAA	National Oceanic and Atmospheric Administration
NSE	Navigation System Error
PEP	Airbus' Performance Engineering Programs Suite
NLP	NonLinear Programming
RADAR	RAdio Detection And Ranging
RMS	Root Mean Square
ROS	Robotics Operating System
RTA	Required Time of Arrival
SESAR	Single European Sky ATM Research
SID	Standard Instrumental Departure
STAR	Standard Terminal Arrival Route
SWIM	System Wide Information Management
TAS	True Air Speed
TBO	Trajectory Based Operations
TCAS	Traffic Collision Avoidance System
TEMO	Time and Energy Management Operations
TIS-B	Traffic Information Service - Broadcast
TMA	Terminal Manoeuvring Area
V2V	Vehicle-to-vehicle
VOR	VHF Omnidirectional Range

I

Introduction

Air travel and air delivery have become an essential part of our lives. As society evolves at each technology breakthrough, new concepts of life, cohabitation and commerce are available. It is not uncommon nowadays to see members of small families spread about the globe, without having to compromise working opportunities with family intimacy. Teleworking and long-distance daily commutes are a part of a huge number of active workers. Especially when last-minute purchases are ringing the door bell at tremendously short waiting times. Even if the sustainability of current state of things is under discussion (very few are actually negating the bad environmental impact of some modern habits), most people believe that, this time, science and technology will save the day (with cleaner transport, green energy, complete up-cycling of waste, etc.).

In all cases, the societal changes that technology (and economy and politics) has enabled, are backed up by more and more adopters who will not give up the achieved *statu quo*. And air traffic, once again, is in the spotlight of the big challenge that this increase in people and goods transportation represents.

As it has already happened in the past, new concepts of operations will have to upgrade current air traffic management (ATM) and air traffic control (ATC). Historically, at the beginning of aviation, the use of air traffic was marginal and therefore coordination between airborne actors was completely lacking of big infrastructures or human interaction beyond the rudimentary 'look out of the window' (*see-and-avoid*). Back then, the effective applications of civil air traffic were very few and mostly focussed on incipient air mail delivery.

Soon after, engines got lighter and more powerful, and the airplanes got faster and with a longer range and higher load capacity. At this point, civil society started taking benefit from the use of aviation, be it for the delivery of packages or the transportaion of people. American and European elites started travelling big distances with relatively *short times*: from Belgium to

Madagascar in under a week for 8000 French Francs (see figure I-1).

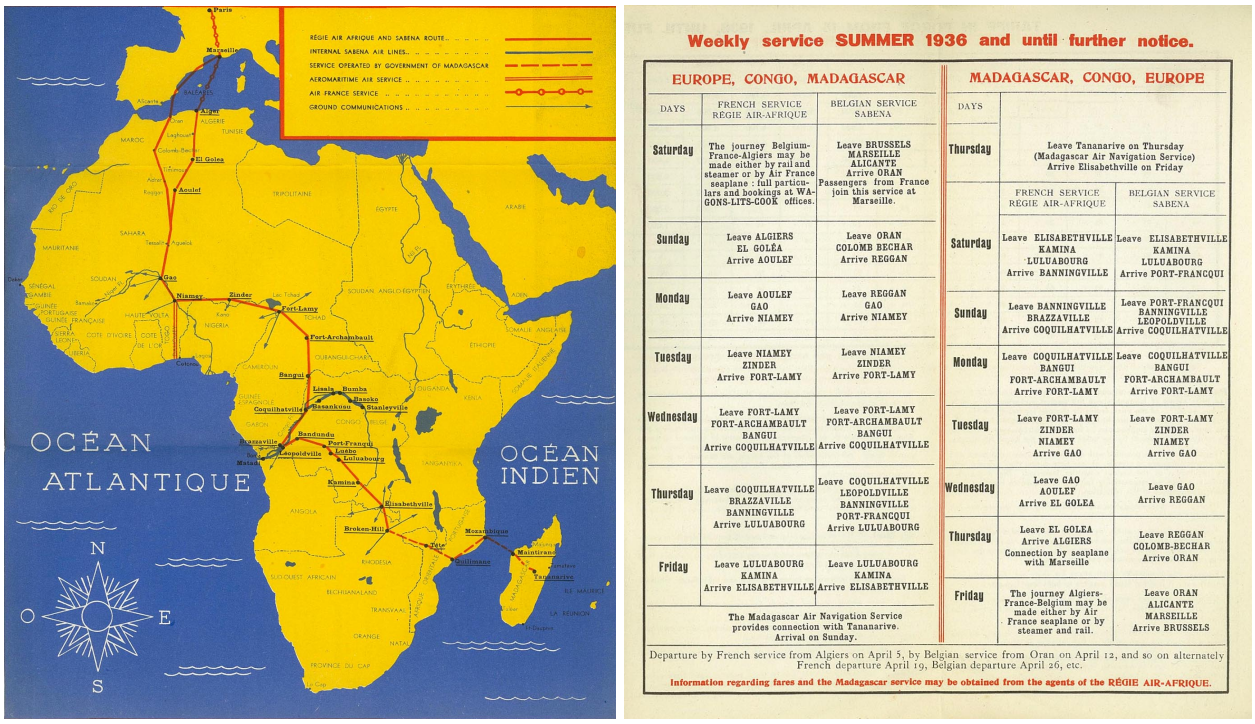

Weekly service SUMMER 1936 and until further notice.

EUROPE, CONGO, MADAGASCAR

DAYS	FRENCH SERVICE RÉGIE AIR-AFRIQUE	BELGIAN SERVICE SABENA
Saturday	The journey Belgium-France-Algiers may be made either by rail and steamer or by Air France seaplane : full particulars and bookings at WAGONS-LITS-COOK offices.	Leave BRUSSELS MARSEILLE ALICANTE Arrive ORAN Passengers from France join this service at Marseille.
Sunday	Leave ALGIERS EL GOLÉA Arrive AOULEF	Leave ORAN COLOMB BECHAR Arrive REGGAN
Monday	Leave AOULEF GAO Arrive NIAMEY	Leave REGGAN GAO Arrive NIAMEY
Tuesday	Leave NIAMEY ZINDER Arrive FORT-LAMY	Leave NIAMEY ZINDER Arrive FORT-LAMY
Wednesday	Leave FORT-LAMY FORT-ARCHAMBAULT BANGUI Arrive COQUILHATVILLE	Leave FORT-LAMY FORT-ARCHAMBAULT BANGUI Arrive COQUILHATVILLE
Thursday	Leave COQUILHATVILLE BRAZZAVILLE BANNINGVILLE Arrive LULUABOURG	Leave COQUILHATVILLE LEOPOLDVILLE BANNINGVILLE PORT-FRANCQUI Arrive LULUABOURG
Friday	Leave LULUABOURG KAMINA Arrive ELISABETHVILLE	Leave LULUABOURG KAMINA Arrive ELISABETHVILLE
	The Madagascar Air Navigation Service provides connection with Tananarive. Arrival on Sunday.	

MADAGASCAR, CONGO, EUROPE

DAYS		
Thursday	Leave Tananarive on Thursday (Madagascar Air Navigation Service) Arrive Elisabethville on Friday	
	FRENCH SERVICE RÉGIE AIR-AFRIQUE	BELGIAN SERVICE SABENA
Saturday	Leave ELISABETHVILLE KAMINA LULUABOURG Arrive BANNINGVILLE	Leave ELISABETHVILLE KAMINA LULUABOURG Arrive PORT-FRANCQUI
Sunday	Leave BANNINGVILLE BRAZZAVILLE Arrive COQUILHATVILLE	Leave PORT-FRANCQUI BANNINGVILLE LEOPOLDVILLE Arrive COQUILHATVILLE
Monday	Leave COQUILHATVILLE BANGUI FORT-ARCHAMBAULT Arrive FORT-LAMY	Leave COQUILHATVILLE BANGUI FORT-ARCHAMBAULT Arrive FORT-LAMY
Tuesday	Leave FORT-LAMY ZINDER NIAMEY Arrive GAO	Leave FORT-LAMY ZINDER NIAMEY Arrive GAO
Wednesday	Leave GAO AOULEF Arrive EL GOLEA	Leave GAO Arrive REGGAN
Thursday	Leave EL GOLEA Arrive ALGIERS Connection by seaplane with Marseille	Leave REGGAN COLOMB-BECHAR Arrive ORAN
Friday	The journey Algiers-France-Belgium may be made either by Air France seaplane or by steamer and rail.	Leave ORAN ALICANTE MARSEILLE Arrive BRUSSELS

Departure by French service from Algiers on April 5, by Belgian service from Oran on April 12, and so on alternately French departure April 19, Belgian departure April 26, etc.

Information regarding fares and the Madagascar service may be obtained from the agents of the RÉGIE AIR-AFRIQUE.

Figure I-1: *From Belgium to Madagascar in under a week for 8000 French Francs in 1936. Source: Björn Larsson*[1]

I.1 The ATC background

To cope with the increase of traffic numbers and complexity, ATM faced the big challenge to upgrade the quasi non-existent system to the complex systems found today around the world. From the very early beginning free-flight to the potential future self-separated technology-enabled free-flight, figure I-2 depicts the big paradigm shift.

Very low traffic levels enabled the very early beginning **laissez faire**. However, this only lasted a few years, and incipient air traffic control services appeared alongside the birth of commercial aviation. Especially at airfields, where the concentration of aircraft was higher, the need for a navigation structure arised, to enable an orderly and expeditious flow of incoming and outgoing air traffic. To this end, visual structured procedures (following landscape marks and manned ground flagging) were set in place in a form of very incipient standard procedures. Low-visibility navigation was assisted by a ground infrastructure, which consisted first with omnidirectional bonfires and later by rotating aerial lighthouses. Soon, the instrumentation of the network (and the cockpit) superseded the rudimentary visual navigation aids, enabling the emergence of the instrument flight rules (IFR) thanks to radio navigation beacons (NDB, VOR, DME) and, more recently, to satellite navigation.

Once in a pre-defined route, and thanks to radio communications and timers, an air traffic controller (ATCo) would have an estimation of the position of aircraft and would predict potential future conflicts. This is known as **procedural control**, and would depend on reliable voice communications between the pilot and the ATCo with periodic voice position reports and bilateral

[1] http://www.timetableimages.com/ttimages/airafr/raf36/

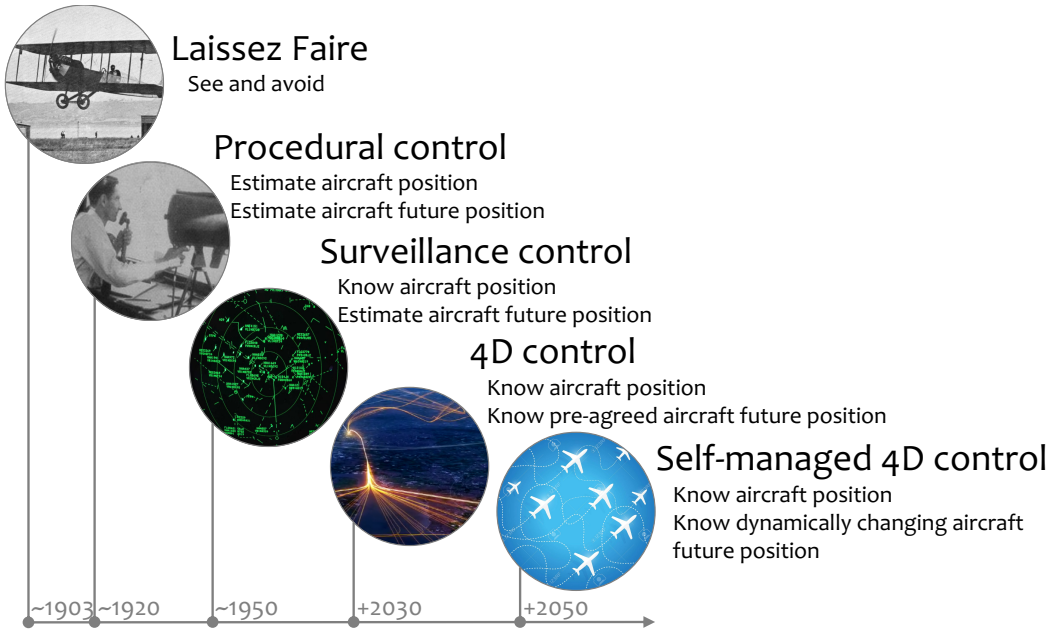

Figure I-2: *Air Traffic Control paradigm shift from the beginning of aviation to the foreseable future.*

interrogation-and-answer.

Thanks to the development of the RADAR technology, and the beginning of systemic information sharing through the installation of onboard transponders, traffic controllers started to *see* the aircraft. This allowed for a more accurate situational awareness and therefore, enhanced the prediction of conflicts, reducing separation minima (and therefore dramatically increasing airspace capacity). This is known as the **radar control**, or the **surveillance control**, which, with more or less technology support and information sharing is the base for the current imperfect system.

Summarising, separation assurance is firstly tackled at a strategic level, via fixed lateral trajectory profiles and imposing altitude and velocity constraints throughout standard procedures, in form of en-route airways, standard instrumental departures (SID), standard arrivals (STAR) and instrument approach procedures (IAP). Additionally, the ATCo surveil the separation at a tactical level and, if required, issue vectoring commands (i.e., heading changes), level off aircraft at intermediate altitudes or restrict speeds at some segments. An example of instrument procedures and ATC radar vectoring is depicted in figure I-3, showing the initial climb phase for Barcelona and how ATCo advisories are cleared to individual aircraft, deviating these from the standard procedures (each line represents an aircraft trajectory, superposed to the SID chart).

This paradigm has been the kernel of air traffic control since the introduction of RADARs, even if technological and conceptual improvements have been gradually introduced since then, mainly regarding **safety** and **capacity** objectives. In the context that the main driver for improvements has been the increase of the number of flights (backed up by a healthy economy and an omission of environmental aspects) the gradual upgrades to the surveillance control have sufficed. However, under the current economical stress and environmental concerns, the mere increase of capacity is no longer enough: it is more and more important that **efficiency**, at all levels, leads the next paradigm shift.

This is the reason why new concepts of navigation such as Continuous Climb Operations (CCO), Continuous Cruise Climbs (CCC), and Continuous Descent Operations (CDO) have appeared in the recent years. Continuous operations benefit from flying an optimal vertical profile

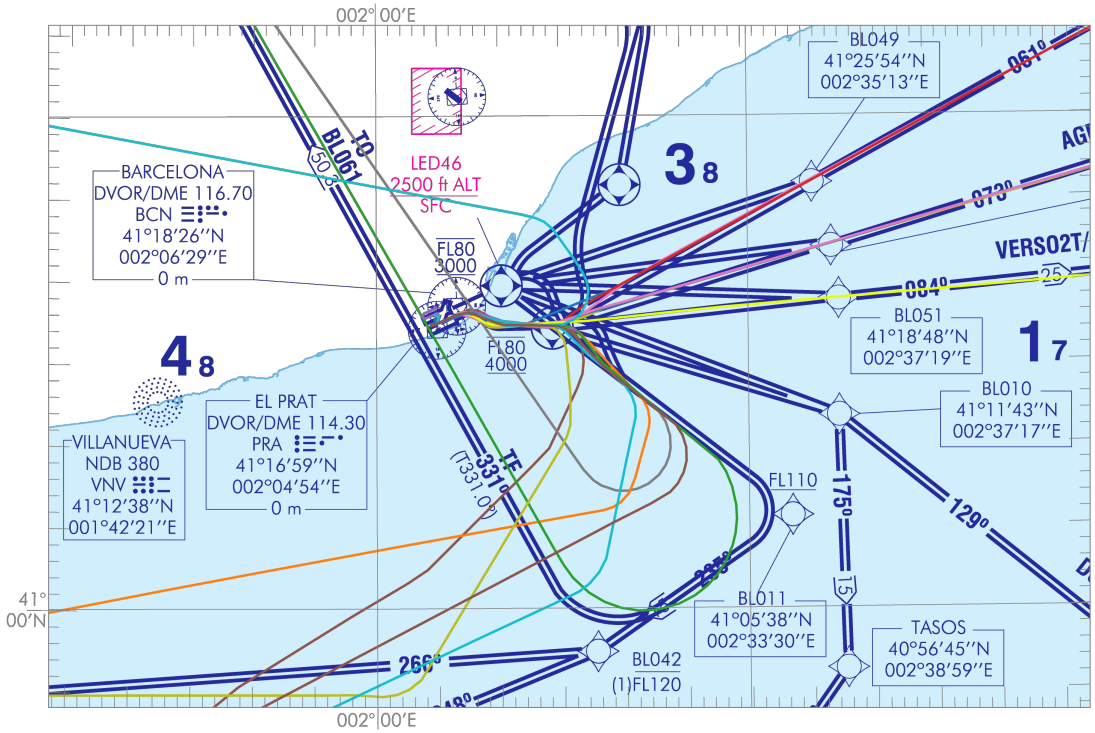

Figure I-3: *Surveillance control at the initial climb phase in Barcelona (instrument departure procedure vs. radar tracks).*

throughout the different phases of the flight, with the adequate airspace design, procedure design, and ATC facilitation. If conditions allow, the departing aircraft will be cleared for high altitudes immediately after take-off, enabling optimal speed and engine thrust setings throghout the climb up to the inicial cruise level (ICAO, 2012; Pérez Castán *et al.*, 2015). Similarly, the arriving aircraft will be allowed to descend continuously and/or at idle engine configuration from the top of descent to the glide slope interception (ICAO, 2010). Finally, during the cruise phase, as the flight progresses and the aircraft mass decreases (upon continuously burning fuel), the optimum cruise altitude increases and therefore the aircraft would benefit from a continuous climb during cruise (Dalmau & Prats, 2015).

Even if continuous operations have demonstrated good fuel reduction, they are greatly dependent on multiple characteristics of each aircraft (such as aircraft performance, mass or operating procedures) and meteorological conditions (Fricke *et al.*, 2017). This results in a great variety of individually *optimal* vertical and speed profiles that complicates the task of predicting aircraft future states and traffic separation, ultimately impacting negatively on airspace capacity (Johnson, 2011). This is why nowadays ATCo restrict the use of CCO and CDO to off-peak hours, where low levels of traffic are found in the terminal manoeuvring area (TMA). Furthermore, CCC is seldom implemented nowadays, except in remote areas such as the north atlantic tracks with a block of flight levels (ICAO, 2016)

These limitations are intrinsic to the current surveillance control, where, mostly due to the technology and the (very reduced-) information sharing between airspace users, the prediction of the aircraft future position is based on a (usually very poor-) estimation. In the following sections, this will be upgraded gradually to the **4D control**, where a business trajectory is shared among airspace users, and the **self-managed 4D control**, where this business trajectory is continuously updated and all actors are legitimated and take the responsibility of keeping separation with others, thus delegating ATC responsibilities to the pilot through the use of airborne separation assurance systems (ASAS) (Eurocontrol, 2002).

I.2 Efficiency vs. capacity in TMAs

The tradeoff between efficiency and capacity is not new, and research has been performed on the integration of continuous operations in all phases of the flight. An example of this, in the TMA, is the Oceanic Tailored Arrivals program, in place at San Francisco airport (**?**). These arrivals are supported by the En-route Descent Advisor (EDA) developed by NASA-AMES, which is able to compute conflict-free optimal descent trajectories and satisfy a given arrival fix metering by issuing speed advisories to participating aircraft (Coppenbarger *et al.*, 2007). Another example is the project Environmentally Responsible Air Transport (ERAT), which developed methods and systems to reduce environmental impact using continuous arrival and departure procedures inside high density TMAs in Europe (ERAT Consortium, 2012). Alternatively, (Chaloulos *et al.*, 2010) propose imperceptible speed adjustments to minimise the risk of potential conflicts and lessen the workload of ATCo, impacting positively into airspace capacity.

More recently, SESAR and NextGen programs have introduced the concept of Trajectory Based Operations (TBO), claimed to be an enabler for trajectory optimisation implementation in an operational environment (Mutuel & Neri, 2013). For example, (Soler *et al.*, 2014a) proposes the implementation of applicable speed and heading advisories to current operations to resolve conflicts in cruise phases using TBO concept. Another example is the *relaxed cruise* presented by (Dalmau & Prats, 2017), where a low climb gradient and/or reduced step climbs are performed throhgout the climb phase in a *pseudo*-CCC whilst seeking a compromise between cost savings and impact on the ATM (specifically regarding capacity). (Bronsvoort, 2014) assesses the application of TBO air-ground synchronisation concepts with current technologies and its predictability issues. Finally, (De Jong, 2014) presents the Time and Energy Management Operations (TEMO), which implements CDO in dense traffic while fulfilling very high accuracy controlled time of arrival constraints (CTA) at different metering fixes. TEMO has shown promising results in human-in-the-loop simulations and in real flight trials, as reported in (Prats *et al.*, 2017).

One requirement for the efficient flow of air traffic (without badly impacting capacity) is the accurate knowledge of aircraft positions, velocity and adequate prediction of future aircraft movements. Without accurate information, maintaining safe separation between aircraft requires much more conservative, and therefore less efficient, methods (Roy *et al.*, 2006; Tadema *et al.*, 2010). Moreover, a large scale implementation of these optimised trajectories (i.e., not only for a small set of aircraft but for all those in a dense and complex TMA) remains an issue that will require more levels of automation. In this regard, the concept of aircraft self-separation is seen as a promising solution. The iFly project[2] claims this concept may safely accommodate up to six times the en-route traffic demand of 2005 (Blom & Bakker, 2011). The distributed nature of this solution provides localised case-by-case efficient near- and mid-term conflict resolution (from minutes to tens of minutes), even if the long-term (hours) efficiency can be included in combination with ground assistance as depicted in (Chaloulos *et al.*, 2008). This will also result in lower ground infrastructure complexity and reduced associated costs compared to a fully centralised solution.

I.3 Information sharing

In a TMA, where a high density of traffic struggles to safely and efficiently navigate towards a destination, cooperation between all involved actors is an important issue to address. This becomes even more important in a future self-separation scenario, under **self-managed 4D control**. The major driver for effective cooperation is the amount and quality of information that is shared amongst airspace users. From everything to nothing, three information sharing cases are considered in this PhD:

[2] http://ifly.nlr.nl

Fully-cooperative

An ideal scenario would assume a fully cooperative situation where ownship trajectory planning benefits from **knowledge of intruder aircraft performance data and intents**. Some implementations of this case assume centralised computation of all traffic optimal trajectories (Soler *et al.*, 2014a). Another strategy would be to delegate the computation of optimal trajectories and conflict resolutions to the cockpit. In that case, each aircraft calculates its own optimal trajectory taking into account the prediction of other traffic future states and then enters in a collaborative decision making process with the potential conflicting aircraft to find the overall best conflict resolution.

Semi-cooperative

Nowadays, airlines are very wary on providing sensitive information to other airspace users (mainly aircraft mass and cost index strategy). Hence, another (less cooperative) solution would be to use a **flight plan** or **flight intent** information to predict other aircraft trajectories, with the assumptions of **unknown aircraft parameters**. This solution relies on Automatic Dependent Surveillance - Broadcast (ADS-B) technology or the implementation of cooperative methodologies such as AIDL (Aircraft Intent Description Language) (Gallo *et al.*, 2007) and SWIM (System Wide Information Management) (SESAR, 2017). In that case, a conflicted user can perform ownship optimisation separating from a prediction of other traffic future states. Again, a real-time collaborative decision making process might be required, in this case to determine which aircraft has the responsibility to keep the required separation from other traffic, for instance.

Non-cooperative

The third case assumes there is (almost) no direct form of information sharing between aircraft. In this case, only **historical position data** (as coming from either ADS-B, if available, or from other surveillance means) can be used on the ownship to predict potential intruder future states (Bezawada *et al.*, 2011). The resulting prediction uncertainty, however, adds complexity (and inefficiency) to the deconflicting problem. A real-time collaborative decision making process is, in this case, hindered by the lack of information sharing from the intruder. Assuming that the intruder might suffer from technical problems (e.g, unavailability of the on-board transceiver) or is otherwise unable or unwilling to cooperate, the conflict resolution is tackled from the ownship. This could be regarded as a degraded *Semi-cooperative* case, where **intents are unknown**.

Depending on the information sharing level, the mentioned real-time collaborative decision making process can be tackled from two different perspectives. On the one hand, aircraft could be required to meet strategically externally imposed constraints (e.g., in form of time or speed advisories) throughout the flight path that would resolve the conflict (**4D control**). On the other hand, it could be effectively decided that the deviation responsibility is established upon one aircraft (the ownship), who should deviate from the other traffic in the problem (intruder(s)) **self-managed 4D control**. This decision of responsibility might be done *ad-hoc*, depending on aircraft parameters (e.g., weight or speed) or network effects (impact to future potential conflicts) or, alternatively, through pre-established convention (pre-agreed between airports, routes, right-of-way, etc).

I.4 Overall strategy of this PhD thesis

The research performed within this doctoral thesis contributes to the research efforts and initiatives, in line with what have been described above. Specifically, a trajectory optimisation methodology is presented which, phase by phase (chapter by chapter), builds from a pure mathematical resolution of an isolated trajectory optimisation problem where the objective is to minimise the

fuel burned, and adding constraints all the way to a fully-cooperative scenario where traffic is optimally separated one another whilst efficiency is the overal goal.

The specific phases to cover this operational applications spectrum that divide the work in this thesis are the following:

Phase 1: Trajectory optimisation

First, we present an optimisation framework that computes efficient trajectories given a set of constraints and a quantifiable objective. The presented framework resolves an optimal control problem formulation where a configurable scenario drives the search for the optimal solution. The lateral and vertical route in the scenario is defined by a flight-plan (described as a set of fixes and legs), which can conform to current procedural standards (such as SID, STAR and IAP) implementing most common path-terminators (ICAO, 2006), or conform to future concepts such as user-preferred routing or waypoint navigation to allow for greater flexibility in the generation of efficient trajectories. Furthermore, the scenario provides other configuration parameters regarding the operational constraints and the nature of the study (optimisation objective, weather features, existence of wind, conflict resolution with other traffic, etc.).

Phase 2: Surveillance control vs. 4D control

In Phase 2 we assume that deconfliction between aircraft is provided through required time of arrival (RTAs) at specific navigation fixes. It is assumed that a ground based algorithm would provide these RTA, in order to ensure that if all actors meet these, all aircraft respect the minimum required separation between them. Assuming this separation mechanism is in place, and using the trajectory optimisation framework described in Phase 1, Phase 2 quantifies the impact in terms of fuel and time consumption of implementing this methodology in a dense TMA.

In this phase, we show how requiring an aircraft to arrive at a waypoint earlier or later (when compared to the individual optimal trajectory) leads to increased fuel burn. In addition, the efficiency of such methods to resolve air traffic conflicts is studied in terms of both fuel burn and resulting aircraft separation. Finally, various scenarios are studied reflecting various airline preferences with regards to cost and fuel burn, as well as different route and conflict geometries for a broader scope of study.

Phase 3: Self-managed 4D control under semi-cooperative conditions

Phase 3, goes one step further and, instead of meeting pre-calculated RTA that resolve the conflict, an aircraft (the ownship, pre-established by strategic decision) is given full freedom to resolve the conflict as desired. We present a conflict-free optimal trajectory resolution methodology on a semi-cooperative scenario, where the only information that is shared among airspace users is the current position (and velocity) and the flight intents.

With this, after making quite uninformed assumptions on sensitive parameters such as the aircraft mass or the cost-index strategy, the ownship predicts the future state of a potential intruder aircraft and calculates its own optimal trajectory that deviates from it (all calculated through the framework described in Phase 1). Furthermore, a conformance monitoring strategy is presented that keeps track of the deviations from the prediction in real-time, leading to a safer and more robust conflict detection and resolution.

Phase 4: Enhancing predictability in self-managed 4D control

The methodology described in Phase 3 is very effective in the detection of inconsistencies between predicted and real trajectories. However, at each new prediction the same parameter biases are encountered and therefore new deviations appear again quickly. Phase 4 builds on top of Phase 3 in an effort to increase predictability, not only by monitoring the adherence

to a prediction, but also by learning from the past in a way to increase the knowledge of the estimated aircraft parameters for more accurate new predictions.

To improve the ownship's knowledge of other aircraft dynamics we propose to continuously integrate the state of the surounding traffic. Specifically, conventional position (and velocity) messages, as coming from ADS-B, are integrated at the ownship. Then, using the optimisation framework described in Phase 1 (which indeed contains biased mathematical models and assumptions), we minimise the error with the known states (position and velocity reports), having the parameters of study (in this case, the mass of the aircraft) as decision variables. We demonstrate the big improvements in predictability and safety that this methodology provides, reaching very low prediction errors with only a few seconds/minutes of past known states.

Phase 5: Self-managed 4D control under fully-cooperative conditions
Finally, Phase 5 presents a very utopic scenario assuming a fully cooperative situation where global trajectory optimisation is possible due to downlink of aircraft performance data and intents. Even if nowadays airlines are very wary on providing such information to other airspace users, and thus such scenario is far from reality, it provides a comparative global optimal reference to other results in this PhD.

I.5 Scope and limitations of this PhD thesis

In order to accomplish the objectives of this PhD thesis, according to the strategy that has been presented in the previous section, the research is subject to serveral assumptions and limitations that define its scope:

- The work in this thesis is mainly focussed on aircraft departures from take-off to an initial cruise level. All provided results are based on this phase of the flight, even if the presented algorithms and methods could be extrapolated to all other phases.
- The trajectory optimisation, prediction and parameter estimation methods presented in this thesis depend on a mathematical formulation of the aircraft dynamics, the flight envelope and the scenario environment. The aircraft performance model that is implemented throghout this thesis work represents an Airbus A320, one of the most commonly used narrow-body aircraft in commercial aviation. Nevertheless, the flexibility of the described framework would seamlessly integrate other types of aircraft.
- In chapter IV, two aircraft are modelled in one single optimisation problem: the ownship and the intruder. During the simulations, both aircraft are mathematically modelled through the same equations and parameters (except for the take-off mass). Furthermore, it is assumed that the ownship predictions of the intruder future states use this exact same model. Even if this stands as a simplification (it is unrealistic to assume that the ownship knows that well the performance parameters of the intruder; again, except for the mass), this chapter proposes an ideal situation where the functioning of methodology is demonstrated.
- This ideal assumption is broken in chapter V where other aircraft predictions are no longer *ideal*. Indeed, even if the *real* trajectory (of both aircraft) is synthesized with a high-fidelity performance model, the predictions of other aircraft (i.e., when the ownship predicts the intruder future states) are computed with a more generic and publicly available performance model. The described methodology is demonstrated to be agnostic to the accuracy or veracity of the prediction model.

- The described framework for trajectory optimisation describes the optimal path that an aircraft should follow with a given set of configurable parameters, conditions and constraints. When not otherwise specifically mentioned, the results of this trajectory optimisation (i.e., the optimal path) is assumed as the *real* path that is flown by the aircraft. In other words, the own computation of a trajectory is assumed as a *truth*, rather than an estimation. When this is not so (e.g., intruder prediction), it is specifically mentioned and the $\hat{}$ mathematical notation is used.

- During the simulations of chapters IV and V, the computational time of generating a new trajectory is neglected. Indeed, every time a deviation is detected and a new computation is triggered, the simulation clock is automatically paused to isolate the results from the uncertainty derived from arbitrarily different times of computation.

- Some of the presented results in this thesis rely on ADS-B position reports and intents. Even if the concept of ADS-B has been utilised, we have not fully implemented the DO-260B standards (RTCA SC-186, 2009) in our simulations.

- In different chapters of this thesis, it is assumed that an undisclosed authority (e.g., the network manager, the ATCo, existing regulations, or even self-managed collaborative decision making) delivers instructions or responsibilities to the aircraft in the scenario. These come in form of RTA or as a decision of who should perform a conflict resolution action (described as *ownship* vs. *intruder* in the different sections of the dissertation). Even if future work sould tackle this decision making step, the work in this thesis presents algorithms and methods to resolve the conflict once this is established, and provides also some tools to ease the decision making process. Furthermore, chapter VI fully removes this dependency.

- Due to the non-linearities of the models used in this thesis, the optimal control problem tackled in this thesis is non-convex, and therefore it can be affected by local minima. Nevertheless, even if a global optimum cannot be formally guaranteed, a lot of effort has been put to mitigate falling in local minima and to ensure that the results are indeed relevant and represent an appealing objective for a potential airspace user. Please note that the concept *global optimal* is still used in some cases in the document to refer to the optimisation of **all** aircraft in the problem as opposed to only **one** (i.e., the ownship).

- Contingencies, such as downgraded guidance, navigation or ADS-B capabilities, engine failure, etc. are not considered in the experiments. In other words, normal operations are assumed in all the experiments.

I.6 Outline of this PhD thesis

The material in this dissertation is organised in six remaining chapters which are summarised as follows:

- **Chapter** II contains the models and methods that have been developed or adapted for this work. In particular, the model describing the dynamics of the aircraft is given along with the definition of constraints, as well as the optimisation problem and the methodology for solving it. This relates to **Phase 1** as described above.

- **Chapter** III shows the results of the quantification of the impact in terms of fuel and time consumption of implementing suboptimal trajectories in a dense TMA driven by RTAs at specific navigation fixes to mitigate the capacity loss of continuous climb operations. This relates to **Phase 2** as described above.

- **Chapter IV** presents a conflict-free optimal trajectory resolution methodology using the optimisation framework described in chapter II in a semi-cooperative scenario, where only current situation (position and velocity) and a conceptual description of what is to happen (flight plan or fligh intents) is shared amongst users. This relates to **Phase 3** as described above.
- **Chapter V** describes a methodology to enhance aircraft trajectory predictability in a semi-cooperative scenario by learning from the past in a way to increase the knowledge of the estimated aircraft parameters for more accurate new predictions. This relates to **Phase 4** as described above.
- **Chapter VI** presents a fully cooperative scenario where global trajectory optimisation is possible due to downlink of aircraft performance data and intents. This relates to **Phase 5** as described above.
- **Chapter VII** gives the conclusions that are drawn from this work and points out some future work that could be done in the direction of the presented research.

II

DYNAMO: a dynamic optimiser

There are multiple approaches to the computation of a trajectory that complies with a set of constraints.

On the one hand, **trajectory prediction** methods provide a straightforward approach to synthesise the four dimensional path that the aircraft will follow through the airspace (Musialek *et al.*, 2010). With a mathematical definition of the aircraft's dynamics (i.e., in form of differential algebraic equations of motion), a very simple trajectory predictor will iteratively *command* the aircraft over (infinitessimal) time steps. In other words, the numerical integration of the aircraft dynamics results in a simple, fast and accurate method to predict the aircraft's trajectory. In this process, *commanding* the aircraft requires making assumptions over the actions that the pilot (or FMS) will take to follow the flight intents. These usually result in establishing a value (or a policy) for the thrust (or throttle setting), the vertical speed (or flight path angle, or angle of attack) and the rate of turn (or bank angle), at miminum. The more complex are the constraints of the problem, the more difficult will be to define these commands, usually leading to complex iterative (and costly) processes to continuously adjust them in order to meet the trajectory prediction methods become inefficient and deliver slow and non-optimal results.

On the other hand, **trajectory optimisation** techniques allow the definition of a cost functional that is minimised while complying with all the problem constraints. This can be approached by means of sampling-based path planning algorithms such as Dijkstra, A^*, RRT^*, etc. (Yang *et al.*, 2014) or stochastic optimisation methods such as genetic algorithms and other evolutionary algorithms (Yan & Cai, 2017). However, such algorithms present a difficult trade-off between an accurate dynamics model and the computational burden of generating the solution space (samples), which can only rely on an heuristic for an informed growth. Another mathematical approach is to formulate a continuous and constrained **optimal control** problem. The fundamentals of an optimal control problem are to find the control law (the *commands*) that drives a constrained system

(defined by the equations of motion and the problem contraints) towards an objective (defined by an optimality criterion function). In other words, this will find the *commands* that guide the aircraft through its planned trajectory (and imposed constraints) all whilst minimising a cost functional (e.g., fuel, time, etc.).

In the literature, there are a few examples that use optimal control for trajectory optimisation in ATM. For instance, (Prats *et al.*, 2011) optimise departing trajectories to reduce noise in the vicinities of an airport. Also, (Soler *et al.*, 2014b) define a mixed-integer optimal control problem for flight planning optimisation purposes. (Visser & Hartjes, 2014) describe a methodology for optimal flight paths between city-pairs minimising environmental footprint and airline cost criteria. Finally, (Prats *et al.*, 2015) present results on continuous descent trajectories in high density traffic with RTAs. Each of these has a similar methodology, but key aspects differ on the application of some mathematical assumptions (some use fixed altitudes, some have no lateral freedom, etc.), and the application scenario, with a different concept of operation (free-routing vs. standard procedures, ATCo restrictions, etc.).

This thesis takes a similar approach to the described literature, building a **flexible trajectory optimisation framework** based on optimal control theory. The following reasons have determined this decision:

Problem complexity The complexity of the described problem almost removes all other options, not only given the complexity of the system dynamics (described by realistic propulsion, aerodynamic and atmospheric mathematical models), but also the amount of constraints in the problem (a route, ATC advisories, airspace restrictions, meteorological conditions, separation assurance, etc.).

Generic framework This thesis proposes the use of an optimisation framework to resolve problems of very different nature: prediction, optimisation and estimation. Furthermore, it is used for the computation of baselines and comparative cases (e.g., conventional ATC advisories or different cooperation levels between airspace users), each requiring different flight phases and constraints. The use of optimal control theory has contributed to successfully achieving this generic approach.

Execution time Finally, even if not a main objective in this thesis, we have explored the possibility of a (near-) real time computation of the results. In our preliminary assessment, the chosen approach offered the best trade-off between the accuracy of the results, the probability of finding local minima and the computational time.

This chapter describes this framework, in relation to the referenced literature, and highlights our contributions beyond the state of the art.

II.1 Aircraft model

As already stated before, the generation of an optimal trajectory creates a 4 dimensional representation of the expected future states of an aircraft. To accurately predict the behaviour of a specific type of aircraft, we rely on mathematical models of the different actuators. In the literature we can find a very wide range of solutions, from very simple and less accurate, to very complex and closer to reality. Depending on the nature of the problem to solve, the solution may require more or less accurate models, faster or slower computational times, etc.

This section is divided into the different aspects that conform a mathematical aircraft model.

II.1.1 Aircraft dynamics

The following list describes three options to mathematically model the movement of an aircraft, from very simple and less accurate, to very complex and closer to reality (and therefore more computational greedy when implemented in an optimisation problem).

Basic kinematic model In these models, only position and time rate of changes are modelled. The model is integrated forward with respect to time, acceleration, velocity, etc.

Point-mass model (3DOF) This dynamic model is deemed realistic enough in most of the papers in the literature, both for trajectory prediction and trajectory optimisation for ATM or on-board guidance applications. Currently, the point-mass model is used in most flight management systems (FMS) available today in commercial aircraft for the internal calculations and predictions. It models the four actuating forces of an aircraft as affecting the centre of gravity (CoG), without taking into account the angular force momenta that lead to roll, pitch and yaw (see figure II-1). This is hence a three degrees of freedom (3DOF) model, which whilst keeping very accurate results, lessen the computational burden that a complete 6DOF model represents.

Many of the studies that implement a point-mass model constraint the space to two dimensions in order to further simplify the complexity of the model. This simplification is very common when studying long-haul flights, where high accuracy lateral movements are deemed negligible (or are resolved independently in a previous step) and for constant-altitude studies (Hartjes *et al.*, 2011; Soler *et al.*, 2011). Whilst these constraint the lateral or vertical movement, there are workarounds that bring full 3D results whilst having only a 2D model in the resolution. On another perspective, this 2D simplification is used in specific phases of the flight where the lateral or vertical movements are restricted to standard procedures (e.g., initial climb or final approach phases) (Wu & Zhao, 2009).

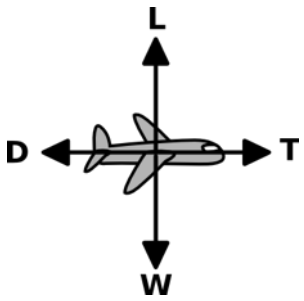

Figure II-1: *The four actuating forces of an aircraft as affecting the centre of gravity in a Point Mass Model.*

Full kinematic model (6DOF) In the literature there are very few examples of full kinematic models applied to aircraft trajectory prediction and optimisation. These pose a very complex set of equations that render the real-time computation of results almost impossible. This is a 6DOF model, which means that all linear and rotational forces and momenta are taken into account when simulating the aircraft states. In civil aviation trajectory optimisation, such models pose a big challenge in computational resolution and their contribution in accuracy (when compared to the 3DOF) is not proved to be extraordinary in this application. In other applications, such as the one described in (Bittner *et al.*, 2012), this high fidelity dynamic model proves very relevant for accurate results.

For the objectives set in this PhD thesis, a 3D point-mass model has been implemented, as a compromise between computational complexity, sufficient accuracy, and the three dimensional space required for the resolution of aircraft conflicts (plus the time).

II.1.1.1 Aircraft controls and states

The election of control variables is a complex task that can highly affect the results, and the computational complexity and time to reach them. Even if the control variables are usually conceptually similar, in each problem, choosing one mathematical representation or another may vary a lot.

As an example, the concept of **thrust** as the control that gives the acceleration of the plane will usually be in the control vector. However, this can be implemented using the thrust itself (Raghunathan *et al.*, 2004), the forward acceleration or horizontal load factor (Mohan *et al.*, 2012), the throttle or relative thrust setting (Houacine & Khardi, 2010), etc. In all cases, the concept is the same, but the differential algebraic equations that model the variation of the state and control variables will differ. Hence, different mathematical resolutions will perform differently in each case.

A similar issue appears with the **lift** force, which can be modelled in the controls using the load factor (n_z, defined as the relation between the aerodynamic lift force and the aircraft weight) (Mohan *et al.*, 2012), the lift coefficient (Bakolas *et al.*, 2011), the angle of attack (Patel & Goulart, 2011) or directly the lift force (Raghunathan *et al.*, 2004) or the flight path angle (Clarke & Park, 2012) if vertical equilibrium is assumed.

Similarly, the **turns**, if modelled, can be implemented as the rate of change of the heading angle (Hartjes *et al.*, 2011) or the aerodynamic bank angle (Prats, 2010).

The controls, identified by the control vector $\vec{u}$, are modelled in this thesis with ϕ as the bank angle, n_z as the load factor and π as the engine throttle setting.

$$\vec{u} = [\ n_z\ \ \phi\ \ \pi\ ] \tag{II.1}$$

The formulation of the state of the problem largely depends on the choices made for the dynamic model as described in the previuos subsections. The states of the problem, identified by the state vector $\vec{x}$, is modelled in this thesis by the spatial location of the aircraft in north (n) and east (e) coordinates, the geometric altitude (h), the true airspeed (v), the aerodynamic flight path angle (γ), the heading (χ) and the mass of the aircraft (m):

$$\vec{x} = [\ v\ \ \gamma\ \ \chi\ \ e\ \ n\ \ h\ \ m\ ] \tag{II.2}$$

II.1.1.2 Equations of motion

Using a point-mass model (3DOF) as explained before, and the controls and states of the problem that have just been presented, the equations of motion are written as follows:

$$\begin{aligned}
\frac{\mathrm{d}v}{\mathrm{d}t} &= \dot{v} &&= \frac{1}{m}(T - D - mg\sin\gamma) \\
\frac{\mathrm{d}\gamma}{\mathrm{d}t} &= \dot{\gamma} &&= \frac{g}{v}(n_z\cos\phi - \cos\gamma) \\
\frac{\mathrm{d}\chi}{\mathrm{d}t} &= \dot{\chi} &&= \frac{g}{v}\frac{\sin\phi}{\cos\gamma}n_z \\
\frac{\mathrm{d}e}{\mathrm{d}t} &= \dot{e} &&= v\cos\gamma\sin\chi + W_e \\
\frac{\mathrm{d}n}{\mathrm{d}t} &= \dot{n} &&= v\cos\gamma\cos\chi + W_n \\
\frac{\mathrm{d}h}{\mathrm{d}t} &= \dot{h} &&= v\sin\gamma \\
\frac{\mathrm{d}m}{\mathrm{d}t} &= \dot{m} &&= -FF
\end{aligned} \tag{II.3}$$

where T is the aircraft thrust, D is the aerodynamic drag, W_n and W_e are the north and east wind components respectively and g is the gravity acceleration. These equations of motion neglect the vertical wind ($W_h = 0$) and the wind shear ($\dot{W} = 0$).

All aerodynamic and engine parameters are represented by continuous polynomials, that ensure continuity for the first and second derivatives as it is required for the numerical resolution of the optimisation problem (explained later in this chapter, section II.2). Aerodynamic Drag (D) forces are modelled considering air compressibility effects, which cannot be neglected for nominal cruising speeds of typical commercial aircraft (between M.78 and M.82 approximately). Tabulated aircraft aerodynamic data has been obtained from Airbus PEP software suite, which provided us with accurate (and certified) values for aerodynamic Drag and engine performance for different flight conditions (further explained below).

II.1.2 Atmosphere and wind

The atmosphere can be modelled using the International Standard Atmsphere (ISA) model, which defines the temperature τ, pressure p and density ρ as functions of geometric altitude:

$$\begin{aligned} \tau(t) &= \tau_o + K_t h(t) \\ p(t) &= p_o \frac{\tau(t)}{\tau_o}^{\frac{-g}{K_t R}} \\ \rho(t) &= \rho_o \frac{\tau(t)}{\tau_o}^{\frac{-g}{K_t R}-1} \end{aligned} \tag{II.4}$$

where R is the universal gas constant and K_t is the standard temperature lapse rate. The magnitudes of origin τ_o, p_o and ρ_o (as would be measured at standard sea level) can be set to calibrate the magnitudes to the conditions of a specific day. For most applications, the ISA model provides enough accuracy, and it is very convenient due to its simplicity.

The following normalised magnitudes are also used:

$$\delta = \frac{p}{p_0}; \quad \theta = \frac{\tau}{\tau_0}; \quad \sigma = \frac{\rho}{\rho_0}; \tag{II.5}$$

Alternatively, if more precision is desired, or a very specific atmosphere condition is needed, the support for GRIB[1] files has been implemented as well. GRIB is an open, international, data format standard that is widely used in the meteorology community to store and share historical and forecast weather data. Its multi-dimensional gridded format, allows for the accumulation of all kinds of weather information in a single file for a specific date (including a validity period) and geographical location (a cube, where sample data is evenly distributed horizontally and vertically). Figure II-2 depicts part of a GRIB file generated by the National Oceanic and Atmospheric Administration (NOAA) with weather information (in this case, magintude and direction of the wind).

The enhanced accuracy of this gridded data, however, requires more complex mathematical approximations. In this thesis work, splines have been used to implement the curve and surface interpolation that provides values (and derivatives) of ρ, p and τ in the continuous space throughout the flight as functions of the altitude and geographic location (and date, since there is usually one GRIB file available for every pre-established time interval (e.g., every fifteen minutes or every three hours)):

[1] General Regularly-distributed Information in Binary form: common format for storing and sharing weather data.

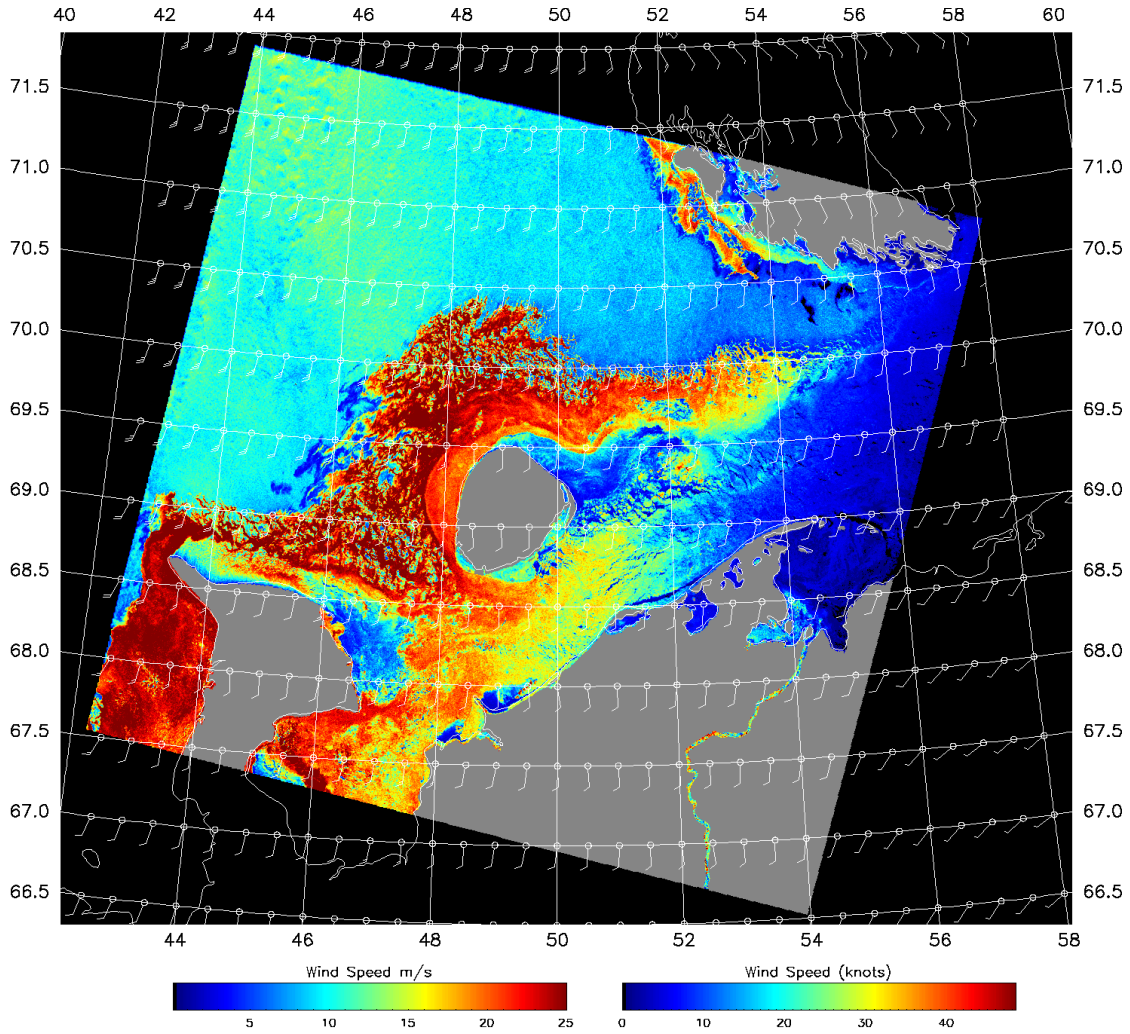

Figure II-2: *Depiction of a GRIB file with the wind information at north western Russia. Source NOAA.*

$$\begin{aligned} \tau(t) &= \Gamma_\tau(e(t), n(t), h(t)) \\ p(t) &= \Gamma_p(e(t), n(t), h(t)) \\ \rho(t) &= \Gamma_\rho(e(t), n(t), h(t)) \end{aligned} \tag{II.6}$$

where $\Gamma_{(\cdot)}$ is the continouous twice differentiable piecewise polynomial interpolation of the gridded data (spline).

Thanks to this technique, not only the atmosphere is modelled more accurately, but also the wind, the arbitrariness of which is well adhered to with the splines. The east (W_e) and north (W_n) wind components are formulated in this thesis as function of the altitude and geographic location (and, again, date):

$$\begin{aligned} W_e(t) &= \Gamma_{W_e}(e(t), n(t), h(t)) \\ W_n(t) &= \Gamma_{W_n}(e(t), n(t), h(t)) \end{aligned} \tag{II.7}$$

An example of a spline interpolation surface is depicted in figure II-3 with the wind magnitude at sea level, as extracted from a GRIB file. To enable depiction (maximum of three-

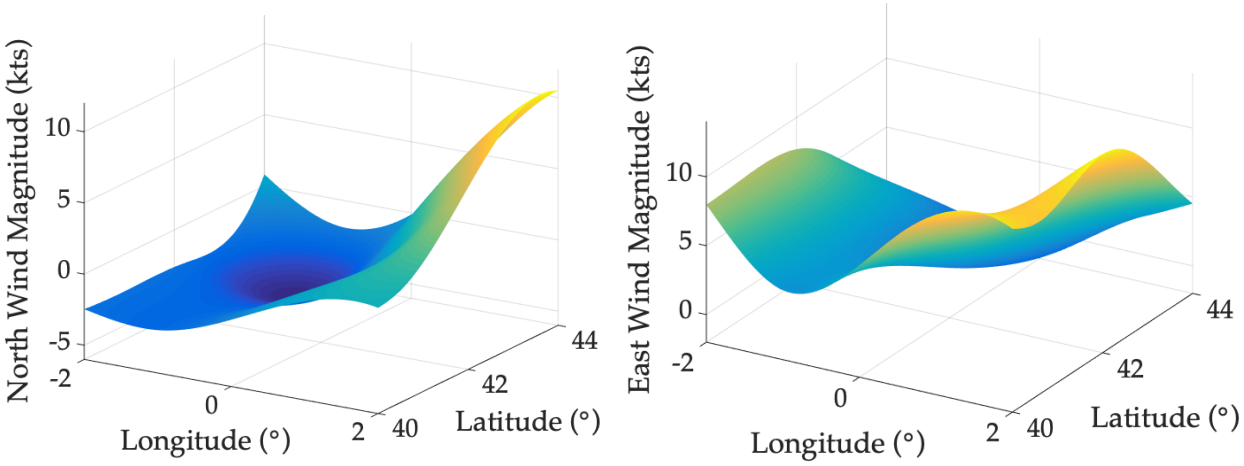

Figure II-3: *Depiction of a spline interpolation of the wind magnitude with respect to latitude and longitude at sea level.*

dimensional space), only the slice at sea level is shown. However, the 4D splines used in this thesis can output values at any altitude inside the measurement range (from sea level to FL400). This enables the computation of the absolute wind magnitude and direction at any geographical location and altitude during the flight.

II.1.3 Aircraft performance model

Modelling the engine thrust and the aerodynamic drag is usually between one of the most complex and unfortunately most inaccurate aspects of trajectory prediction and optimisation. Also, and directly related to its complexity, performance parameters are usually not very disclosed. In this thesis, two main performance models have been implemented:

BADA Eurocontrol's Base of Aircraft Data (Eurocontrol, 2011) has a very simplified set of equations and data files to calculate the fuel flow on a big amount of aircraft types and different phases during the flight. BADA provides the equations and the relevant coefficients for a big collection of aircraft to model the drag, thrust and fuel flow. In this thesis, BADA family 3 has been implemented. The formulation of the mathematical model can be found in the user manual for BADA (Eurocontrol, 2011), and therefore its details are not included here.

Airbus PEP Directly coming from the aircraft manufacturer, the Performance Engineer's Programs suite provides a huge amount of tabular data that can be used to model thrust, drag and fuel flow coefficients for any Airbus model in any aerodynamic and engine configuration (Prats, 2010). The implementation of a mathematical model from the tabular data is not straightforward and requires fitting techniques. These, create continuous variables that are worked out from the tabular coefficients and give the specific thrust and drag for the different values of the true airspeed (TAS) or Mach (M), altitude and aerodynamic settings. In this thesis, a highly parameterised polynomial fitting has been implemented, the formulation of which is described in the following subsections.

II.1.3.1 Engine thrust

In the nominal aircraft, the throttle directly commands the revolutions of the engine fan ($N1$). The maximum revolutions of the engine fan $N1_{max}$ and the residual revolutions, when the throttle is zero ($N1_{idle}$) are modelled with a third degree polynomial approximation as:

$$N1_k = \sum_{i=0}^{3}\sum_{j=0}^{3} c_{ij}^{k}\theta^i M^j \quad k \in \{max, idle\}\,. \tag{II.8}$$

Following the same methodology, thrust T and fuel flow FF are also modelled by a third order polynomial as a function of the reduced revolutions of the engine fan ($N1/\sqrt{\theta}$) and M:

$$\begin{aligned} T &= n_e\delta\sum_{i=0}^{3}\sum_{j=0}^{3} c_{ij}^{T}\left(\frac{N1}{\sqrt{\theta}}\right)^i M^j \\ FF &= n_e\delta\sqrt{\theta}\sum_{i=0}^{3}\sum_{j=0}^{3} c_{ij}^{FF}\left(\frac{N1}{\sqrt{\theta}}\right)^i M^j \end{aligned} \tag{II.9}$$

being n_e the number of engines of the airplane.

II.1.3.2 Aerodynamic drag

The aerodynamic drag is modelled as:

$$D(t) = \frac{1}{2}\rho(t)Sv^2(t)C_D(t) \tag{II.10}$$

where C_D is the drag coefficient and S the wing area.

The drag coefficient is expressed as a function of the lift coefficient C_L, v and M. This relationship considers air compressibility effects, which cannot be neglected for nominal cruising speeds of typical commercial aircraft (between M.78 and M.82 approximately). In this paper, a polynomial fitting similar to the model proposed in (Kaiser *et al.*, 2011) is used, giving a very accurate approximation of the drag coefficient:

$$C_D(t) = C_{D0}(t) + K(t)(C_L(t) - C_{L0}(t))^2 \tag{II.11}$$

C_L is expressed as:

$$C_L(t) = \frac{2n_z(t)m(t)g}{\rho(t)Sv^2(t)} \tag{II.12}$$

Coefficients C_{D0}, K and C_{L0} depend on the flaps/slats setting and M. For each aircraft configuration these coefficients are obtained after a fitting function process with aircraft aerodynamic data obtained from PEP's database. A generic notation $(\cdot)$ of the piecewise equation for C_{D0}, K and C_{L0} is defined as follows:

$$(\cdot)(t) = (\cdot)(v(t)) = \begin{cases} (\cdot)_\varphi & \text{if} \quad v(t) \leqslant v_{\varphi\to\varphi-1} \\ (\cdot)_{\varphi-1} & \text{if} \quad v_{\varphi\to\varphi-1} < v(t) \leqslant v_{\varphi-1\to\varphi-2} \\ \vdots & \\ (\cdot)_1 & \text{if} \quad v_{2\to1} < v(t) \leqslant v_{1\to0} \\ (\cdot)_0 & \text{if} \quad v(t) > v_{1\to0} \end{cases} \tag{II.13}$$

where $(\cdot)_i$ is the aerodynamic coefficient corresponding to flap/slat configuration i, $v_{i\to j}$ is the operational speed where the transition from configuration i to j is performed and φ is the total amount of flap/slats different configurations.

For clean configuration (corresponding to $(\cdot)_0$ in eq. (II.13)), C_{D0}, K and C_{L0} consider air compressibility effects as already stated, modelled as:

$$\begin{aligned} C_{D0_0} &= a_0 + \Delta a_1 M \\ K_0 &= b_0 + \Delta b_1 M + \Delta b_2 M^2 \\ C_{L0_0} &= c_0 + \Delta c_1 M + \Delta c_2 M^2 \end{aligned} \tag{II.14}$$

where a, b, and c are coefficients for the second degree polinomial curve fitting.

II.2 Trajectory optimisation problem

As described in the introductory paragraphs of this chapter, we propose to solve the trajectory optimisation problem using optimal control theory techniques.

Although there are some methods to solve an optimal control problem analytically, see for instance (Franco *et al.*, 2010; Franco & Rivas, 2014) and the references therein, these depend on big mathematical simplifications such as singular arc approximation, as well as very limited operational applications (constant altitude and speed, etc.). For the same reasons stated before, these simplifications are unacceptable in the problem we are solving in this PhD thesis.

Numerical methods propose an effective resolution of the optimal control problem, specially as more and more computational power becomes available. Notably the following two options have been widely explored:

- **Indirect methods**, involving the calculus of variations and the Maximum Principle of Pontryagin, and
- **Direct methods**, which transform the continuous (and thus infinite) original optimal control problem into a (discrete and finite) nonlinear programming optimisation (NLP) problem.

The first type of methods try to find the necessary conditions for optimality (Bryson & Ho, 1975). These conditions result in a two-point (or, in the case of a complex problem, a multi-point) boundary-value problem which is often extremely difficult to solve, like in our case.

Given the limitations of the indirect methods, the approach more widely applied nowadays is the direct method, which converts the infinite-dimensional original problem (the continuous functions that describe the dynamics of an aircraft) into a finite-dimensional optimisation by applying three fundamental steps (Betts, 2010):

(a) Convert the dynamic system into a problem with a finite set of variables (also called transcription method or collocation); then

(b) solve the finite-dimensional problem using a parameter optimisation method, (i.e., solving an NLP problem); and finally

(c) assess the accuracy of the finite-dimensional approximation and if necessary repeat the transcription and optimisation steps.

The following subsections describe this constrained multiple-phase optimal control problem and its resolution using direct collocation methods in more detail.

II.2.1 Problem formulation

A trajectory optimisation problem can be divided into one or more consecutive phases. Let $\vec{x}^{(i)}(t) \in \mathbb{R}^{n_{x^{(i)}}}$ be the state vector describing the trajectory of the aircraft at phase $i \in \{1, ..., N\}$ over time $t \in \mathbb{R}$ in the time period $[t_0^{(i)}, t_f^{(i)}] \subset \mathbb{R}$ and $\vec{u}^{(i)}(t) \in \mathbb{R}^{n_{u^{(i)}}}$ the control vector that leads to a specific trajectory in that particular phase. The goal of an optimal control problem is to find the best control vector functions for each phase that minimise a given cost functional $J : \mathbb{R}^{n_{x^{(1)}}} \times \mathbb{R}^{n_{u^{(1)}}} \times \cdots \times \mathbb{R}^{n_{x^{(N)}}} \times \mathbb{R}^{n_{u^{(N)}}} \to \mathbb{R}$, defined over the whole time period $[t_0^{(1)}, t_f^{(N)}] \subset \mathbb{R}$:

$$J\left(\vec{x}^{(1)}(t), \vec{u}^{(1)}(t), \vec{x}^{(2)}(t), \vec{u}^{(2)}(t), \ldots, \vec{x}^{(N)}(t), \vec{u}^{(N)}(t)\right). \tag{II.15}$$

The objective function J defines the problem functional that will be minimised by the algorithm. Notice that the cost functional may depend on quantities computed in each of the N phases. Moreover, the value of $t_f^{(i)}$ is a decision variable itself and will be fixed by the optimisation algorithm.

We have formulated an optimal control problem, the solution to which minimises the objective defined in eq. (II.15). The state and control vectors for each phase i are defined as a subset of $\vec{x}$ as described in eq. (II.2) and $\vec{u}$ as described in eq. (II.1), respectively. This generic formulation would eventually allow for each phase of the problem to take a different state and control vector, depending on the specific requirements of the phase. However, in reality, we have used the full vectors in all phases in the different problems throughout this PhD thesis due to the very similar nature of the phases, as explained further down in this chapter.

In order to guarantee a feasible and acceptable trajectory, as a result of this optimisation process, several constraints must be considered. In particular, the dynamics of the system (dynamics of the state vector), expressed by the non-linear differential equations (II.3), are established by non-linear vector functions $\vec{f}^{(i)} : \mathbb{R}^{n_{x^{(i)}}} \times \mathbb{R}^{n_{u^{(i)}}} \to \mathbb{R}^{n_{x^{(i)}}}$ as:

$$\frac{\mathrm{d}\vec{x}^{(i)}}{\mathrm{d}t} = \dot{\vec{x}}^{(i)}(t) = \vec{f}^{(i)}\left(\vec{x}^{(i)}(t), \vec{u}^{(i)}(t)\right). \tag{II.16}$$

In addition, the solution might satisfy some algebraic event constraints $\vec{e}^{(i)} : \mathbb{R}^{n_{x^{(i)}}} \times \mathbb{R}^{n_{u^{(i)}}} \times \mathbb{R}^{n_{x^{(i)}}} \times \mathbb{R}^{n_{u^{(i)}}} \to \mathbb{R}^{n_{e^{(i)}}}$ (i.e. initial and final conditions at the different phases), expressed in the general form with vector functions:

$$\vec{e}_L^{(i)} \leqslant \vec{e}^{(i)}\left(\vec{x}^{(i)}(t_0^{(i)}), \vec{x}^{(i)}(t_f^{(i)}), \vec{u}^{(i)}(t_0^{(i)}), \vec{u}^{(i)}(t_f^{(i)})\right) \leqslant \vec{e}_U^{(i)}. \tag{II.17}$$

some algebraic path constraints $\vec{h}^{(i)} : \mathbb{R}^{n_{x^{(i)}}} \times \mathbb{R}^{n_{u^{(i)}}} \to \mathbb{R}^{n_{h^{(i)}}}$ such as

$$\vec{h}_L^{(i)} \leqslant \vec{h}^{(i)}\left(\vec{x}^{(i)}(t), \vec{u}^{(i)}(t)\right) \leqslant \vec{h}_U^{(i)}. \tag{II.18}$$

and simple bounds on the state, control and time variables (box constraints):

$$\begin{aligned} \vec{x}_L^{(i)}(t) \leqslant \vec{x}^{(i)}(t) \leqslant \vec{x}_U^{(i)}(t), \qquad & t_{0_L}^{(i)} \leqslant t_0^{(i)} \leqslant t_{0_U}^{(i)}, \\ \vec{u}_L^{(i)}(t) \leqslant \vec{u}^{(i)}(t) \leqslant \vec{u}_U^{(i)}(t), \qquad & t_{f_L}^{(i)} \leqslant t_f^{(i)} \leqslant t_{f_U}^{(i)}. \end{aligned} \tag{II.19}$$

In the previous notation, $(\cdot)_L \in \mathbb{R}^{n_{(\cdot)}}$ and $(\cdot)_U \in \mathbb{R}^{n_{(\cdot)}}$ are respectively the lower and upper bounds for these constraints. It should be noted that equality constraints can be defined by setting the lower bound equal to the upper bound, i.e. $(\cdot)_L = (\cdot)_U$.

Table II-1: *Constraints in the optimal control problem*

Constraint	Definition
Operating airspeeds	$V_{MCA} \leq v_{CAS}(t) \leq V_{MO}$ $M(t) \leq M_{MO}$
No deceleration allowed	$\dot{v}_{CAS}(t) \geq 0$
No descent allowed	$\dot{h}(t) \geq 0$
Minimum climb gradient	$h(t) \geq 0.033s(t)$
Load factor	$0.85 \leq n_z(t) \leq 1.15$
Bank angle	$-25\,^\circ \leq \phi(t) \leq 25\,^\circ$

Even if apparent in the mathematical notation, it is worth emphasising that equations (II.16) to (II.19) are defined for each phase $i \in \{1, ..., N\}$. Therefore, for those problems that span over more than one phase, this set of equations would be repeated N times, and the compilation of **all** the equations for **all** phases would be the full mathematical definition of the problem constraints. In other words, this allows the dynamics of the system, the event, path and box constraints to be different in each phase.

To ensure that the consecutive phases are correctly linked one another in compliance with the dynamic models, and that they relate to the time continuum they represent, the following constraint applies to the state vector:

$$\vec{x}^{(i+1)}(t^+) - \vec{x}^{(i+1)}(t^-) = 0;\ i = 0, \dots N-2 \tag{II.20}$$

II.2.2 Operational constraints

The dynamic constraints of the problem, defined by eq. (II.16), are particularised with the dynamic model as described in eq. (II.3). Besides the equations of motion, the problem is further constrained by additional equations that take into account several operational restrictions.

Table II-1 depicts the constraints considered in the optimisation problem throughout the thesis work. Many of these are operational constraints, either to stay within the flight envelope (for instance, V_{MCA} for the minimum aircraft control speed in the air and V_{MO} for the maximum aircraft operating speed) or comply with ATM constraints such as CAS profiles and ground obstacle avoidance. Others, are imposed to deliver realistic results in some of the experiments: disallowing deceleration and descent throughout the climb phase and imposing a minimum climb gradient to guide the optimiser to operationally feasible results (and prevent numerically optimal results such as too long on-ground acceleration phase, zero-energy final state or wiggly vertical profiles, to name a few). Additionally, bounding constraints on n_z and ϕ are defined following civil aviation standards mainly related to passenger confort (Jacobson & Rudrapatna, 1974).

Since the operating speeds are always expressed in calibrated airspeed (v_{CAS}) or mach (M) the following equations have been implemented to relate these to the true airspeed (v):

$$\begin{aligned} v_{CAS} &= \sqrt{\frac{2p_0}{\mu\rho_0}\left[\left(\delta\left(\left(\frac{\mu v^2}{2R\tau}+1\right)^{\frac{1}{\mu}}-1\right)+1\right)^{\mu}-1\right]} \\ M &= v/\sqrt{\gamma_a R\tau} \end{aligned} \tag{II.21}$$

where $\mu = \frac{\gamma_a - 1}{\gamma_a}$, γ_a is the specific heat ratio of the air and R the perfect gas constant.

The along path distance (s) is used in the minimum climb gradient, and is modelled as:

$$\frac{\mathrm{d}s}{\mathrm{d}t} = \dot{s} = \sqrt{\dot{e}^2 + \dot{n}^2} \tag{II.22}$$

Furthermore, other operational constraints are defined by velocity, lateral, vertical and time constraints required by the specific air traffic management procedures in place. This would be the case for velocity restrictions at some flight legs, altitude restrictions at certain airspace volumes, as well as the flight route (as defined in the flight plan or the instrumental standard procedure). Therefore, different phases of the problem enable and disable different constraints as required, as further explained in the following subsection.

II.2.3 Multiphase modelling

Aircraft trajectories can be divided into multiple flight phases, each with different **performance configuration and operational contraints**. For example, during the initial climb phase of a departure, an aircraft will be at maximum take-off thrust climbing without the possibility of turning or making changes to the aerodynamic configuration up to 400ft (ICAO, 2006). Actually, many studies in the literature do not contemplate this phase, given the low degrees of freedom that pose these operational constraints. The subsequent phases, following this initial climb phase, are defined by the different and sequential aerodynamic changes (flaps/slats retraction). These aerodynamic configuration changes are typically executed at predefined speed steps and result in different aircraft performance parameters in each phase, modelled by different equations and coefficients in the matematical model.

Besides, the departing aircraft follows an **ATM route defined by a set of vertical, lateral, speed and time constraints** described in the published instrument flight procedure (e.g., a SID), which are specified at specific legs or waypoints in the procedure. Additionally, such constraints may also be issued by an ATCo at a tactical level, along with one or several RTAs in a 4D trajectory scenario (TBO).

Recapitulating, the two paragraphs above describe two *disconnected* types of phases:

- those related to **performance** of the aircraft (e.g., changes in flaps, gear, etc.)
- those related to **ATM procedures** (waypoints, speed/altitude constraints, RTA, etc.).

In other words, the order of which the **performance** events occur is independent (*disconnected*) to the order of which **ATM** events occur. For example, a geographical fix on the procedure could come before or after the moment the aircraft transitions from one aerodynamic configuration to the following one. Even for the same aircraft type, depending on the weather conditions and the mass of the aircraft the order of these events will differ and it is impossible to know beforehand. Therefore, the multiphase formulation in section II.2.1 cannot be used simultaneously for the two types of disconnected phases. Due to the nature of optimal control problems, the unordered use of phases becomes a challenge not easily solved.

A possible solution to tackle this challenge is to reformulate the optimisation problem into a mixed-integer non-linear programming problem and use integer decision variables to find the optimal sequence of ATM and operational phases. A fine example of this approach for aircraft trajectory optimisation is given by (Bonami *et al.*, 2013). This method, however, increases the numerical complexity of the problem and might negatively impact the computational time to obtain a solution.

Another solution is to use continuous and twice-differentiable switching functions to model certain phase changes. This method has the negative side-effect that it adds non-linearities to the model (greater computational times and possible convergence difficulties), and the minor drawback of having a transition effect around the switching value. Both issues are directly related, since a less steep function at the switching point (and thus smoother for the NLP Solver) results in a bigger transition effect, and vice versa. Hence, a trade-off must be sought (Hartjes *et al.*, 2010).

In this thesis, we have used these switching functions to take into consideration the changes in aerodynamic configurations. The following equation reformulates piecewise eq. (II.13) in a single continuous equation that models the aerodynamic coefficients throghouth the whole flight, taking into account all changes in flaps/slats settings:

$$(\cdot)(t) = (\cdot)(v(t)) = \sum_{i=1}^{\varphi} (\cdot) i \Upsilon_i \tag{II.23}$$

The switching function itself is described in this thesis with the notation Υ and is defined as follows:

$$\Upsilon_i = \left[\frac{1}{2} + \frac{1}{\pi}\arctan(k_{i-1\to i}(v(t) - v_{i-1\to i}))\right] - \left[\frac{1}{2} + \frac{1}{\pi}\arctan(k_{i\to i+1}(v(t) - v_{i\to i+1}))\right] \tag{II.24}$$

where $v_{i\to j}$ is the operational speed where the transitioning from configuration i to j is performed and $k_{i\to j}$ determines the steepness of the transition

With this, in our work the ordered list of fixes defining the lateral and vertical route (**ATM procedures**) define the different optimal control phases as described in the problem formulation in section II.2.1. Each phase contains a flight leg, from one specific origin to one specific objective. Independently to these phases, the changes in aircraft **performance** configuration happen at the desired time thanks to the switching functions. This enables us to optimise a full trajectory from a set of initial conditions to a set of final conditions, through a set of 4D constrains (e.g, fixes along the route with RTAs) and undergoing through the different aircraft configuration (gear-up, flaps retraction, etc.) using a constrained multi-phase optimal control problem.

II.3 Optimisation framework

The optimisation framework described in this chapter integrates different modules. The software tool has been mainly developed in C++ and General Algebraic Modelling System (GAMS[2]). The core part of the optimiser is written in GAMS, given the facility and robustness it provides to implement optimal control problems and the multiple NLP solver engines to which it seamlessly links. All other software modules are written in C++, including a wrapper to the core functionality. Thus, we can dynamically define and load scenarios (described by a Flight Plan and many other problem parameters), prepare them for the optimisation and gather the results once done.

The flexibility of the described framework allows for an easy implementation of different flight profiles, from completely unconstrained continuous operations, to defined standard procedures such as Noise Abatement Departure Procedures (NADP), standard instrument departures and arrivals (SID, STAR), etc. as well as any ATC constraint. Furthermore, the flexibility of the C++ approach opens the core optimisation framework to real-time applications, including continuous real-time monitoring and multi-agent interactive simulations. This section describes in more detail the definition of scenarios and the implementation choices.

[2] http://www.gams.com

II.3.1 Definition of scenarios

A scenario characterises the problem that needs to be solved. There are multiple types of information, which are relevant to the problem defintion, as follows:

General optimisation options

These include the following:

- settings intrinsic to the **formulation and execution of the optimal control problem** and the NLP solver such as the collocation method (euler or trapezoidal), number of collocation points per phase, choice of NLP solver, maximum time for convergence, etc.
- **scenario settings** such as meteorological conditions, altimeter barometric reference (QNH), weather model (ISA vs. GRIB), wind, etc.
- **aircraft settings** such as aerodynamic configuration, type of aircraft, cost index, dynamic model (BADA vs. PEP), etc.
- **problem type** such as individual optimisation, cooperative intruder, parameter estimation, etc.

Trajectory choices

The route describes the desired flight trajectory of an aircraft regarding both the lateral and vertical profiles as well as other constraints along the flight. This is described as a list of parameterisable waypoints. Each waypoint is caracterised by the following parameters: id, latitude, longitude, altitude, speed, RTA, heading and type.

Almost all parameters can be left blank, which means that a vast typology of flight legs can be defined, mimicking the path-terminators defined in ICAO documentation (ICAO, 2006). One example of this would be a course to an altitude path terminator, which would be described by a heading and a final altitude, and leaving latitude and longitude unspecified. Another example would be a direct to a fix, which would specify a latitude and longitude, ignoring altitude and heading.

Additionally, time and speed restrictions or advisories as published in the aeronautical information publications (strategic) or provided from ATCo (tactic) can be specified in the RTA and speed fields.

Types of waypoints caracterise other aspects of the leg to the waypoint such as, for example, freedom or restriction to perform turns, acceleration/deceleration legs, etc.

The generic definition of each waypoint in a route plus the caracterisation of the optimisation problem and scenario configuration provides high flexibility in the definition of the problem statement, which results in a vast number of optimisation problems that can be solved with this framework. The different chapters in this thesis describe different typologies of problems which are effectively resolved using the said flexibility.

II.3.2 Software design

The framework is formed by two main functional blocks: the optimisation core (named DYNAMO for DYNAMic Optimiser), and the execution functionality layers (named SIMULATOR). Figure II-4 depicts the different modules of the system.

The following paragraphs describe each of these two functional blocks in detail. Then, next section describes how these modules work together for the resolution of complex optimisation problems.

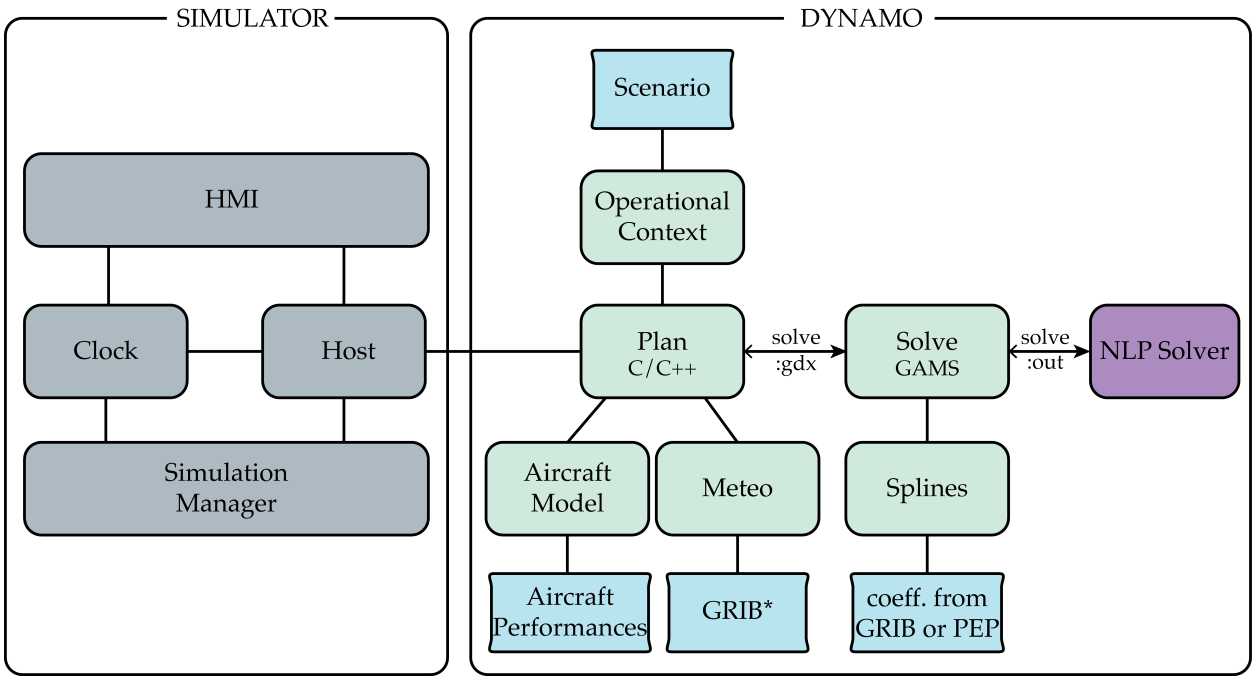

Figure II-4: *Architecture of the optimisation framework. (*) GRIB files are only used if selected in the scenario. Otherwise, ISA is assumed.*

DYNAMO The optimisation core of the framework. It consists of the following modules:

Plan Principal interface of the optimisation core with the exterior. From an incoming scenario (which is defined by the scenario file plus the aircraft performance coefficients and the meteorological condition datasets), prepares all structures to be ready for optimisation and provides the results, when available.

Solve From the structures prepared by the *Plan* module, interfaces the NLP solver, providing the required information when requested (Jacobians, Hessians, etc.).

NLP Solver Solves a non-linear programming problem, using the structures that come from the *Solve* module. Examples of solvers that have been evaluated are IPOPT and CONOPT.

Splines Models virtually any kind of curve and surface using splines. The module can be used to generate a spline from a dataset and to poll values from an existing spline. This module uses the open source library *einspline*[3], based on basis splines (B-splines). As explained in the different chapters, in this thesis the splines are used to model aircraft performance, wind, atmosphere and aircraft trajectories.

Meteo Contains the dataset that is used to generate the meterological conditions (wind, temperature and pressure). The data is fetched by the module *Plan*, which then uses the *Splines* module to generate the curves that are later used in the optimisation process.

Aircraft Model The dataset that models the aircraft performance. This includes tables and coefficients that model, for an aircraft type and configuration, the aerodynamic drag and the thrust force.

[3] http://einspline.sourceforge.net/

Operational Context The constraints that model the desired trajectory, including including the parameters that have been selected in the scenario file described in section II.3.1.

SIMULATOR A set of tools that, using the optimisation core (DYNAMO), create the wrapping elements to form the virtualisation environment that enable the resolution of diverse complete optimisation problems (including real-time requirements, batch study sensitivity analyses and multi-agent problems). It consists of the following modules:

Host This is the main executable of the whole optimisation framework. It stands as a simplification of an aircraft flight management system in the way that it can trigger the calculation of a trajectory given a flight plan, it can define specific constraints for a waypoint (which then trigger a new calculation of the trajectory), and it can even guide an ownship aircraft to follow the planned trajectory. Notice that this module does not simulate the aircraft dynamics: at every clock tick, it merely retreives the updated position from the already calculated trajectory and publishes it to the simulation ecosystem.

Clock Keeps a time tick (either real-time or fast-forward/slow-forward) which is then used from the other modules in the SIMULATOR to advance all aircraft (all *Host* concurrent instances) in a simulated environment through their routes. The *Clock* module is paramount for the virtualisation of multi-agent real-time (or virtual-time) problems.

Simulation Manager Plays, pauses, speeds-up, slows-down and jumps-forward/backward the simulated clock at the *Clock* module.

HMI Shows in a 3D synthetic environment all aircraft in the simulation. It also displays other releveant information about the simulation such as distance between aircraft, among other assets. This module is only used for the real-time (or virtual-time) monitoring of the execution of the simulation.

II.3.3 Functional Workflow

In the previous sections of this chapter, the framework has been described and all its elements identified. This final section of this chapter describes the flow of events that lead from a complex problem to its resolution, using the described tool. First, we describe the flow of events within DYNAMO to solve an isolated optimisation problem. Then, we describe how DYNAMO is used in collaboration with the SIMULATOR to resolve more complex problems.

II.3.3.1 Isolated optimisation

The atomic functionality of the optimisation framework is to solve an individual optimisation problem consisting of one single aircraft flying along a route, with a specified cost functional. The resolution of this problem consists of a single execution of the optimisation framework, covering the following steps, in the order they appear in the list:

- *Plan* module:

  Read scenario file Open and parse the scenario file to create the software data structures in memory, corresponding to the scenario definition. If everything is correct, the data

structures created in this step correspond to the whole scenario in C++ (an aircraft model, a weather model, an atmosphere model and the operational context). Alternatively, this module returns immediately if errors are found in the scenario file, such as missing parameters, wrong values or an inconsistent configuration is found.

Generate nominal trajectory Using the data structures created in the previous step, a forward integration algorithm is executed to generate an initial guess to the optimisation problem. This algorithm uses the differential algebraic equations as described in section II.1 plus a couple of assumptions regarding the control variables to generate a feasible trajectory, yet not the optimal one (plus, some constraints will still not be consistent with the scenario). This trajectory will be used to initialise all variables of the NLP solver to ease the search for the optimal solution.

Most of the times, however, during a complex problem resolution, the nominal trajectory will be issued from a previous trajectory optimisation. As an example of this is found during a sensitivity analysis, where only one parameter changes from one trajectory optimisation execution to another (e.g., the RTA). This results in a faster convergence to a feasible solution.

Prepare execution files The results of the previous step are written into GAMS Data eXchange protocol files (GDX). Additionally, some structures that will be needed in GAMS are already written in the GDX, such as initial conditions, initial collocation points, linking structures, etc. This allows for more flexibility in the definition of scenarios, and eases the GAMS code which ultimately provides better performance.

Launch GAMS Finally, launch a GAMS process instantiating the *Solve* module using the GAMS Application Programming Interface (API) and the C++ standard process calls. Then, this process will freeze until the GAMS process returns.

- *Solve* module:

Read problem definition The problem definition is read from the GDX file, written in the previous steps.

Initialise all GAMS structures Initialise all sets, tables, variables, and equations to the values specified in the GDX file.

Run optimisation Prepare and run the optimisation. Link to the NLP solver specified in the scenario definition. Internally, GAMS prepares the structures to run the NLP solver, which include such things as the number of variables, constraints, sparsity, number of nonzero elements in the 1st and 2nd derivatives matrices (Jacobian and Hessian), number of nonlinear variables, etc. Additionally, in the search for an optimal solution, the solver will call back GAMS functions to evaluate the evolution of the mathematical model at every optimisation step in form of the equations: the derivatives of all equations (Jacobian and Hessian), the objective and constraint functions, etc. GAMS already provides the said methods if the model is correctly defined (using conventional resolution of the equations and automatic differentiation to evaluate 1st and 2nd derivatives)(GAMS, 2019).

Alternatively, one can implement a callback mechanism to provide custom results for these methods. This provides the mechanism to implement virtually any kind of external evaluation function, more complex than conventional polynomials. In our case, this is specially useful as it allows us to model parts of the mathematical model in form of splines using the *Splines* module. As piecewise polynomials (and therefore cannot be formulated with a single equation), splines are not directly available using conventional GAMS formulation, but are however very convenient as these can approximate very accurately complex physical phenomena (weather, atmosphere, engine performance, aircraft trajectories, etc.).

Write results Once the optimisation has finished (either because an optimal point has been reached or because one cannot be found) the GAMS structures (sets) that define the state variables and controls contain the resulting values for each collocation step. These structures are saved into a GDX file using conventional GAMS calls and then the GAMS process finishes.

- *Plan* module:

Read results When GAMS process exits, the dormant C++ process wakes up and reads the GDX file with the results.

Work with results In a successful execution of the optimisation algorithm, the resulting structures contain the values for the state and control variables at each time step. This effectively means that a complete 4D trajectory is provided (latitude, longitude and altitude at each time), with all aircraft states at all time steps (i.e., velocity, mass, angles, thrust, aerodynamic configuration, etc.), among all other auxiliary parameters used during the optimisation (e.g., wind, engine states, aerodynamic forces, etc.).

These results are then contextualised to the specific problem that was being resolved and used accordingly, either to provide an individual optimisation result or to feed other parts of the optimisation problem.

As already stated, this isolated optimisation can be then part of a complex problem as has been introduced in chapter I through the different Phases of the thesis, and is further detailed in the following subsection.

II.3.3.2 Complex problem resolution

To solve the technical and operational challenges that are faced in this thesis, the optimisation framework is used, not in isolation, but as part of a more complex problem. This problem can be of a *static* nature or a *dynamic* nature:

Static A static problem is faced when an assessment of a specific situation has to be performed in the form of a sensitivity analysis. The generation of optimal trajectories is not dependent to real-time, changing, events. A set of trajectories is generated for a controlled environment (deterministic), where only one specific parameter changes at each optimisation, to assess the impact that this parameter has to a specific objective of the study.

Dynamic A dynamic problem, on the other hand, is one that requires the optimisation of one or more trajectories in real-time (or even fast/slow-forward) to be effectively evaluated:

flying optimal trajectories all whilst monitoring for unexpected events and resolving (in real-time) when these occur. The initial conditions of every execution are unknown beforehand, and depend on non-deterministic events (uncertainty), and are only learned as long as the problem (the flight(s), the environment, etc.) evolves.

For both static and dynamic problems, DYNAMO is used as the core functional block for the production of optimal trajectories when required. The SIMULATOR functional block appears only for dynamic problems, where there is a need of a clock and a real-time visualisation of the situation and the algorithms' performance. Even so, the *Host* module (situated in figure II-4 at the SIMULATOR's side) stands as the main entry point (the executable) for all types of problems.

Thus, the *Host* can represent one aircraft in a multi-agent problem (i.e., one per aircraft) or can represent the static point of entry of a sensitivity analysis. In this latter case, the logic is implemented in the *Host* to allow the execution of multiple trajectory optimisation processess in an automated environment (either iterative in a single executable or simultaneous in a multithreaded architecture, depending on the dependency to previous results during the calculation of subsequent executions). For sensitivity studies and wide range analyses this functionality is paramount for the generation of the required results in an efficient way.

A section named *Framework set-up* appears in all relevant chapters with further details on the exact implementation of this architecture to resolve the specific chapter's problem.

III

Operating cost sensitivity to required time of arrival commands

In the current concept of operations, standard navigation procedures (air routes) are in place in such a way that they minimise the number of potential airborne encounters (conflicts) at a strategic level. Yet, in busy terminal manoeuvring area (TMA) conflicts may still appear and it is very common that air traffic controllers (ATCo) act tactically by deviating aircraft from their nominal (optimal) path giving direct heading instructions (the so called *radar vectors*) and/or levelling-off individual aircraft to ensure horizontal and/or vertical separation between aircraft, thus removing any remaining conflict.

These open instructions usually prevent (or difficult) continuous operations such as continuous descent operations (CDO) and continuous climb operations (CCO) under heavy traffic, resulting in an increased operational cost, both in fuel burned and/or flight time.

One of the main proposals to allow optimal profiles in high traffic conditions is the concept of trajectory based operations (TBO), which relies on pre-established conflict-free efficient trajectories. Described within both SESAR and NextGen programmes, the most common and well-accepted implementation of this concept is based on time advisories throughout the trajectory in form of required time of arrival (RTA) at specific fixes along the route. Preliminarily, this looks like an advantageous concept when compared to the current paradigm, but, again, the strict time requirements will prevent the aircraft to fly their optimal profile.

With the objective of further assessing the use of time metering within TBO, this chapter tries to answer the following two main questions:

- **how bad** is the impact of RTAs to the operational cost of previously (individually-) optimal departures?

- **how good** is the sole use of RTAs for separation purposes?

Using the optimisation framework presented in chapter II we propose cost-optimal trajectories in a dense traffic area. Aiming at **continuous vertical profiles** while minimising the negative impact on airspace capacity, 4D optimal flight paths are computed with **strict time constraints** at fixes along the route. In this chapter, we fix the lateral path of aircraft along the strategically pre-established route (either due to the requirement fo follow a standard instrumental procedures, or due to a pre-agreed reference business trajectory under TBO). Then, when the ATCo acts tactically, issuing time advisories to resolve the remaining conflicts, the aircraft are consequently deviated from their optimal vertical and speed profiles (again, respecting the fixed pre-agreed lateral trajectory). Thus, for each new RTA, the optimisation framework provides **the best trajectory that complies with this time metering**, minimising the negative impact to the operational cost.

The objective is to assess the impact on the total cost of assigning RTAs along the fixed route, as well as evaluating their effectiveness in traffic separation. The operating cost is computed with respect to the airline's cost index strategy, in a sensitivity analysis regarding RTAs, cost index and distance to the conflict.

The following sections are organised as follows.

- Section III.1 lays out the particularities on the dynamic model of the aircraft and the problem formulation, including the flight phases and operational constraints applied to the generic approach described in chapter II.
- Section III.2 describes the scenario that has been implemented in the case study.
- Section III.3 describes the set-up of the simulations for the demonstration of the chapter's objectives.
- Section III.4 presents the results divided into three separate sections:
  - section III.4.1 presents a sensitivity study of fuel to the different RTAs and its success in conflict resolution;
  - section III.4.2 presents a sensitivity study of the total cost to the different RTAs and Cost Index values, with its impact to the conflict geometry; and
  - section III.4.3 presents a sensitivity study of the total cost to the different RTAs and the distance to the RTA fix.
- Finally, section III.5 presents the author's conclusions relative to this chapter.

III.1 Problem formulation

This section describes the additions to the formulation presented in chapter II to achieve this chapter's specific objectives. Specifically, the cost functional is presented (the objective of the optimisation) and a new constraint for a fixed lateral route that enforces the aircraft to strictly follow the prescribed instrumental procedure.

III.1.1 Optimisation objective

Our goal is to find the best trajectory that minimises the following cost functional:

$$J = \sum_{i=1}^{N} \int_{t_0^{(i)}}^{t_f^{(i)}} FF(\vec{x}^{(i)}, \vec{u}^{(i)}) + CI \mathrm{d}t. \tag{III.1}$$

The Cost Index (CI) scalar relates the cost of time (C_t) to the cost of fuel (C_f):

$$CI = \frac{C_t}{C_f} = \frac{[€/\text{min}]}{[€/\text{kg}]} = \left[\frac{\text{kg}}{\text{min}}\right] \tag{III.2}$$

This allows to not only optimise by the cost of fuel (and therefore be as fuel-efficient as possible) when $CI = 0$, but also to take into consideration the operating cost of time which is usually related to the staff stipends, maintenance issues, passenger satisfaction, etc., when $CI > 0$ (Airbus, 2002). Not surprisingly, see for example how, for an unvariable C_f, an increase of wages will make flying faster (and hence increasing the fuel consumption) a more interesting option with regards to minimising the total operating cost. Airlines take very seriously the decision of the CI value before each flight.

It is worth noting this value is usually scaled for the different FMS: each brand takes different input ranges. Example FMS input value ranges are [0-99] (Smiths FMS) and [0-999] (Sperry and Honeywell FMS) for Airbus fleet (Airbus, 1998) and [0-200], [0-500], [0-999] and [0-9999] for Boeing fleet (Roberson, 2007). In this thesis, we have assumed unscaled cost index values with the units [kg/min].

III.1.2 Modelling a fixed lateral route

The fixed lateral route is a new constraint in the problem we have formulated in chapter II. To implement this constraint, one could remove e and n from the state vector defined in (II.2) and leave only s as the along track distance aggregation and fix the values of χ as function of s. The control variable ϕ could also be removed in this case, as it is completely bound by the fixed χ (note that *fixed* does not mean constant). To keep DYNAMO as flexible as possible, we have opted for the option of keeping e and n as state variables, but constrain them as described in the following paragraphs (in this case both χ as a state variable and ϕ as a control variable are actually bound to the values that lead to the constrained e and n).

Because a trajectory can be a very complex curve, and due to the nature of the optimal control problem, we rely on polynomial fitting to model the constrain of the fixed lateral route (Gong & Sadovsky, 2010). To this end, we find the cost-optimal trajectory of each aircraft (as their baseline optimal reference, following the desired route, unconstrained to other traffic), which is then approximated with curves represented by basis splines (B-splines).

Specifically, the baseline reference curves of the trajectory, generated through the process described in the previous paragraph, are modelled with two splines that represent the ownship's east (Γ_e) and north (Γ_n) coordinates over the along path distance (s):

$$\begin{aligned} e(t) &= \Gamma_e(s(t)) \\ n(t) &= \Gamma_n(s(t)) \end{aligned} \tag{III.3}$$

Then, upon the fixed-route-, RTA-, constrained problem, the solver iteratively calls these curves that represent the geographical position, and the e and n variables in the state vector are constrained following these over s. More details about the baseline pre-process and the subsequent constrained optimisations are provided in section III.3, further down in this chapter.

Effectively, through many different simulations during the development of this thesis, this solution has proved very reliable and robust, showing good performance. Specifically, cubic B-splines have been used, which are continuous twice-differentiable functions represented by piecewise polynomials of order three. As opposed to higher degree polynomials, these provide an accurate fitting and have been demonstrated to perform well with NLP optimisation (Betts & Cramer, 1995) as they can be very smooth.

As a matter of fact, the root mean square (RMS) of the error between the resulting polynomial approximation and the original trajectory is negligible.

III.2 Case study

A typical conflict that is encountered within a TMA is usually due to the close proximity of two airports (like it happens for instance in the Bay Area around San Francisco airport or in the New York Area, and mostly all over Europe) or between departures and arrivals in the same airport. For the purpose of this chapter, we have prepared a scenario following close-to-real life operations in two major airports in the Catalonia region. The Airbus A320, a typical twin-engine narrow-body aircraft, has been simulated in all the cases explained below.

Aircraft departing Barcelona (LEBL) and Reus (LERS) airports have been considered and we have focused in two simultaneous departures from each airport creating an eventual conflict. In Reus, the current eastwards departure procedure BCN1S makes a long detour to strategically deconflict departing traffic with inbound and outbound traffic of Barcelona airport (see figure III-1). In SESAR and NextGen, with the concept of TBO, these long detours may be replaced by pre-cleared 4D trajectories. As an example, (Dahlberg *et al.*, 2018) proposes the flexibilisation of terminal routes and separating the traffic pre-tactically by time and space constraints at the merging points. In a similar manner, in this chapter we propose that the aircraft departing from Reus take a new, more fuel efficient, straight departure route as depicted in the same figure.

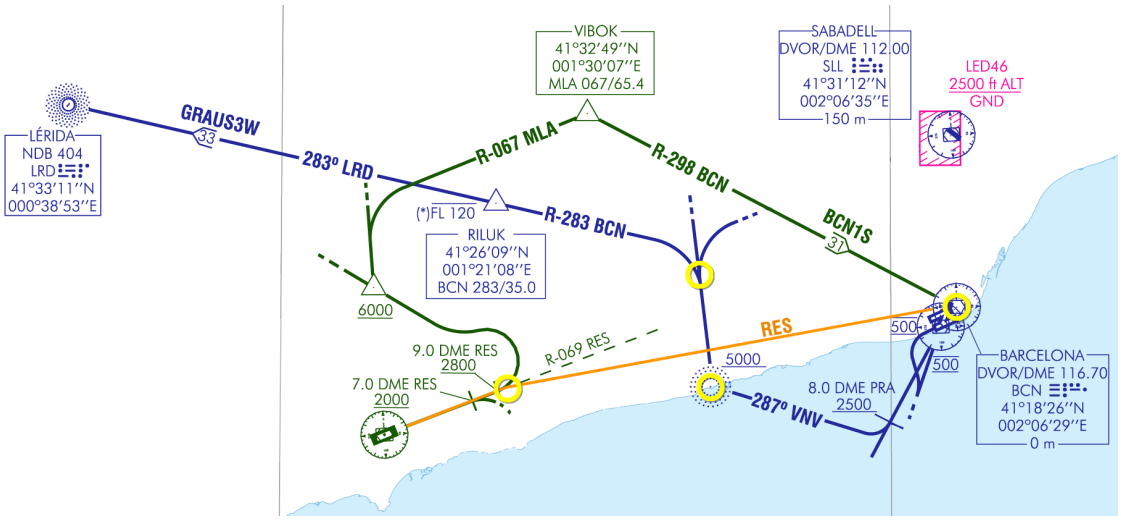

Figure III-1: *Published standard instrument departures for Barcelona (GRAUS3W, blue) and Reus (BCN1S, green) and proposed direct route (RES, orange).*

Let us call by RES the trajectory of an aircraft departing from Reus and following this new departure and by BCN, the trajectory of another aircraft that departs Barcelona to the west through the GRAUS3W standard departure procedure (SID). Figure III-1 shows the lateral routes as resulting from the optimiser, overlaid on the charts defined in the Spanish aeronautical information publications (AIP) (ENAIRE, 2012; ENAIRE, 2010).

This new direct route from Reus is more likely to create conflicts with traffic in Barcelona. A conflict is defined when the minimum required vertical and horizontal separation between two aircraft is violated. Current radar separation minima range from 3 NM to 5 NM in horizontal and 1000 ft to 2000 ft in vertical, depending on technical and environment related aspects (ICAO, 2001). In this thesis, the values of 3 NM and 1000 ft have been selected as these are usually used in TMA

around main airports.

Indeed, two aircraft departing at approximately the same time with a similar take-off mass enter in conflict soon after take-off. Therefore, some action is required to prevent the loss of separation. The following paragraphs describe potential actions broken into different cases. RES and BCN trajectories are simulated through all cases with the same ending condition at cruise altitude of FL320 and final speed of Mach 0.73.

Case A: Baseline
In this case a cost-optimal baseline scenario has been defined from the ground to cruise altitude without traffic related constraints. Effectively, these optimal trajectories cannot be flown due to a loss of separation with the other aircraft, but they lay out the resulting conflict geometry and this case is also used as the cost-optimal reference trajectory for comparison with all other cases.

Case B: RTA at a fix
Following 4D TBO concepts, the strategy to keep lateral separation between aircraft could be to assign an RTA requested time of arrival at a certain fix along each aircraft's route so they reach the conflicting area at an earlier or later time, thus preventing the conflict. The exact time deviation that is needed is unknown and will vary for every scenario under study. This is why, in order to fulfil the objective of this chapter, we have defined a set of feasible earlier and later RTAs, aiming at the quantification of the impact in fuel that such non-optimal time requests pose to the aircraft. These set of simulations have a fixed lateral route as described in section III.1.2. Therefore, requesting faster or slower trajectories will only have an impact on the vertical and speed profiles of the aircraft. The fix to which the RTA is requested depends on the geometry of the conflict and is explained below.

Case C: Level-off segment
Current ATC procedures tend to resolve this type of situation by issuing directives to at least one of the involved aircraft, typically resulting in a level-off flight segment. The duration of this segment depends on the TMA complexity and ATC practices. In this study a level segment of 18 NM has been simulated, which was found to be the average segment length in a study in New York and Paris TMAs (Thompson *et al.*, 2013).

With the optimisation framework described in chapter II, cases A to C are studied as follows. First, we find out at what latitude and longitude the trajectories enter in conflict along their fuel-optimal trajectories (case A). From this geographical location we then select the adequate fix in each aircraft's flight plan where the RTA will be requested (see yellow circles in figure III-1 for proposed fixes in the example). For earlier RTAs, the selected fix will be the one that comes after the geographical encounter (we want to clear as fast as possible the conflicting leg). For later RTAs it will be the one before (we want to arrive later at the conflicting leg).

We then iteratively assign earlier and later times to the corresponding fix, starting at the optimal time of overfly up to the earliest and latest feasible RTA respectively (case B). Initial and final conditions (including speed) are kept equal for all cases to enable fair comparison. Each new trajectory gives different fuel consumption, and modifies the conflict geometry, possibly completely removing it. Finally we compare it to current operations assuming a level-off segment (case C).

In an effort to adapt the optimiser to current climb operations, the CAS profile is restricted throughout the climb procedure as shown in table II-1. In short, CAS decelerations are not allowed. However, earlier RTAs will most probably need higher speeds to meet the RTA and will not be able to comply with the final speed constraint at the ending point. To make this possible, we introduce an optional deceleration phase (at constant $\dot{v}_{CAS}$) that only happens immediately after the RTA is met to allow the aircraft to slow down to the desired speed. This deceleration phase is only allowed in the calculation of trajectories having earlier RTAs.

III.3 Framework set-up

To demonstrate this chapter's objectives, a range of simulations have been performed using the optimisation framework described in chapter II. Given the fact that the outcomes of the study presented in this chapter are addressed on a static nature (i.e. a generic assessment, as opposed to an active actor on a real-time environment), the optimisation framework is used in isolation to generate individual trajectories. The relevant parameters of each individual trajectory are then stored for the comparison and presentation of the global results.

The functional workflow for the different simulations described in section III.4 is the following, taking the sofware design nomenclature that has been presented in chapter II:

Scenario file Using a scenario editor, prepare the scenario file with all parameters that represent the trajectory of study. The type of aircraft, the route, the cost index, constaints, and all other configuration items relevant to the current simulation are carefully specified (see section II.3.1). In the case study, one scenario file is needed for each case (A to C) and for each route (BCN and RES).

Baseline Compute the baseline optimal trajectory (Case A) for the scenario file using DYNAMO. This provides, not only the lowest cost trajectory, but also the fixed lateral route and the desired time of overfly of the fix(es) where an RTA can be issued. Besides, this trajectory is used as a nominal trajectory (guess) to the NLP to all subsequent executions to decrease the number of non-conformities at the problem initialisation for a faster and more efficient trajectory optimisation.

Fixed route The baseline trajectory is given to the *Splines* module to generate the set of static curves that model the fixed lateral routes, which will be used during all subsequent optimisation executions within the study.

RTA At this point, an iterative process starts to compute all relevant results for the trajectory of study. Each iteration step consists of the following:

- Modify the scenario parameters (increase/decrease the RTA at the specified fix, as described in section III.2)
- Run the optimisation process using DYNAMO
- Store the results

Level-off segment Compute the equivalent to current day operations through a level-off segment (Case C). This is used as a comparative result.

Results Prepare the results from the big automatically generated dataset and display them through tables and charts.

The process described above (except the manual definition of the base scenario files) is automated through the *Host* module, within the SIMULATOR functional block. This module is used as a main executable and configured to work autonomously all the way to achieving the study results, which are presented in the following section.

Furthermore, we study the sensitivity of the results to CI and to the distance to the RTA fix. Both studies need to run the whole workflow presented above multiple times, one for each value of study. To this end, we use the same approach: an automated process inside the *Host* module that iterates through all the values (e.g., $CI = 0\,\text{kg/min}$, $CI = 10\,\text{kg/min}$, etc.), running a complete RTA workflow for each one.

III.4 Numerical results

This section lays out the numerical results for the different cases (A to C) described in section III.2. First of all, we study the impact of RTAs applied individually to one trajectory, or in combination between two trajectories. At the end, two sensitivity studies are presented: one towards cost index and another one towards distance of encounter of the RTA fix.

III.4.1 Numerical results for $CI = 0\,\mathrm{kg/min}$

This section shows numerical results involving comparisons for all cases when $CI = 0\,\mathrm{kg/min}$ (i.e. only fuel is minimised). First, Case A trajectories are computed (as displayed in figure III-1), where the aircraft fly fuel-optimal trajectories for both departures regardless of the potential conflict at the crossing point. Then, the sensitivity study for Case B is studied individually (only one aircraft receives an RTA, section III.4.1.1) and in combination (both aircraft receive an RTA, section III.4.1.2), and is compared with case C.

III.4.1.1 Individual RTAs

The results for case B are summarised in figure III-2, showing the differences in fuel and time with respect to the baseline scenario (Case A) for different RTAs. It should be noted that $\Delta\mathrm{RTA} = 0\,\mathrm{s}$ means no time deviation from the original optimal trajectory (Case A). Furthermore, we have analysed two possible situations: BCN is the ownship and must change the trajectory according to the new RTA and vice-versa. In both cases, the intruder is always flying its corresponding optimal trajectory of Case A.

Given the different geometries in BCN and RES trajectories, the RTAs of study are not the same. Fore example, BCN has 33 NM of along track distance before reaching the fix where earlier RTAs are applied, whereas RES has a longer stretch: 43 NM. This explains why the magnitude of the earliest feasible ΔRTA for BCN is lower than for RES, which has a longer stretch to gain speed. For later ΔRTA things are inverted, with BCN having the possibility of reaching the fix where the later RTAs are applied at $\Delta\mathrm{RTA} = +204\,\mathrm{s}$ whereas RES can only go as far as $\Delta\mathrm{RTA} = +68\,\mathrm{s}$, mainly because the latter has a shorter leg to generate the delay (specifically, BCN has 23 NM and RES 9 NM).

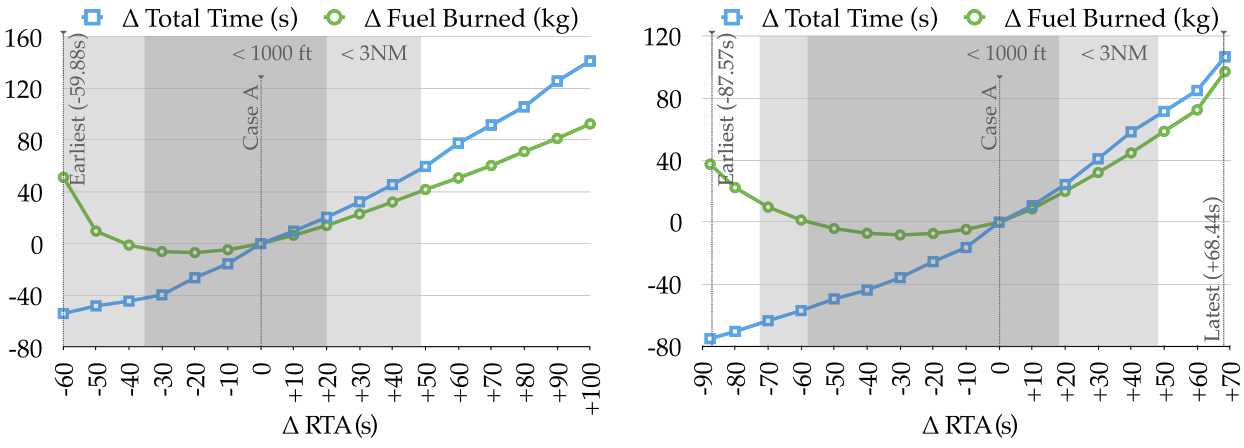

(a) Ownship: BCN, Intruder: RES.

(b) Ownship: RES, Intruder: BCN.

Figure III-2: *Increase in fuel burned and trajectory time evolution for different RTAs in case B.*

The expected conclusion is that in general earlier and later RTAs are less efficient than the optimal reference for both depicted trajectories. However, for some earlier ΔRTA this is not the

case. The reasons for that are found in the introduction of the deceleration phase after the metering fix, as described at the end of section III.2. Without this phase, calibrated airspeed (CAS) decelerations are not allowed, which indirectly restricts the vertical profile (for the same true airspeed (TAS), CAS decreases as the altitude increases). However, from the optimiser's perspective, it is more fuel-efficient to climb at a higher speed with a deceleration phase at the end (see figure III-3). For this reason, the optimiser reaches lower fuel consumptions than the *more restrictive* optimal reference. Other solutions would involve restrictions in TAS instead of CAS (less restrictive in the altitude profile), but this poses a big shift in air operations and has been deliberately kept out of the scope of this study. Still, acknowledging this aspect, the results in fuel are perfectly valid for the proposed sensitivity analysis.

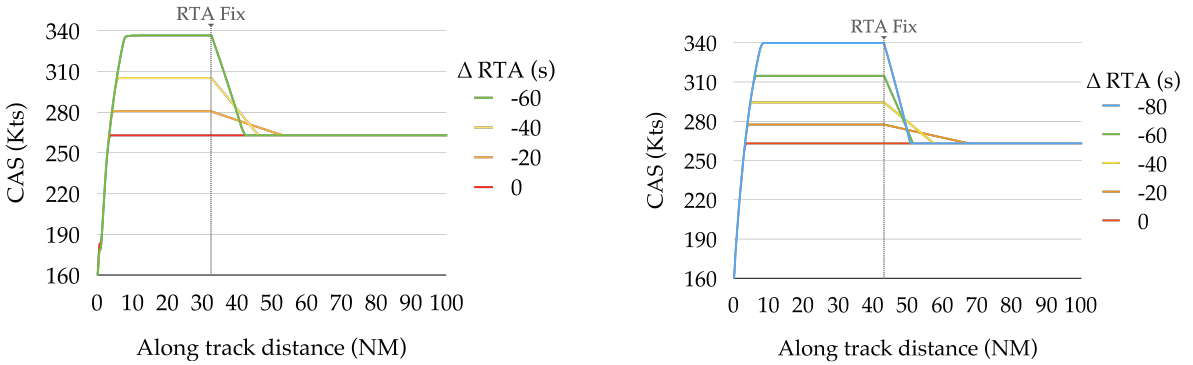

(a) Ownship: BCN

(b) Ownship: RES

Figure III-3: *CAS profile for some earlier RTAs in BCN and RES trajectories.*

As previously explained, the baseline case A does not keep the required horizontal and vertical separation of 3 NM and 1000 ft, respectively, between the involved aircraft. In figure III-2 we have presented a sensitivity study of the impact of different RTA to the fuel consumption. But how do these RTA perform at keeping the required separation between aircraft? Figure III-4 shows the observed minimum aircraft horizontal separation (S_h) for each RTA of study. Additionally, the observed minimum vertical separation when the horizontal separation is not granted (i.e. less than 3 NM) is defined as $S_v|_{S_h<3\,\mathrm{NM}}$.

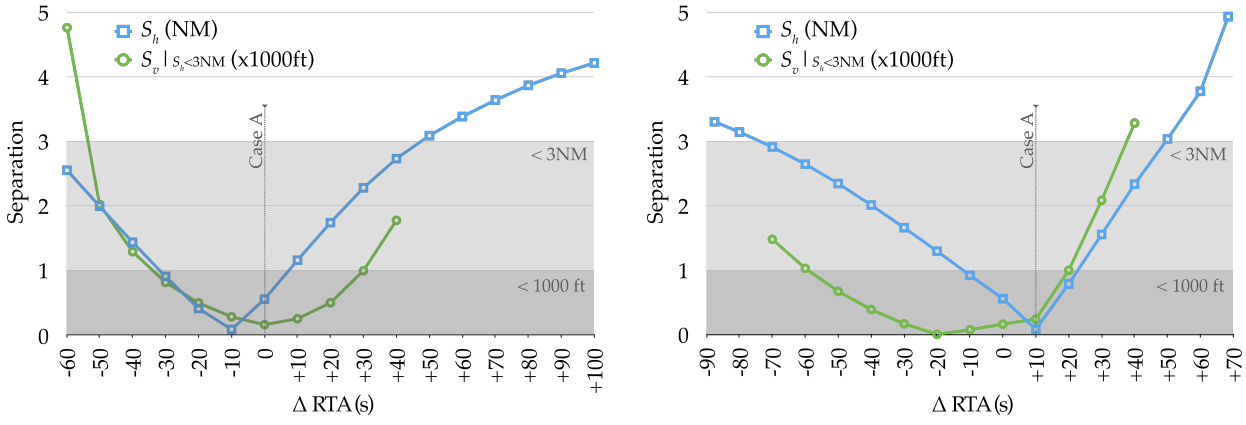

(a) Ownship: BCN, Intruder: RES.

(b) Ownship: RES, Intruder: BCN.

Figure III-4: *Minimum aircraft separation between ownship and intruder for different RTAs in case B with $CI = 0\,kg/min$.*

As an example, if BCN aircraft would reach the conflicting leg 50 seconds later than its fuel-optimal time, it would completely remove the conflict by keeping the required minimum hori-

zontal separation with RES throughout the flight. Contrasted with figure III-2, this represents a $41.9\,\text{kg}$ increase in fuel, reaching the final point $60\,\text{s}$ later. Similarly, RES could itself prevent the loss of horizontal separation by reaching the area $80\,\text{s}$ earlier, with a fuel increase of over $22.3\,\text{kg}$, gaining $70\,\text{s}$. However, from figure III-4, it is clearly visible that the vertical separation is always achieved before the horizontal. Effectively, the conflict could be removed with the use of RTAs (e.g. RES$+20$, RES-60, BCN$+30$ or BCN-40) with fuel increases ranging from $-1\,\text{kg}$ to $23\,\text{kg}$.

The small impact in fuel can be explained because both aircraft are climbing and a slight early vertical deviation will keep the $1000\,\text{ft}$ separation without further efforts. In comparison, a level-off phase imposed to one of the aircraft (case C) would represent $47.6\,\text{kg}$ more, with a total flight duration 68 seconds longer than the fuel-optimal path (RES) or $50\,\text{kg}$ and $73\,\text{s}$ (BCN). Some of these figures are summarised in table III-1.

Table III-1: *Summary of costs for some representative examples of cases A, B and C*

Case	Description	ΔFuel (kg)	ΔTime (s)	S_h	$S_v\|_{S_h<3\,\text{NM}}$
Case A	Optimal Reference	0.00	0.00	0.56	154
Case B.1	$\Delta\text{RTA}_{\text{BCN}} = +50\,\text{s}$	$+41.9$	$+60$	3.09	-
Case B.2	$\Delta\text{RTA}_{\text{RES}} = -80\,\text{s}$	$+22.3$	-70	3.14	-
Case B.3	$\Delta\text{RTA}_{\text{BCN}} = +30\,\text{s}$	$+23$	$+32$	2.28	1000
Case B.4	$\Delta\text{RTA}_{\text{RES}} = +20\,\text{s}$	$+19.8$	$+24$	0.79	1000
Case C.1	Level-off phase BCN	$+47.6$	$+68$	0.88	4028
Case C.2	Level-off phase RES	$+50$	$+73$	0.38	3830

III.4.1.2 Combined RTAs

Previous results are based on issuing time constraints to only one of the involved aircraft. The study to apply an RTA to both aircraft would most surely require smaller ΔRTAs, with a presumably lower increase in fuel overall. Effectively, this study is depicted in figure III-5, where different RTAs have been given to both trajectories and the minimum horizontal separation between aircraft is depicted. As for the previous results, this study calculates the fuel-optimal trajectories for both routes, which constitute the baseline $\Delta\text{RTA}_{\text{BCN}} = 0\,\text{s}$ and $\Delta\text{RTA}_{\text{RES}} = 0\,\text{s}$, and then recalculates the trajectories iteratively incrementing and decrementing the reference by $10\,\text{s}$.

Compared to the previous results, this figure shows, for example, how delaying the RTA to BCN by about 30 seconds, and at the same time advancing the same amount to RES, the required horizontal separation would be granted, only implying an overall increase in fuel of $14.7\,\text{kg}$, much less than the results showed above. Similarly, BCN $\Delta\text{RTA} = +20\,\text{s}$ and RES $\Delta\text{RTA} = -50\,\text{s}$ would result in $\Delta\text{Fuel} = 9.9\,\text{kg}$.

Other successful cases can be drawn from figure III-5. It presents, for the given situation and predicted trajectories, the best conflict resolution using RTAs for horizontal separation. However, these results raise the need for better predictability in aircraft operations (Bronsvoort, 2014), since the predictions are used to assign the RTAs for separation. In such situation, the RTA could also be designed for vertical separation, giving thus even more efficient conflict resolution results.

III.4.2 Sensitivity study to cost index

To this point, the results shown are based assuming the airlines are looking for the fuel-optimal trajectory (i.e. $CI = 0\,\text{kg/min}$). Currently, however, this is seldom the case, due to fluctuations

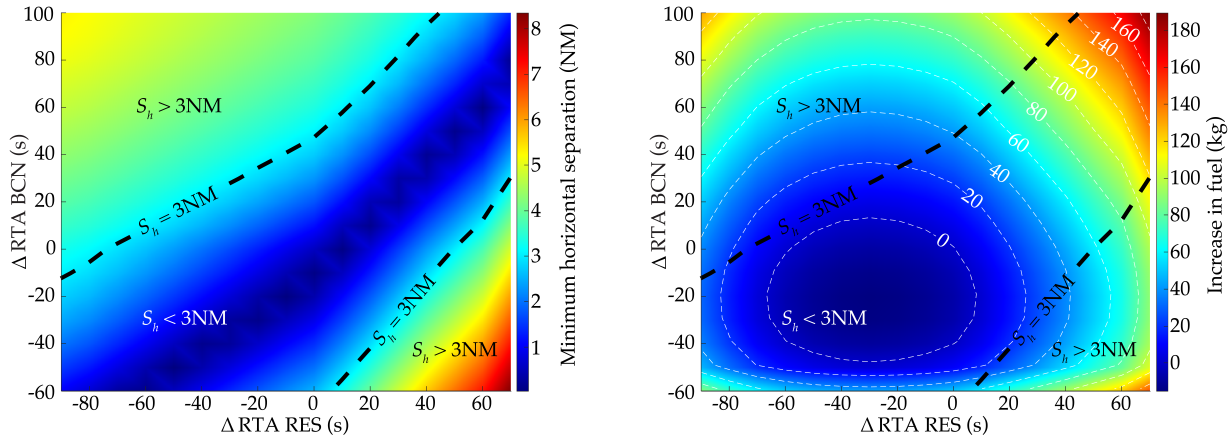

(a) Minimum horizontal separation (S_h). (b) Accumulated increase in fuel.

Figure III-5: *Effectiveness and impact in fuel of different RTAs for both trajectories in case B and $CI = 0\,kg/min$.*

in fuel cost and its relation to other airline costs (mainly related to staff), as well as constraints in time. In order to broaden the scope of the current work, this section extends the previous sections' results to account for multiple CI values.

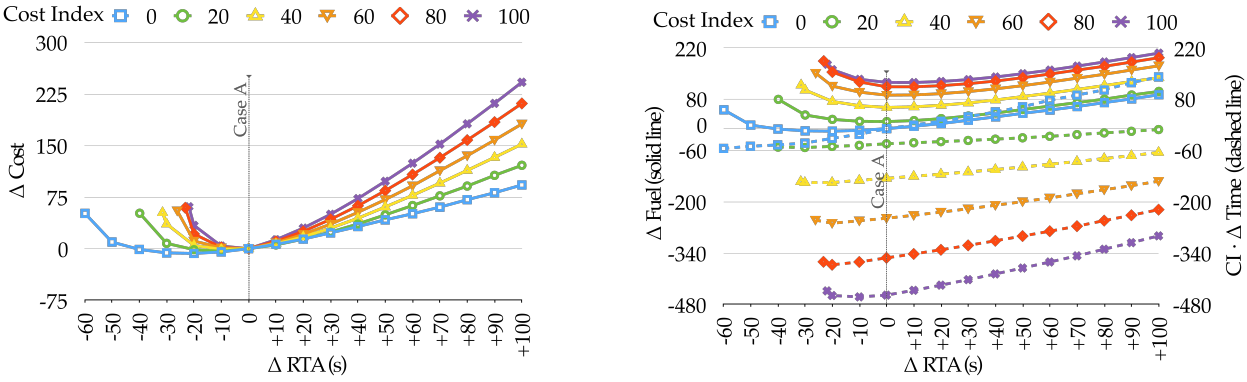

(a) Total Cost (b) Fuel and Time

Figure III-6: *Evolution of total cost, fuel and time for different CI and different RTAs in case B (Ownship: BCN).*

Figure III-6 repeats the results shown for case B with different example CI values ranging from $CI = 0\,$kg/min (fuel only) to $CI = 100\,$kg/min. For each CI value, a new baseline trajectory (case A) is generated. Then, the ΔRTAs in figure III-6 are with respect to each CI reference optimal.

Figure III-6(a) shows the cost evolution with respect to each CI reference optimal. Not surprisingly, figure III-6 shows how for bigger CI values, later RTAs become more and more costly. However, for earlier RTAs the situation is similar: for a same ΔRTA, for higher CI values, higher costs are seen. This means that even if the time dimension is more and more important in the cost function, the gains in time that faster trajectories render are hindered by the increase in fuel to achieve such trajectories. Besides, for higher CI values, the baseline case A is in itself faster when compared to lower CI. Hence, advancing the RTA demands, for higher CI, great amounts of added fuel, for not as big a time gain.

This can be better seen in figure III-6(b), where a breakdown of the cost function described by eq. (III.1) is presented. It shows the evolution of fuel (solid line) and $CI \cdot Time$ (dashed line) of

each new trajectory with respect to the fuel-optimal reference (Case A). It shows how, even if the dashed line (time dimension) decreases, the solid line (fuel dimension) increases as much, or even more, for many of the cases in earlier RTAs. It is also worth noting that for $CI = 80\,\text{kg/min}$ and $CI = 100\,\text{kg/min}$, the results are very similar. This is due to the fact that in both cases, trajectories are approaching maximum speed values. Furthermore, this demands very low vertical speeds, so that reaching the required cruise altitude for the available along path distance is much more difficult.

The different CI values also have an impact on the separation between the ownship and the intruder. In order to keep this study to an assumable number of pages and figures, but without loss of generality, we only vary the CI of the ownship (BCN, in the example) while we assume the intruder (RES) has $CI = 0\,\text{kg/min}$. Figure III-7 presents an example.

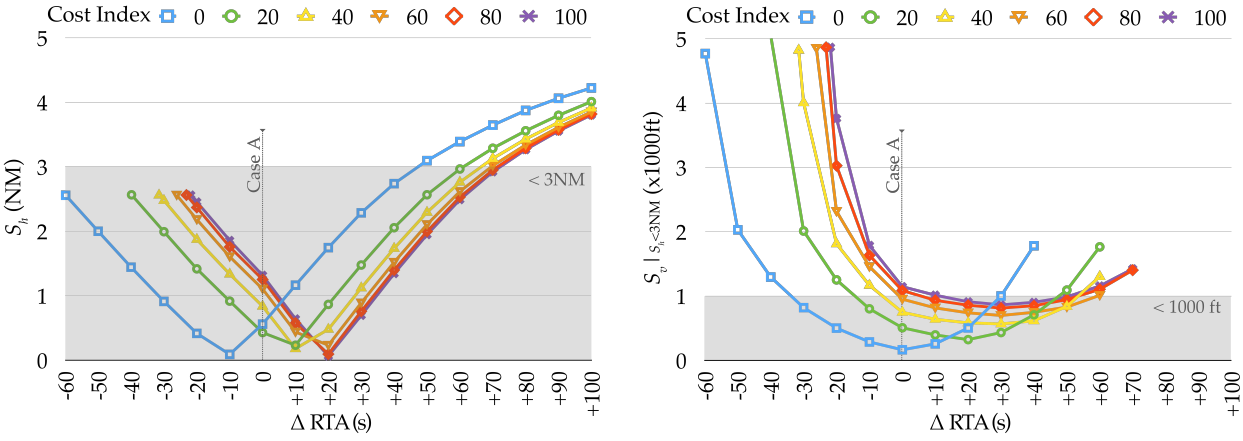

(a) Horizontal Separation (S_h)

(b) Vertical Separation ($S_v|_{S_h<3\,\text{NM}}$)

Figure III-7: *Minimum aircraft separation between ownship and intruder for different RTAs in case B with different CI (Ownship: BCN, Intruder: RES with $CI = 0\,\text{kg/min}$).*

The minimum horizontal separation between BCN and RES is similar for the different CI with a small shift in the time dimension. This is to be expected, since bigger CI values fly faster, therefore the required ΔRTA to reach the fix at a specified time instant grows. As expected, the required horizontal separation cannot be granted for earlier RTAs regardless of the CI value (the earliest feasible time is the same), and a bigger ΔRTA will be needed to keep separation with a later RTA (ΔRTA is computed with respect to each CI optimal baseline, which is faster). More interesting is the fact that for a CI greater than $60\,\text{kg/min}$, the vertical separation in case A is already granted. The reason for that is that higher CI values have higher speeds, which result in shallower vertical profiles.

At the end, we can conclude that as the CI value increases, the resulting cost to imposed ΔRTAs is higher. However, the different values of CI have a big impact on the conflict geometry, and therefore when estimating the possibility of a loss of separation, it is very important to know the airline strategy, or at least to propose different solutions to the conflict so the airlines can take part in the decision making.

III.4.3 Sensitivity study to the distance of the RTA fix

In the previous sections we have based all the results on two trajectories departing Barcelona and Reus airports. To complement this study, it would be interesting to provide results for a larger set of scenarios, including other routes, other conflict geometries, etc. Given the fact that such study would require extensive data sets, and even so, it would be impossible to cover all possible

situations, we have created a generic study that provides results that can be extrapolated to a big range of scenarios. This study is based on the assumption that the most important cause of fuel increase for a given RTA is related to the distance that the aircraft can use to comply with the time constraint.

The study is defined by one departing aircraft in a straight climbing trajectory that is requested an RTA at a fix, located at a specific along track distance from the runway. Figure III-8 presents results for all feasible RTAs at intervals of 10 s, for different locations of the RTA fix (from 10 NM to 100 NM, every 10 NM). In it, the white space represents RTAs that are not achievable given the operational restrictions. As expected, we observe that for shorter distances there is a smaller number of feasible trajectories. Also, the increase in fuel for negative ΔRTA grows at higher rates than for positive ΔRTA. This is also true for shorter distances when compared to longer distances.

Regardless of the lateral route defined by the SID, the impact on fuel will mainly depend on the distance between the moment that the RTA is issued and the RTA fix. In the case where a departing aircraft would encounter more than one conflict throughout the climbing phase, each conflict would be resolved by the adequate RTA, and would hence be treated as an individual problem. Therefore, the results presented in this section are applicable to a wide range of scenarios and conflict geometries.

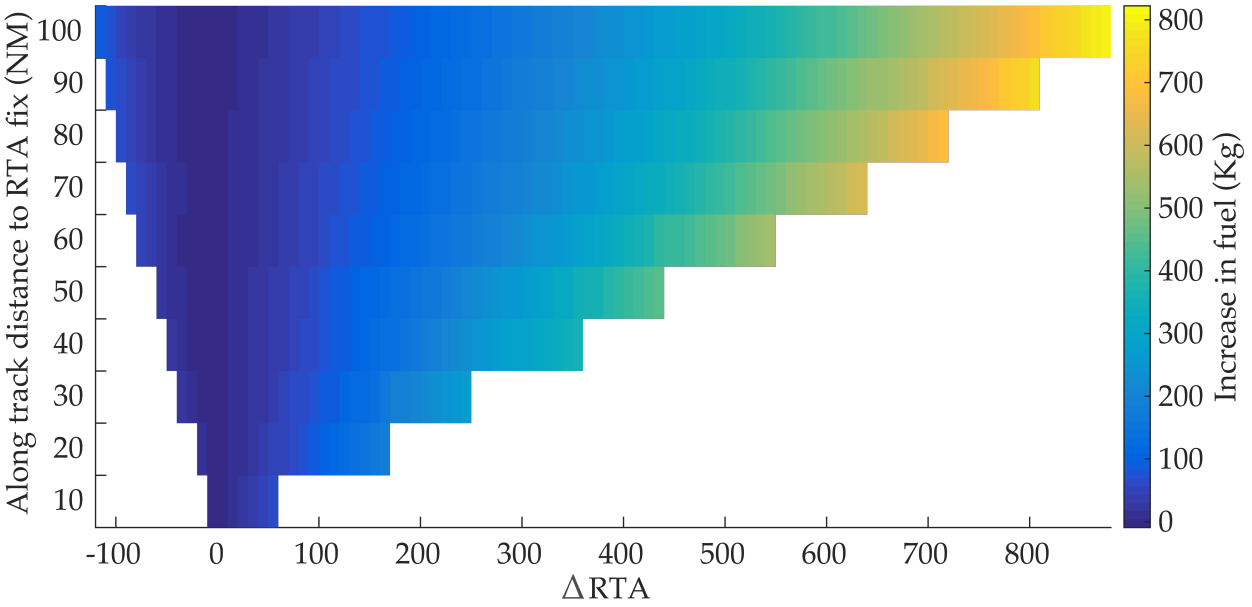

Figure III-8: *Sensitivity study of fuel to the distance of the RTA fix.*

III.5 Conclusion and further work

In this chapter we have particularised the framework described in chapter II to produce optimal trajectories along a strategically deconflicted fixed lateral route, while meeting imposed time constraints for airspace capacity and aircraft separation objectives. A sensitivity study has been developed that includes many cases and RTAs to assess the impact in fuel that sub-optimal trajectories pose.

As expected, RTA produce higher costs when compared to unrestricted continuous operations. However, when compared to imposing a level-off phase (as current ATCo may impose for

tactical separation), the gains are considerable, reaching very low increases in cost when the RTAs are defined in collaboration to all aircraft involved in a potential conflict. Moreover, results show that vertical separation is easier to achieve than horizontal separation. Also, as a side effect, an interesting result shows how adding a deceleration phase at the climbing procedure might cause lower fuel consumption. Even if this would not be foreseen in current climb operations, it should be further quantified to assess its benefits.

We have presented a specific scenario where this framework could work as assistance to decision making for separation assurance with minimum cost impact using RTAs. The granularity of the different RTAs and CI of study is small enough so the ATCo could easily quantify at each moment the impact in fuel of the available conflict resolution strategies and the required security buffers to account for uncertainty. However, such results are based on performance data that is, currently, not shared between airspace users (e.g. aircraft mass, cost index, etc.). Furthermore, weather predictions and updates should be taken into account for better accuracy. Therefore, there is still a need for further research in air traffic predictability in order to make this concept operational.

In the following chapters, instead of delegating the task fo separation to the ATCo (as it is done today in the current surveillance control ATM paradigm), each aircraft will be responsible for the maintenance and monitoring of the separation between itself and the other traffic. This will describe a more futuristic scenario where the main benefit will be that each aircraft is always the owner of its own trajectory computation and therefore has more control over how to overcome potential conflicts with intruding traffic following its own (the airline's) interests.

IV

Self-separated 4D control with conformance monitoring

This chapter proposes an optimal trajectory resolution methodology that computes **efficient conflict-free trajectory** based operations (TBO) in a dense traffic terminal manoeuvring area (TMA) on a self-separated paradigm using the optimisation framework described in II. The methodology assumes a *Semi-cooperative* scenario (as described in section I.3), where only current situation (position and velocity) and a conceptual description of what is to happen (flight plan or fligh intents) is shared amongst users. Given ADS-B (Automatic Dependent Surveillance - Broadcast) current position and intent information, we predict the future state of potential intruder aircraft and use this nominal trajectory as a constraint in the ownship trajectory optimisation process, resulting in a (presumably) conflict-free optimal trajectory.

Long-term predictions, however, can lead to big deviations, specially in this semi-collaborative scenario where very sensitive parameters from the intruder are unknown (e.g. mass, cost-index). To overcome the problems associated with prediction errors, we present a methodology that **continuously monitors the conformance of the intruder** predicted trajectory with regards to the real flight evolution: a linearised Kalman filter keeps track of the target by estimating the deviations of its actual trajectory from its nominal trajectory, issuing a warning when an appropriate threshold is exceeded.

The results show how this framework resolves the problem of uncertainties in the trajectory predictions and results in a **safer and more efficient conflict resolution**. This deconfliction aims at tactical traffic separation either because strategic deconfliction is non-existent, or it has failed due to unexpected events and uncertainties at the time of execution.

The following sections are organised as follows:

- Section IV.1 lays out the particularities on the dynamic model of the aircraft and the problem formulation, including the flight phases and operational constraints applied to the generic approach described in chapter II and the conformance monitoring implementation.
- Section IV.2 describes the set-up of the simulations for the demonstration of the chapter's objectives.
- Section IV.3 describes the scenarios and results that have been obtained.
- Finally, section IV.4 presents the author's conclusions relative to this chapter.

IV.1 Problem formulation

This chapter uses the same optimisation objective as the previous chapter III, formulated in eq. (III.1), which takes into account the flight operating cost including the time and fuel components. However, we include separation assurance constraints and a new conformance monitoring strategy, as described in the following sub-sections.

IV.1.1 Separation assurance

Requiring separation from other traffic is an added constraint in the problem. Figure IV-1 depicts a block diagram of the proposed methodology, involving an aircraft (the ownship) separating from surrounding traffic (one intruder).

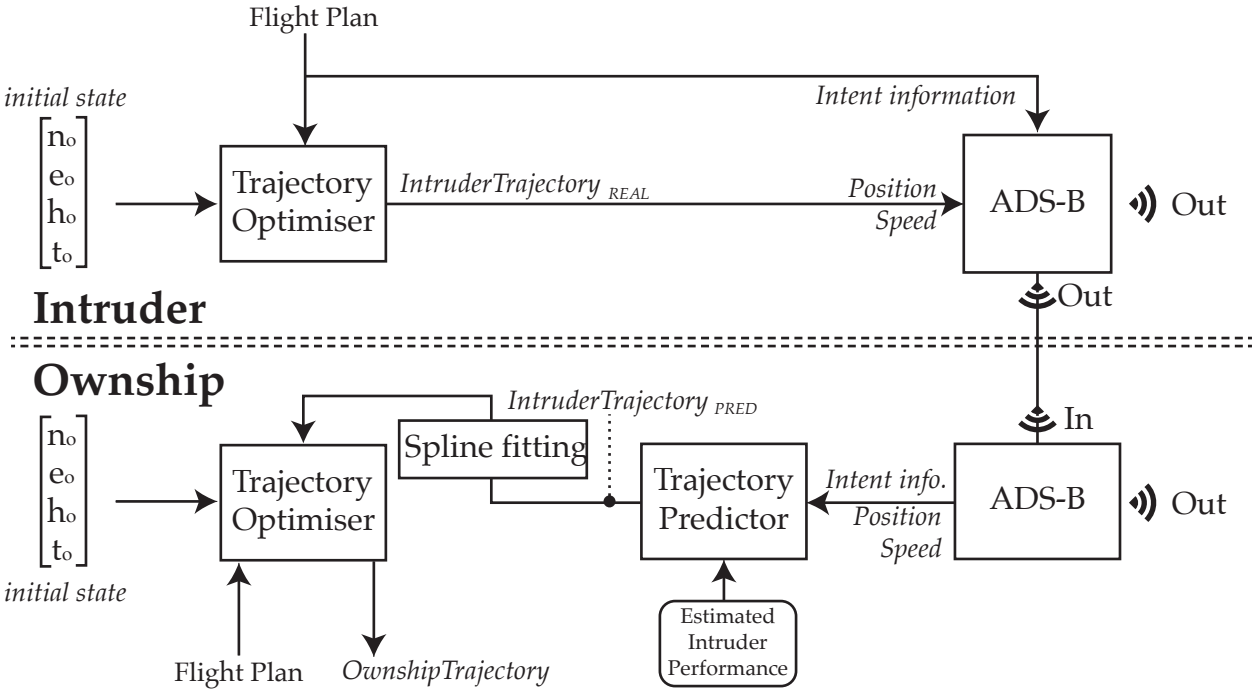

Figure IV-1: *Block diagram of the proposed aircraft separation methodology*

To generate a trajectory that maintains the required minimum separation from an intruder, the ownship collects the following required data from the other aircraft:

Updated position and velocity To be used as the initial state for the prediction algorithm.

Flight plan or short-term intents The next couple of waypoints (two or three suffice) as these represent the expected route that the aircraft will follow. The more information coded in these intents, the more accurate the prediction will be. In this thesis we have assumed geographical information only (latitude, longitude mainly, and altitude restrictions if provided), but time and velocity information as calculated in real time by the flight management system would render the prediction more accurate.

Type of aircraft To be used to select the performance model and parameters (i.e., nominal values for drag coefficients, mass, etc.)

This information could come from a fully implemented ADS-B protocol as specified in (RTCA SC-186, 2009) or other transmission protocols and frameworks such as TIS-B or SWIM. In this thesis we have assumed ADS-B as the data exchange technology (and message format), where the above-mentioned required information is directly accessible, or easily extrapolated, from the identification message, position message and intent message. This information is then used to predict the intruder future states (i.e., from the current intruder's position and velocity, following the flight intents, using the aircraft type performance) and calculate the ownship optimal trajectory that keeps the required separation.

Note that the separation strategy described in this section is easily extrapolated to multiple conflicts. The following subsections describe the different parts of the methodology in further detail.

IV.1.1.1 Intruder trajectory prediction

Prediction methods in the literature are usually based on the numerical integration of the intruder aircraft dynamics with specific assumptions required to close the degrees of freedom in the dynamic equations (in form of throttle setting, vertical speed, flight path angle, etc.) (Musialek *et al.*, 2010). These usually lead to complex iterative (and costly) processes to adjust the controls in order to meet the published intents. Instead of fixing such controls (and adjust them when we see that we do not comply with a specific constraint), we propose to use an optimisation method, which will modulate the controls as required in order to comply with the set of constraints.

This method allows for more complex predictions and can potentially provide more accurate results when many restrictions apply to a trajectory. Specially, when a flight plan is available that follows a defined lateral route or when multiple constraints have to be met at one fix (e.g., altitude and time). Given the fact that more than one trajectory will be available as a solution to the prediction problem (e.g., climb first vs. accelerate first), our strategy does not just provide one of the possible trajectories that meets the constraints (the one that the given fixed controls have generated), but it provides the one that is most cost effective (assuming an optimisation objective given by eq. (III.1)). Obviously, the more accurate the intents are, the better the prediction will be.

This is implemented in our framework using the exact same problem formulation as used when optimising an onwship, only that the state vector variables will in this case represent the intruder modelled states, as opposed to the ownship's.

The remaining challenge is how to model this moving target in our optimisation problem as continuous and twice differentiable functions needed by the NLP solver. Similar to the approach described in chapter III, section III.1.2, the list of 4D points coming from the predicted intruder trajectory is fit by a set of basis splines (B-splines), which provide an accurate curve fit and have been demonstrated to perform well with NLP optimisation. Again, this solution has proven to be very reliable, robust and have good performance in our simulations.

In this case, our approach is to create three different splines that represent the estimated intruder's east ($\hat{e}_i$), north ($\hat{n}_i$) and altitude ($\hat{h}_i$) coordinates over time (t):

$$\begin{aligned}\hat{e}_{\mathrm{i}}(t) &= \Gamma_{\hat{e}_{\mathrm{i}}}(t)\\ \hat{n}_{\mathrm{i}}(t) &= \Gamma_{\hat{n}_{\mathrm{i}}}(t)\\ \hat{h}_{\mathrm{i}}(t) &= \Gamma_{\hat{h}_{\mathrm{i}}}(t)\end{aligned} \tag{IV.1}$$

At the ownship optimisation process, the algorithm repetitively queries these curves that represent the dynamic obstacle (intruder) at each time of sample (t). With this strategy, a new constraint in the problem ensures that the required separation minima is kept at all times, as described in the following section.

IV.1.1.2 Separation volume

Current RADAR separation minima specify lateral and vertical separation independently (as explained previously in the document, in this thesis we use 3 NM and 1000 ft respectively). The two components are specified independently due to the big difference in dynamics between the horizontal and vertical planes, forming a cylindrical protection volume. Thus, a *conflict* appears when there is a risk of an aircraft entering this protection volume unless a separation action is taken. This could lead to a loss of separation and eventually to a near mid-air collision or ultimately a fatal encounter.

The cylindrical separation volume constraint can be described with the following disjunction:

$$g_h(t) \geq 0 \vee g_v(t) \geq 0 \tag{IV.2}$$

where g_h and g_v are the horizontal and vertical separation constraints; with d_h and d_v, respectively, the required horizontal and vertical separation values:

$$\begin{aligned}g_h &= \sqrt{(e(t) - \hat{e}_{\mathrm{i}}(t))^2 + (n(t) - \hat{n}_{\mathrm{i}}(t))^2} - d_h\\ g_v &= \Big(h(t) - \hat{h}_{\mathrm{i}}(t)\Big) - d_v.\end{aligned} \tag{IV.3}$$

As stated before, NLP solvers require continuous and twice differentiable functions, and it is obvious that a cylinder does not comply with this. To solve this issue one can reformulate eq. (IV.2) with continuous functions as follows (Raghunathan *et al.*, 2004):

$$\begin{aligned}\lambda_h(t)g_h(t) + \lambda_v(t)g_v(t) &\geq 0\\ \lambda_h(t) + \lambda_v(t) &= 1\\ \lambda_h(t), \lambda_v(t) &\geq 0\end{aligned} \tag{IV.4}$$

where λ_h and λ_v are two continuous variables that, with the second and third constraints in (IV.4), enforce the logical OR in this formulation. The nature of this formulation, however, will presumably add complexity to the solver, increasing computational times and increasing the risk of local minima.

Other strategies could bring better convergence to the algorithm with the cost of a less accurate representation of the separation volume. This would be, for example, in case of a sphere (Mohan *et al.*, 2012) or an ellipsoid (Menon *et al.*, 1999). These are geometrical forms that can be expressed by a single equation and, specifically to our problem, enforce separation by form of inequations. In contrast to the current cylindrical specification, the sphere is highly inaccurate as

it treats lateral and vertical separation equally and ellipsoids are also inaccurate at the horizontal extremes (i.e., the vertical separation is soon lost when going towards the horizontal edges).

Alternatively, a specific case of super-ellipsoids, the supereggs, can be parameterised in a way to form a geometrical shape very close to that of the cilindrical protection volume. Effectively, these are very similar to ellipsoids but maintain the vertical separation longer, to a steeper end. They can be represented by the following equation:

$$\left(\frac{(e(t)-\hat{e}_{\mathrm{i}}(t))^2+(n(t)-\hat{n}_{\mathrm{i}}(t))^2}{{d_h}^2}\right)^q+\left(\frac{(h(t)-\hat{h}_{\mathrm{i}}(t))^2}{{d_v}^2}\right)^q\geq 1 \tag{IV.5}$$

where q is the steepness coefficient of the superegg. A higher value is closer to the representation of a cylinder but more complex for the convergence of the algorithm. In our computations, $q=3$ has provided a good trade-off.

Although it is out of the scope of this thesis to thoroughly study each strategy, we have implemented both the cylindrical disjunction described in eq. (IV.4) and the supereggs inequation described in eq. (IV.5). The first strategy, as expected, fully respects the cylindrical protection volume but the non-linear nature of it results in the optimisator falling into local minima easier. The second strategy shows a slightly less accurate representation of the protection cylinder (i.e., the vertical separation is found to be slightly less than the required minima when the horizontal separation is at its bounds), but presents less non-linearities for the model, and thus performs very well on the optimisation engine.

With an adequate choice of superegg coefficients, the inaccuracies of the superegg as compared to the cylinder have been demonstrated to be very small and, therefore, the results in this chapter use this strategy.

IV.1.2 Conformance monitoring

In addition to calculating a conflict-free situation, the target traffic prediction is continuously monitored to account for uncertainties in the prediction process. The conformance monitoring methodology is depicted in figure IV-2 and described in the following paragraphs.

The method is the combination of an intruder reference trajectory (as predicted from the ownship, detailed in the previous sections) and a target tracker based on limited information from ADS-B (i.e., position and velocity). We define a linearised Kalman filter with six states, which account for the difference in position and velocity between the predicted trajectory and the true ADS-B reports:

$$\vec{y}=[\ \Delta e\ \ \Delta n\ \ \Delta h\ \ \Delta\dot{e}\ \ \Delta\dot{n}\ \ \Delta\dot{h}\ ]^T \tag{IV.6}$$

where Δ represents the difference of the state between actual and nominal trajectory. The measurement equation is given by:

$$\vec{z}=\vec{y}+\vec{v} \tag{IV.7}$$

where $\vec{z}$ is the measurement and $\vec{v}$ is the measurement noise with covariance matrix $\boldsymbol{\mathcal{R}}$. $\boldsymbol{\mathcal{R}}$ is derived from Navigation Accuracy Category for Position (NACp) and Navigation Accuracy Category for Velocity (NACv) from ADS-B messages. The state transition equation from time epoch $k-1$ to time epoch k is defined as:

$$\vec{y}_k=\boldsymbol{\mathcal{P}}_k\vec{y}_{k-1}+\vec{w}_k \tag{IV.8}$$

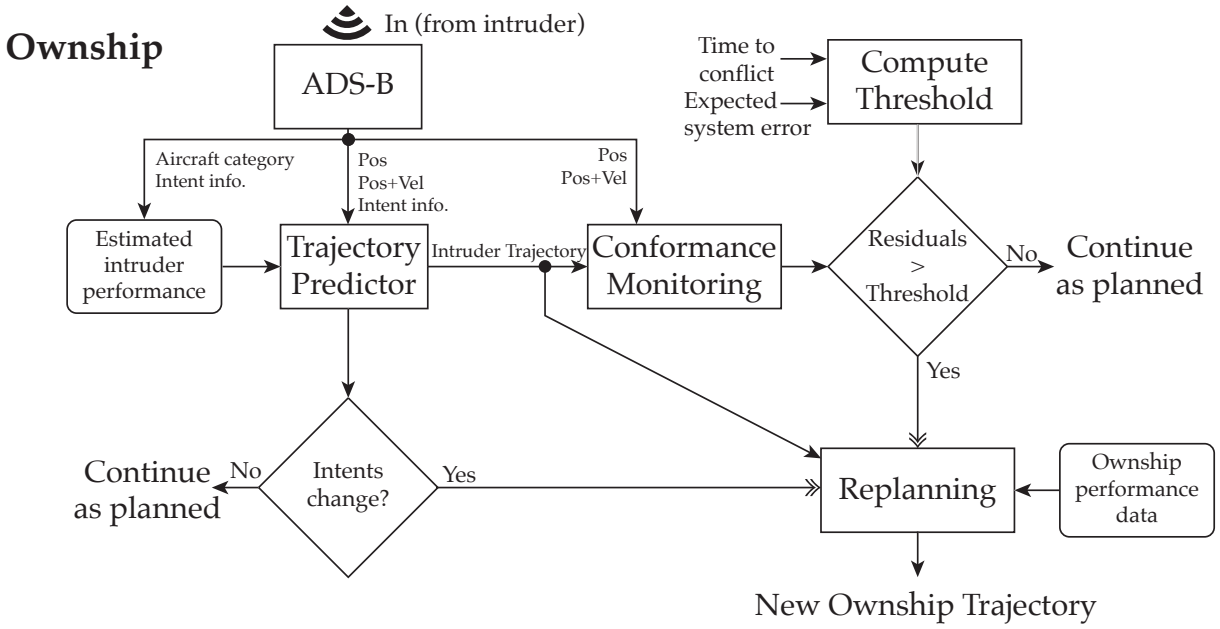

Figure IV-2: *Flow chart of the proposed methodology of separation assurance with conformance monitoring.*

where $\mathcal{P}_k$ is the state transition matrix for a constant velocity model (Brown & Hwang, 2012) and $\vec{w}_k$ is process noise reflecting the uncertainty in the dynamics model for the flight operation. The covariance matrix for $\vec{w}_k$ is the state transition covariance matrix $\mathcal{Q}$.

Note that the constant velocity model is applied to the trajectory deviation rather than the aircraft dynamic model, as it is obvious that aircraft is not flying constant velocity during departure flight phase.

The mechanisation of the filter states allows to take into account the history of the observables (ADS-B reports), reducing the noise from the position and velocity reports and the ability to perform a short-term prediction. With this method, the conformance monitoring is directly interpreted from the state variables of the filter. In other words, as opposed to a mere comparison between the state of the intruder and the predicted trajectory, the presented method allows to take into account the history of all measurements/reports from the ADS-B receiver to come up with estimates and predictions that are more accurate (lower noise) than the instantaneous reports.

The state vector is compared to a pre-defined threshold to determine whether a new prediction of the intruder's trajectory has to be calculated and, consequently, a new trajectory replan is required for the ownship. The values of the pre-defined threshold are based on typical navigation system error (NSE), flight technical error (FTE), and the aircraft dynamics. The choice of the threshold is a trade-off between minimising the possibilities of missed detection and false alarm. The threshold values used in the example in the following section are typical or conservative values for demonstration purposes. A performance analysis for the optimal choice of the threshold is left for future work.

IV.2 Framework set-up

The algorithms and methods presented in this chapter are part of a real-time aircraft situation, where they play an active role in the execution of the flight. To successfully achieve our demonstration objectives, we have prepared a simulation environment where all aircraft fly according to

a time clock (the SIMULATOR). Each aircraft in the simulation (in this case the *ownship* and the *intruder*) follows its own assigned route, which has been previously calculated through the execution of an isolated trajectory optimisation process (DYNAMO). The optimal baseline is used by the *Host* as the real trajectory which is flown by the aircraft. However, the ownship is expected to deviate when it encounters a conflict with the intruder. Therefore it needs to predict the intruder's trajectory and take it into account during the optimisation process. Furthermore, the conformance monitoring runs in parallel at all times.

The simulation framework presented in this section does not only provide all the functionality regarding the clock (play, pause, fast-forward, slow-forward, jump, etc. through the SIMULATOR) and regarding the aircraft flight execution (prediction, optimistion, calculation of the flight position at the published time, etc. through the *Host* module and DYNAMO) but also provides the communication framework that mimicks the ADS-B channel, where all required information is shared among airborne users. This channel is implemented using the Robotics Operating System (ROS[1]), which simplifies the implementation of messaging between processess and provides a big flexibility and performance. Furthermore, ROS has many tools to visualise the status of all nodes in the network, as well as all messages being sent and received, tools both textual and graphical, which allow for an effective and accurate monitoring of the simulation progress.

The funcional workflow at the *Host* module of the ownship (once the required scenario file has been defined) as conceptually depicted in figures IV-1 and IV-2 is the following:

Prediction Compute the predicted intruder's trajectory using DYNAMO.

Baseline Compute the own baseline optimal trajectory using DYNAMO and taking into account the predicted intruder's trajectory. Store this trajectory as the *real* trajectory of the aircraft.

Time-tick At every time tick, the *Host* has to perform the following actions:

- Compute the current state of the aircraft (position, velocity, angles, etc.) from the baseline trajectory at the published time-tick.
- Publish the state of the aircraft through the dedicated ADS-B bus.
- Receive the state of the intruder through the dedicated ADS-B bus.
- Monitor the conformance of the intruder to the expected trajectory. If the difference between the expected and the real intruder's position is over a specific threshold, launch a replan that will perform the Prediction and Baseline steps.

Results All steps and results of the simulation are logged to prepare the desired outcomes and display them through tables and charts.

This workflow is depicted in figure IV-3 as a summary of the flow of events at the software level.

IV.3 Numerical results

A typical conflict that is encountered within a TMA is usually due to the close proximity of two airports (like it happens for instance in the Bay Area around San Francisco airport or in the New York Area, and mostly all over Europe) or between departures and arrivals at the same airport.

[1] http://www.ros.org

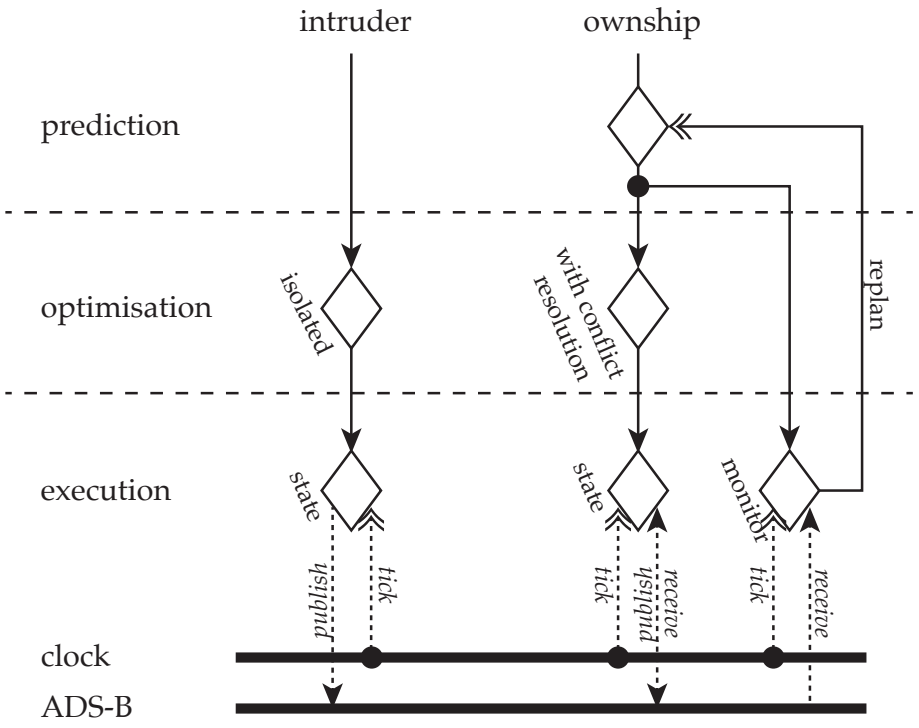

Figure IV-3: *Functional workflow of the simulation framework with self-separation and conformance monitoring.*

IV.3.1 Scenario setup

A similar scenario setup than the one described in the previous chapter is used for the purpose of this chapter. The described routes from Barcelona and Reus airports are flown by two similar aircraft simultaneously, which, as previously stated, enter in conflict soon after take-off. Therefore, some action is required to prevent the loss of separation. This situation could be estimated just before take-off, since every aircraft has a (fairly)accurate prediction of its own future states. However, due to the very limited degree of information sharing between airspace users, it is much more difficult from an external entity (e.g., another aircraft) to synthesise such accurate predictions of other traffic: sensitive data such as aircraft weight and performance data remain unknown.

To reflect this issue, we simulate the situation where the ownship (BCN) predicts the intruder (RES) trajectory and deviates from it. To demonstrate the functionality of the conformance monitor we assume that both aircraft have similar performances, but that the onwship underestimates the intruder's take-off mass (5% lower).

In this example, both aircraft are flying a departure procedure with a required navigation performance of RNP 0.3. In other words, nominally, the target aircraft should never have a lateral deviation of more than 0.6NM (two-sigma containment radius) from the nominal trajectory (RTCA SC-181, 2003b). As a result, if the target aircraft is found to be deviating more than 0.6NM, it is likely due to an intentional change of flight path or mismodelling of the nominal trajectory. Therefore, 0.6NM is used as the lateral position deviation threshold for monitor. Similarly, 250ft (RTCA SC-181, 2003a) is used as the threshold for the vertical position deviation and a conservative value of 5m/s is used for the velocity threshold. A NACp of 10 (corresponding with 95% estimated position error of 10m horizontally and 15m vertically) and NACv of 3 (corresponding with velocity error of 1m/s horizontally and 5ft/s vertically) (RTCA SC-186, 2002) are used to define the measurement covariance matrix $\mathcal{R}$.

IV.3.2 Simulation results

The induced prediction errors lead to time, speed and, more evidently, vertical deviations. Such deviations are easily detected by the conformance monitor. Figure IV-4 shows the intruder position and velocity deviations from the actual trajectory to the nominal trajectory. The red dashed lines are the different thresholds, which define replan triggers. In this example, the first replan triggers at $t = 53s$, both due to the vertical position and vertical speed components (blue line). Subsequent predictions (dark orange, yellow, purple and green) are triggered due to the deviations on the vertical position component only. This is only due to the specific depicted example, and other cases could be sought that triggered replans due to deviations in any of the other state variables.

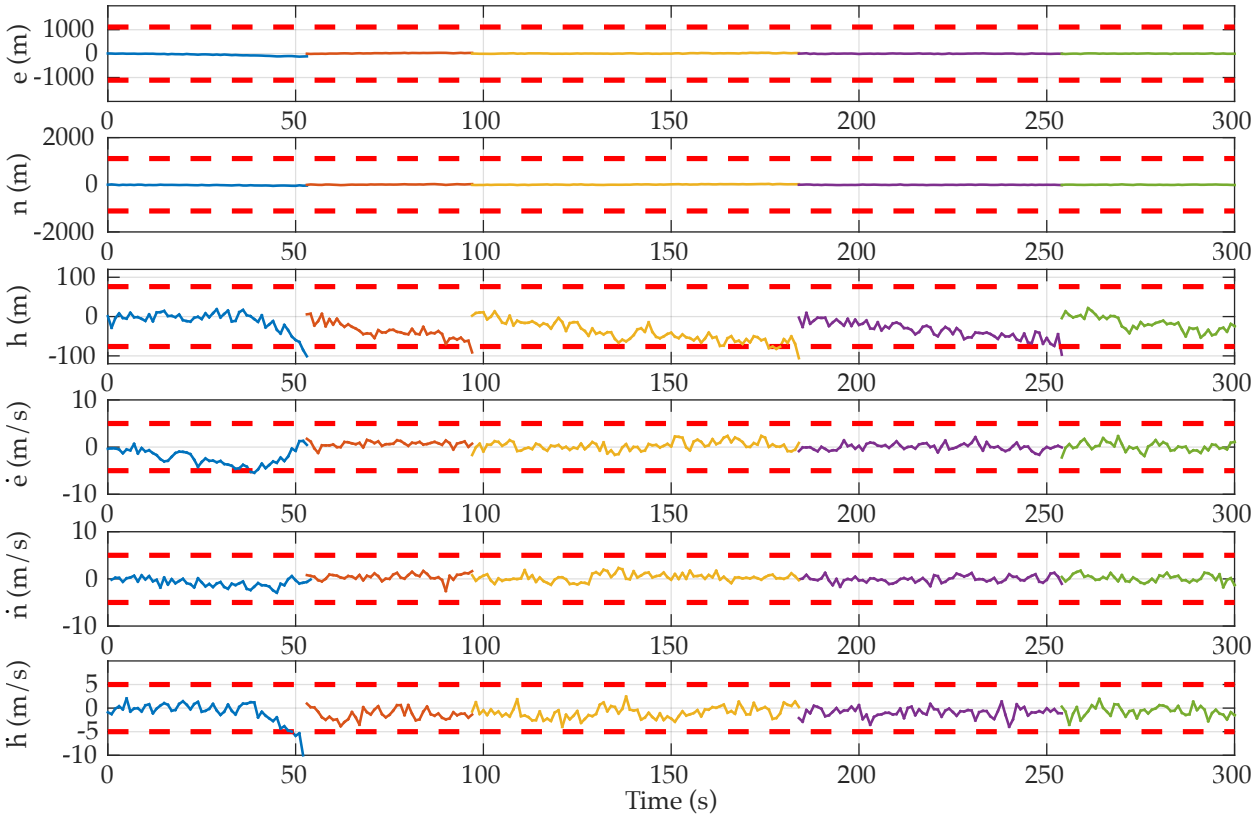

Figure IV-4: *Intruder state vector deviation showing the prediction errors and the trespassing of the threshold at each replan.*

With the objective of maintaining separation from the intruder after each new prediction, the ownship generates new trajectories that deviate from the initial plan as the predicted conflict evolves. In this specific case study, even if the optimiser is given flexibility to deviate both horizontally and vertically, the conflict is resolved with deviations on the vertical profile only: both aircraft are climbing and minor changes in the vertical profile give the required vertical separation throughout the flight, having a negligible impact on the fuel consumption. Figure IV-5 shows this vertical deviation for the different replans (the solid line represents the trajectory that is effectively flown by the ownship, whereas the dashed line depicts what it would have flown if no new replan had been triggered). It is clear how each replan activity creates greater vertical corrective actions and at an earlier time (the initial plan is actually unaware of the conflict due to the prediction errors). See for instance how replan at $t = 184s$ starts deviating earlier than replan at $t = 97s$.

Figure IV-6(a) shows the vertical separation between the ownship and the intruder's predicted trajectory, up to the point where the conflict occurs (after the depicted loss of horizontal

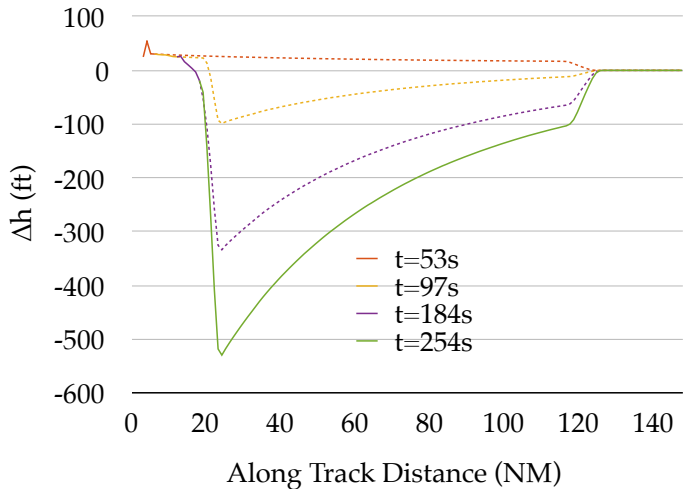

Figure IV-5: *Vertical deviation from the initial plan performed by the ownship at each replan in order to deviate from the updated predicted intruder trajectory.*

separation between seconds 300s and 350s, no more conflicts are encountered between the two aircraft). Effectively, the minimum separation is always respected from the optimiser's perspective. However, in reality this would not be the case, as presented in figure IV-6(b), due to the errors in the predictions. Furthermore, even if the vertical separation between both aircraft at the loss of horizontal separation is increased at every replan, it never reaches the required 1000ft in the presented case. This is explained by the fact that the last replan happens at $t = 254s$, some $50s$ ahead of the conflict, which is enough time for the prediction to grow some error but without triggering a replan (the vertical threshold in the conformance monitoring is set to 250ft).

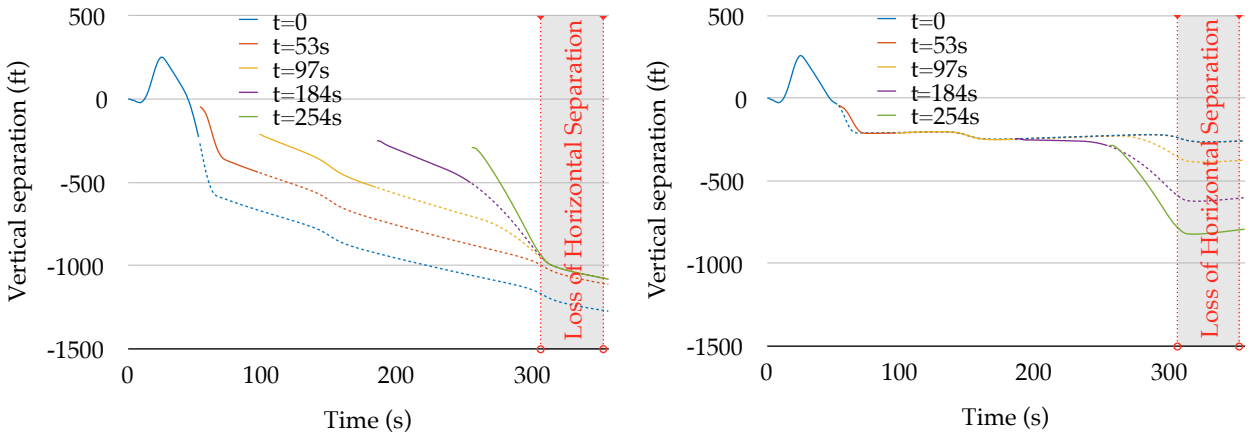

(a) Predicted Separation

(b) Real Separation

Figure IV-6: *Vertical separation between the ownship and the intruder.*

This issue could easily be overcome by increasing the required vertical separation at the optimisation procedure with a buffer accounting for the conformance monitor threshold plus other uncertainty sources. Indeed, figure IV-7 shows how the conflict is finally removed when the ownship optimisation algorithm specifies a minimum required separation of 1250ft (other uncertainty sources are here ignored). Besides, the conformance monitor could have an adaptive threshold which would decrease as the two aircraft get closer. Additionally, a mass estimation algorithm could be run at each replan to learn from the intruder's past states and produce more accurate

predictions, resulting in earlier and more efficient corrective actions (this is solved in next chapter).

It is worth noting that in the example, the increase in fuel of the resulting trajectory (with all the replans) is negligible when compared to the optimal baseline (less than 0.004%).

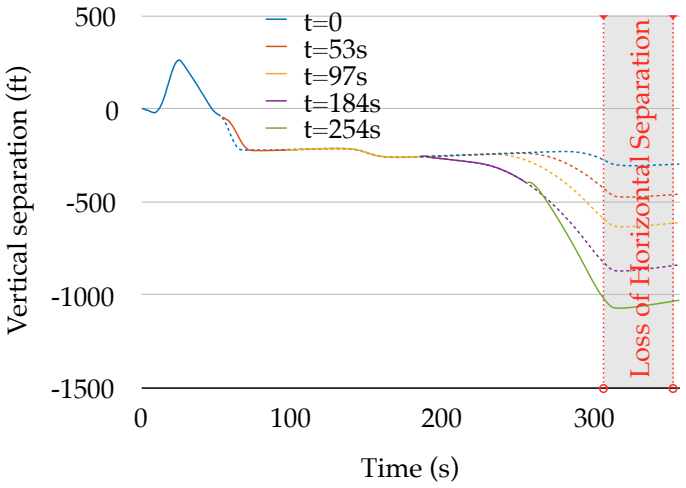

Figure IV-7: *Vertical separation between the ownship and the intruder's real trajectory with a required minimum vertical separation of 1250ft.*

The application of the described methodology in the example results in an evident enhancement of the conflict resolution. Without it, the ownship would most probably have disregarded the intruder as a potential conflict, due to the big errors in the initial prediction. Thanks to the conformance monitoring, as the flight progresses, the ownship is more and more aware of the conflict and has more time to react.

Therefore, the resulting trajectory amendment to avoid the conflict is not only more robust to intruder prediction uncertainties but also more efficient than ATC path stretching or level-offs (as typical tactical interventions to maintain aircraft separation), since it is the outcome of a trajectory optimisation process of the ownship. However, due to the latent inaccuracies in the prediction model, the prediction of the intruder's future states quickly become obsolete as they deviate greatly from the reality. Even if these deviations become apparent through the conformance monitoring strategy, which triggers consequent updates of the ownship trajectory (again, an optimisation process to resolve the presumed upcoming conflict), the short validity of the predictions could result in too many replans and eventually to (too-)aggressive manoeuvres due to the lack of earlier action. This could be easily prevented with an adaptive trajectory prediction strategy, reducing the underlying obsolescence of the predictions and therefore enabling earlier reaction. This is further explored in the next chapter.

IV.4 Conclusion and further work

In this chapter we have enhanced the framework for optimising 4D trajectories described in the previous chapters to present a self-managed 4D control strategy consisting of an optimal resolution of conflicts based on the predicted evolution of traffic. Given the fact that trajectory estimates of intruding traffic can be very inaccurate, techniques for target tracking and conformance monitoring have been introduced. Hence, replans occur either when new information arrives, or when the tracker alerts of a deviation from the expected trajectory.

We have described the functional modules and data sharing for an implementation of a *semi-cooperative* scenario. However, other cooperative cases could easily be integrated in the model. In the case of a more cooperative scenario, both aircraft would individually compute own deviations (assuming they were *the ownship*) and would together (or through a third party) agree on who (between the two) would effectively manoeuvre. This decision should be based on a set of comparable variables, such as consumed fuel, the resulting time of arrival, right-of-way, altitude to the ground, safety, etc. Chapter III shows some metrics (only based on time and fuel) that could help on taking this decision. In a completely *non-cooperative* case, the trajectory prediction could only rely on current and historical data to produce the immediate future states. On the contrary, in a *fully-cooperative* case the solution to the conflict could actually be calculated as the global optimal: all aircraft would manoeuvre slightly to remove the conflict in shared responsibility. This last case is presented in chapter VI.

Additionally, even if only one conflict is assumed in the results, the implemented separation strategy is easily extrapolated to multiple conflicts, treated sequentially. This would obviously pose other problems such as network effects (solving a local conflict could result in even more conflicts in the future) and therefore should be further studied in future work.

Finally, we have presented a realistic example based on an operational scenario. In the depicted case, thanks to the conformance monitoring, the different replans reveal an initially unexpected conflict. Effectively, the conformance monitoring could be enhanced to propose enhancements to the prediction models and assumptions as the Kalman filter learns. In de depicted example, as it is quite apparent that the predictor is always overestimating the altitude, the estimated mass of the aircraft could be slightly increased at each replan. Therefore, mass and cost index strategies could be corrected using ADS-B historical data. This is presented in the following chapter.

Given the flexibility with which the scenarios can be defined in our tool, it could easily be extended to a wider variety of scenarios. These scenarios could include the use of incorrect performance parameters in the predictor, tactical flight plan changes (i.e., once airborne), diversion due to weather, non conformance to fligh plan of non-cooperative aircraft, etc. In future work, an exhaustive set of tests could be defined to demonstrate the performance of the proposed methodology in a sensibility study. This should also be used to study the adequacy of the triggering threshold value.

The self-separated optimisation and conformance monitoring algorithms described in this chapter are laying out the basis for an interactive (vehicle-to-vehicle: V2V) autonomous air traffic management framework. Nowadays, last-minute collision avoidance is already performed semi-autonomously: TCAS advisories are provided through a V2V interaction, and it is the pilot who acts according to these. In a future situation, thanks to the presented paradigm, a similar interaction could happen in tactical coordination upon a conflict resolution for separation management (e.g., who should deviate?), as briefly described in the second paragraph of these concluding remarks.

V

Mass estimation for an adaptive trajectory predictor

Air traffic predictability is paramount in the air traffic system in order to enable concepts such as Trajectory Based Operations (TBO) and higher automation levels for self-separation. Whereas in simulated environments 4D conflict-free trajectory optimisation has shown good potential in the improvement of air traffic efficiency, its application to real operations has been very challenging due to the current lack of information sharing between airspace users. Consequently, such operations are still very limited in scope and rarely attempted in dense traffic situations. Better predictability of other traffic future states would be an enabler for each aircraft to fly its user preferred route without decreasing safety in a self-separation context. But this is not an easy task when basic aircraft parameters such as aircraft weight, performance data or airline strategies are not available at the time of prediction. This leads to uncertainties in the prediction of aircraft future states.

A lot of effort has been put into enhancing the sharing of information between aircraft users (López-Leonés *et al.*, 2007; SESAR, 2017), although the specific contents are still subject of debate and the implementation of such paradigm is still far in the future. On the other hand, many techniques for trajectory prediction are avaiable in the literature (Musialek *et al.*, 2010). Furthermore research is being done with the purpose of using the aircraft past states to enhance ground based predictions (Warren & Ebrahimi, 1998; Schultz *et al.*, 2012; Alligier *et al.*, 2012; Alligier *et al.*, 2014). Most of these algorithms are based on analytical models that iteratively correct the aircraft weight estimation with each new received track data minimising the energy rate differences with the projected energy rate using a simplified dynamic model.

Along these lines, this chapter presents a **unified framework** for **trajectory optimisation**, **prediction** and **parameter estimation** with the purpose of enhancing predictability of air traffic

operations whilst proposing optimal trajectories and conflict resolution in a dense traffic area. Given different spatial and temporal constraints along with the definition of specific objective functions for each purpose, the same problem formulation described in II provides optimisation, prediction and estimation functionalities.

Chapter IV, has already presented part of this framework: an aircraft trajectory computes its own optimal resolution of a conflict in a self-separation paradigm with conformance monitoring. In the current chapter, two major changes are introduced:

Intruder performance model

In the previous chapter, the performance model to compute the *ownship trajectory* and the *intruder prediction* was identical (Airbus' PEP in both cases). This could be somewhat realistic when airlines have many aircraft models in their fleet (and therefore access to real performance data) and can infer the performance of the intruder. However, this is only partially true as same models have sometimes different configurations (engines, winglets, etc.) which will soon lead in big differences in the modelled thrust and drag. And besides, what if the airline does not have a specific model?

What we are proposing in this chapter is to open a new perspective where the ownship is unaware of the specific performance parameters of the intruder, and must default to the use of the more generic BADA equations, parameters and nominal values to predict the intruder future states.

Parameter estimation

In the previous chapter, the conformance monitoring would trigger a new replan as soon as the deviation between the *actual* and *planned* state (position and velocity) of the intruder would be greater than a specific threshold. However, for each new replan, a latent bias in the prediction model would produce equally fast deviating predictions.

As a major contribution in this chapter, we introduce a parameter estimation strategy to make better and better predictions: as the situation evolves, ADS-B published messages are used to learn about other aircraft dynamics. This information forms a trail of past states that the estimation model uses to converge to more accurate parameters (e.g., unknown *intruder* initial mass). Accordingly, the prediction is continuously regenerated as the knowledge of the other traffic grows (i.e., longer trail). The ownship then uses this updated prediction to detect any potential changes in the conflict geometry and generates a new self-separated trajectory. It is shown how this enhanced prediction enables efficient conflict detection and resolution.

For the simplification of the understanding of the results in this chapter, the conformance monitoring presented in chapter IV has been removed. This is, the replans are not triggered after a deviation is detected on the intruder prediction, but on a specific timely basis. The different sections present different results in figures and charts that have different replan triggers (e.g., every 100 s or every 25 s). Each time, the replan rate is carefully selected to provide the adequate granularity required for the results without negatively impacting the legibility of the resulting charts.

The following sections are organised as follows:

- Section V.1 lays out the particularities on the dynamic model of the aircraft and the problem formulation, including the flight phases and operational constraints applied to the generic approach described in chapter II and the parameter estimation implementation.
- Section V.2 describes the set-up of the simulations for the demonstration of the chapter's objectives.

- Section V.3 describes the scenarios and results that have been obtained.
- Finally, section V.4 presents the author's conclusions.

V.1 Problem formulation

Conflict-free trajectory optimisation in dense traffic conditions has a very complex implementation due to many factors that introduce uncertainties at different levels. As already briefly mentioned, the framework described in this chapter tries to unify three main aspects in an effort to minimise such inaccuracies: trajectory prediction, parameter estimation and trajectory optimisation. These functionalities work together interconnected in order to achieve better predictability for a safer and more efficient self-separated air traffic system. The concept of operations is summarised in figure V-1 and the main modules described in the following subsections. The problem formulation of the optimisation engine, which provides core functionality of each module, is described in chapter II. Its use for trajectory optimisation and trajectory prediction is almost identical and has already been covered in previous chapters, whereas some slight modifications occur for parameter estimation.

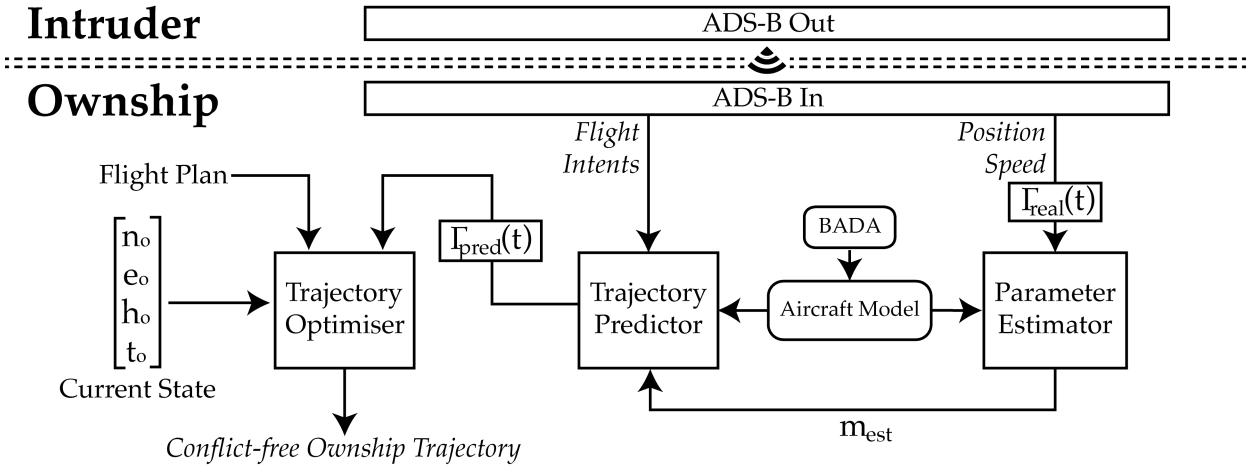

Figure V-1: *Self-separated optimisation framework concept diagram.*

V.1.1 Mass estimation

The core part of the parameter estimation framework is based on exploiting the known states of the intruder trajectory. Using ADS-B messages, the ownship generates a trailing trajectory that positions the intruding aircraft along the time (in the past). The longer this trailing trajectory, the more can be extracted from it. Then, an optimisation process is performed, which, as opposed to finding the cost-optimal trajectory as described in previous chapters, finds the initial mass that produces a trajectory that minimises the error to this trailing trajectory.

To do so, we use a slight modification of the optimisation framework described in chapter II. This parameter estimation framework is thus based on the same basic structure, state and control variables, and only some additional constraints and a different cost function are proposed to achieve the specific objectives.

Specifically, as shown in the right-hand side of figure V-1, the position and speed reports coming from the published ADS-B messages of the intruder, are interpolated at the ownship to create the four splines that represent the known intruder's east (e_i) and north (n_i) coordinates,

altitude (h_i) and velocity (v_i) over the time (t):

$$\begin{aligned} e_\mathrm{i}(t) &= \Gamma_{e_\mathrm{i}}(t) \\ n_\mathrm{i}(t) &= \Gamma_{n_\mathrm{i}}(t) \\ h_\mathrm{i}(t) &= \Gamma_{h_\mathrm{i}}(t) \\ v_\mathrm{i}(t) &= \Gamma_{v_\mathrm{i}}(t) \end{aligned} \tag{V.1}$$

These are referenced as $\Gamma_{real}(t)$ in the figure and are an input to the parameter estimation optimisation problem, the cost function of which defines the root mean square (RMS) of the deviations as follows:

$$J = \sum_{i=1}^{N} \int_{t_0^{(i)}}^{t_f^{(i)}} \left[(e_\mathrm{i}(t) - e(t))^2 + (n_\mathrm{i}(t) - n(t))^2 + (h_\mathrm{i}(t) - h(t))^2 + (v_\mathrm{i}(t) - v(t))^2 \right] \mathrm{d}t. \tag{V.2}$$

Effectively, this means that at the parameter estimation process the solver will minimise the deviations between the variables in the state vector (actually, e, n, h and v) and the observed trailing trajectory. Please note how in this case the variables in the state vector represent the intruder modelled state, not the ownship's.

Also, as opposed to the trajectory optimisation and trajectory prediction problems, where the primary outcome of the optimisation problem is a 4D trajectory, in the mass estimation problem **the main outcome is an *equivalent mass*** that produces a trajectory that is the closest to what the aircraft has actually flown. Therefore, the constraint on the initial mass of the problem is removed (in the previous chapters all state variables are bound at the initial value), so the optimiser is free to find the aircraft take-off mass that minimises the cost functional.

Finally, with the purpose of helping find a feasible and optimal solution, we remove some other constraints of the problem. Given the fact that the trailing trajectory is the most accurate information we have about the intruder, operational constraints defined in section II.2.2 regarding aircraft performance or basic flight intents are removed. Indeed, using the BADA model in the parameter estimation optimisation problem could mean that some of these constraints are unfeasible with regards to exactly following the real lateral and vertical trailing trajectory and the speed profile as reported by the ADS-B position reports and modelled with the curves in eq. (V.1). Doing so really helps the optimisation problem on finding the *equivalent mass*.

Even if the *equivalent mass* is most probably biased with respect to the real mass, it renders the closest results to the real trailing trajectory. This bias is explained by the differences in the performance model (real vs. BADA) and problem simplifications and assumptions. Nevertheless, this biased *equivalent mass*, when used for the prediction of the intruder trajectory (with the same performance model and problem assumptions as used in the parameter estimation problem) will deliver results that are presumably closer to the reality than other values for the mass (including the exact real mass).

V.1.2 Trajectory prediction and optimisation

After the mass estimation process, the *equivalent mass* is available as an intput to the trajectory predictor (middle box in figure V-1). The prediction approach has already been explained in section IV.1.1.1. However, for reasons already stated in the introductory section of this chapter, we have considered here a different perspective of the knowledge of the dynamic model of the intruder. The following assumptions apply:

(a) Since we do not have an enhanced and accurate dynamics model of the intruder, assuming we can work out the type of aircraft, we use BADA to model the dynamics of the state variables and provide nominal parameters. Among this nominal parameters, there is the take-off mass, which BADA defines for each type of aircraft.

(b) We assume that the basic aircraft intents are available in form of a list of geographical points that represent the lateral (and potentially vertical) route. Such information could be available in form of ADS-B messages or other concepts such as AIDL (Aircraft Intent Description Language) (Gallo *et al.*, 2007) and SWIM (System Wide Information Management) (SESAR, 2017).

Similar to the problem described in chapter IV, the output of the trajectory predictor is the estimated trajectory of the intruder which is then approximated with splines (referenced as $\Gamma_{real}(t)$ in figure V-1). This intruder fixed trajectory is then used an input at the trajectory optimiser (left box in figure V-1).

V.2 Framework set-up

The demonstration of this chapter's objectives are built on top of the simulation environment described in chapter IV, section IV.2. The main change from the workflow described there is the addition of an estimation step, previous to the prediction step. The funcional workflow at the FMS module of the ownship (as conceptually depicted in figure V-1) is the following:

Estimation Estimate the intruder's equivalent take-off mass using DYNAMO and taking into account the stored track of previous positions of the intruder. If no historical information is available (i.e., the very first plan), this step is skipped and the nominal mass from BADA is assumed.

Prediction Compute the predicted intruder's trajectory using DYNAMO taking into account the estimated take-off mass of the intruder as calculated in the previous step.

Baseline Compute the own baseline optimal trajectory using DYNAMO and taking into account the predicted intruder's trajectory. Store this trajectory as the *real* trajectory of the aircraft.

Time-tick At every time tick, the FMS has to perform the following actions:

- Compute the current state of the aircraft (position, velocity, angles, etc.) from the baseline trajectory at the published time-tick.
- Publish the state of the aircraft through the dedicated ADS-B bus.
- Receive the state of the intruder through the dedicated ADS-B bus and store it to form a historical track of data of the intruder. This track of data is used at the Estimation step.
- Monitor the conformance of the intruder to the expected trajectory. If the difference between the expected and the real intruder's position is over a specific threshold, launch a replan that will perform the Estimation, Prediction and Baseline steps.

Results All steps and results of the simulation are logged to prepare the desired outcomes and display them through tables and charts.

This workflow is depicted in figure V-2 as a summary of the flow of events at the software level.

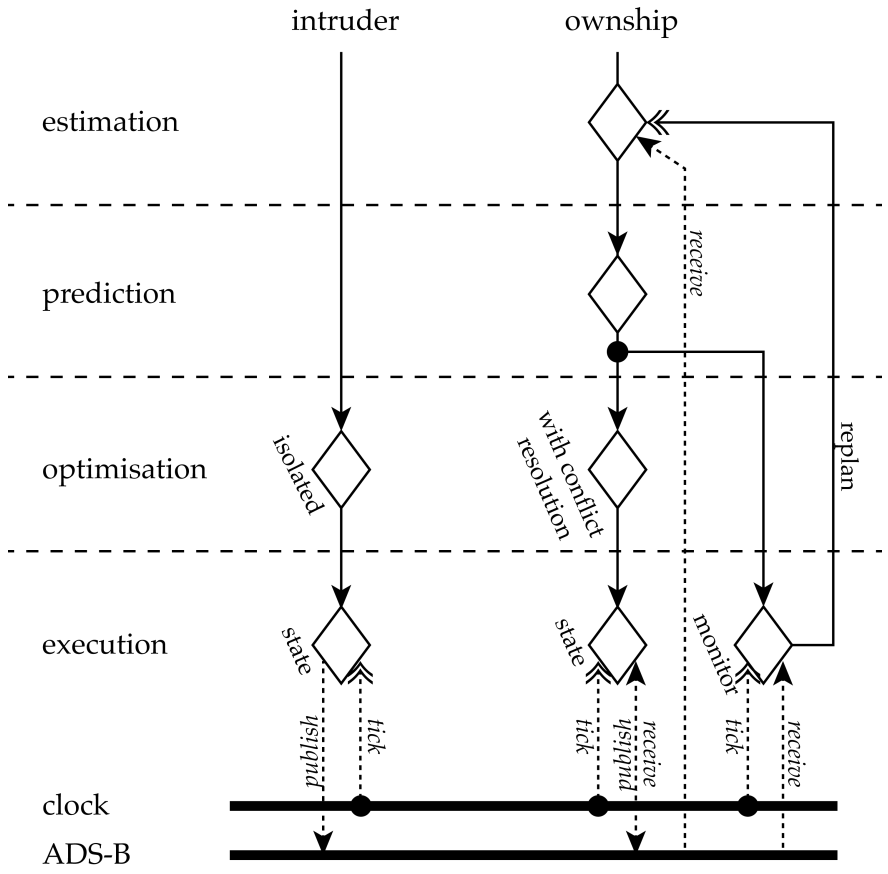

Figure V-2: *Functional workflow of the simulation performed for the demonstration of this chapter's objectives.*

V.3 Numerical results

In the previous chapter, we have presented a study case where a bad assumption of an intruder's mass produces very inaccurate trajectory predictions. To cope with the issue, a conformance monitoring algorithm has been presented that relaunches a new prediction every time the errors jump over a specific threshold. However, due to unchanged wrong assumptions, the new predictions quickly deviate again and rew replans are triggered (see figure IV-6).

This chapter presents the same scenario setup. Again, the same ownship (BCN) is expected to deviate from the same intruder (RES), but due to the already covered limited degree of information sharing between airspace users, the ownship knows very little about the intruder. In this case, the ownship uses BADA nominal parameters and coefficients when predicting the intruder trajectory. In this scenario, this represents a deviation of almost 11% of the actual mass of the intruder (as well as an undetermined bias in the performance model issued by the differences between BADA and PEP).

Besides, and as already said in the introductory paragraphs of this chapter, the conformance monitoring strategy is removed from this scenario. Instead, the replans are triggered on a timely basis. This isolates of the parameter estimation results so these can be read without any interference from external factors. The different results in this section show different trigger rates, based on the readibility of the produced results and plots. The selected trigger rate is directly marked in the plots as the *time of prediction*.

The following subsections deliver results on different situations and aspects of the problematic presented by this scenario.

V.3.1 Vertical predictability

This section presents results on the effectiveness of estimating the mass of the intruder towards prediction accuracy. To do so, two cases are presented as follows:

Case A: Without parameter estimation
The ownship uses the BADA performance model to predict the intruder trajectory. The required unknown parameters are filled with the nominal values of the intruder's aircraft type in BADA. The intruder's basic flight intents are shared through an ADS-B message as a list of fixes (geographic coordinates). Besides, each aircraft broadcasts the current state (position and velocity) through an ADS-B message. This is equivalent to chapter IV, with the added difference that the prediction engine uses BADA instead of Airbus PEP suite.

Case B: With parameter estimation
Same as case A, but once the aircraft takes-off, the ownship uses the intruder's past and current state (from ADS-B) to infer a more accurate value of the intruder's aircraft mass for subsequent predictions.

In all cases, the ownship generates an initial prediction of the intruder trajectory with the said assumptions and assuming both aircraft start flying at $t = 0\,\mathrm{s}$ and do not deviate from their own individually cost-optimal trajectory (i.e., without self-separation). After take-off, a new prediction is generated every $25\,\mathrm{s}$ with the following updated values: current intruder's state (position and velocity, as coming from ADS-B) and, if applicable, updated parameters (i.e., mass in case B).

Figure V-3(a) shows the vertical deviation between each prediction and the reference truth for case A. It can be seen how at each new prediction (for visualisation purposes not all replans are shown), the magnitude of the error decreases sightly, mainly because each time the current position and velocity is corrected and the remaining trajectory is shorter. However, the new prediction deviates rapidly, with a similar rate than the previous calculations. This is expected, since each new prediction has the same parameter assumption errors.

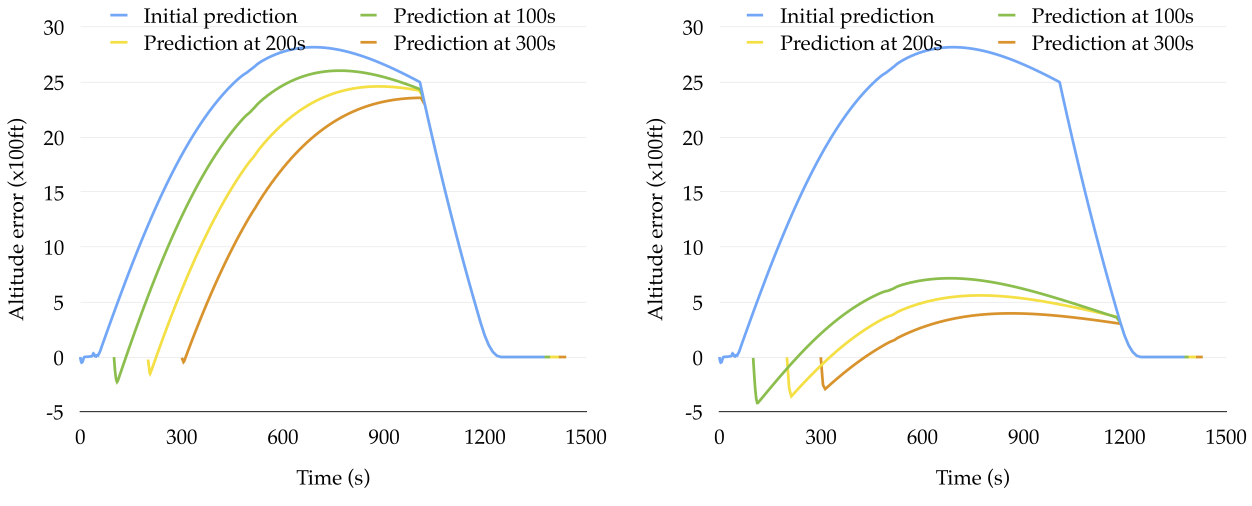

(a) Case A (b) Case B

Figure V-3: *Vertical deviation between the intruder predicted trajectory and the reference truth after each replan for cases A and B.*

This behaviour is, to some extend corrected with case B, as seen in figure V-3(b). As expected, the magnitude of the error for the initial prediction is the same as in case A, since no further information about the intruder is available yet (before take-off). However, the subsequent calculations

have remarcably lower altitude errors. This is thanks to a better estimate of the intruder's equivalent mass (see figure V-4). See how this estimation becomes better and better for later predictions and is confined to vertical errors lower than 700ft (and better) for the whole climbing phase (more than 15 minutes look ahead time). This is due to the fact that a bigger amount of information is available when the parameter estimation process is run (longer trajectory trail), and thus a better mass estimation is produced.

Even if globally the vertical error decreases highly, the moments immediately after the replan are actually worsened. This is due to the fact that the prediction model (based on optimisation), with the new inferred mass and BADA model, finds lower operational costs at higher altitudes. Therefore, the predicted trajectory initiates with a brief acceleration phase (to gain velocity before the steeper climb) that momentarily repercutes negatively on the vertical rate. This could be compensated at the prediction side by expanding the estimation process to further assumptions (besides mass), to enhance the dynamic model and its parameters as a whole. Surely enough, when such parameter deviations are completely removed, and only the mass is wrong (i.e., the utopic case where the aircraft dynamics model of the intruder is very accurate, as assumed in chapter IV), the mass is immediately estimated with no error at all: the optimiser finds the equivalent mass (in this case, equal to the actual mass) without much difficulty.

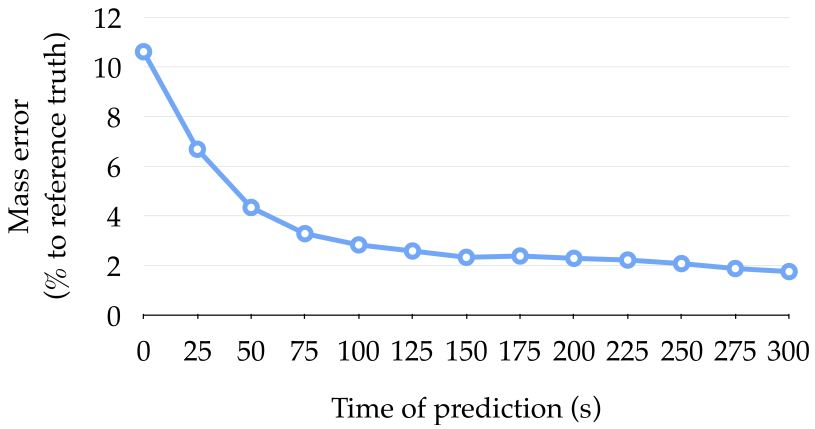

Figure V-4: *Predicted mass error at each replan.*

As already briefly mentioned, this parameter estimation model is actually not intended to infer the real value (and, hence, we should not expect a convergence to the 0% in figure V-4). As said, this process produces an equivalent mass value that minimises the error between the real trajectory trail and a predicted trajectory with BADA. The intrinsinc inaccuracies of this model, bias the estimation process. The effort is then to enable sufficient correcting parameters, which can be estimated, to allow for a prediction model that can be brought closer to the reference truth. This chapter sets the grounds for the authors to continue researching on this matter.

V.3.2 Along track predictability

Surprisingly, despite the proved gains in vertical predictability, figure V-5 demonstrates that along track predictability is not ameliorated with the estimation of the mass alone.

The main reason for this is the difference in flight dynamic models and the way we synthesise the trajectory prediction (which assumes optimisation in fuel). Consequently, BADA model prefers to fly at faster speeds given the fact that these provide lower fuel consumptions at the given estimated mass. To cope with this issue, the parameter estimation model should be enhanced to account for the errors in the calculation of dynamic forces such as drag and thrust and

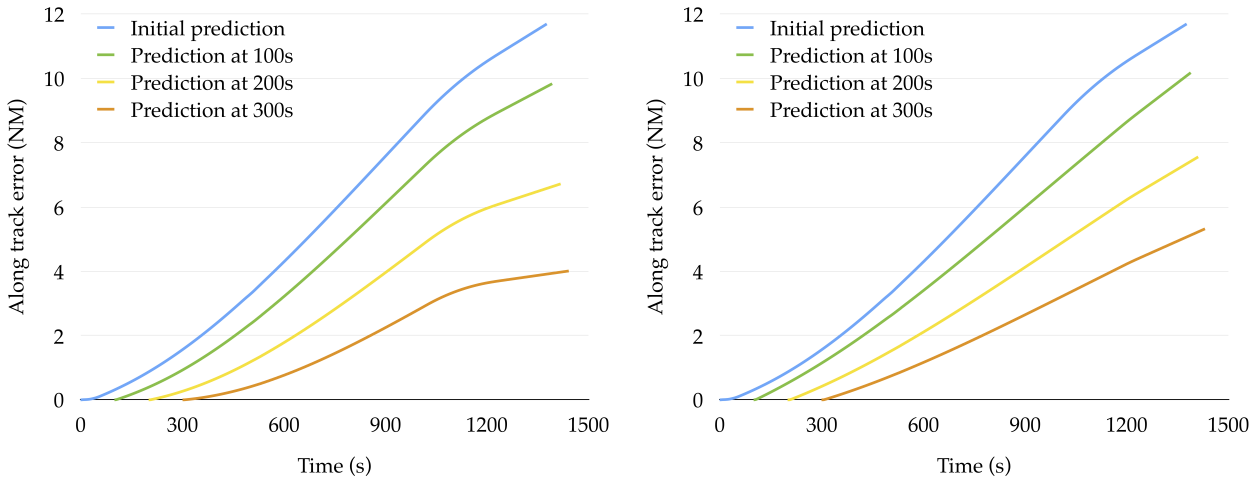

(a) Case A (b) Case B

Figure V-5: *Along track deviation between the intruder predicted trajectory and the reference truth after each replan for cases A and B.*

also the fuel flow dynamics. Alternatively, improved flight intents sharing between aircraft could also help with this issue, as presented in section V.3.4.

Nevertheless, this does not hamper the effective detection of the conflict and its resolution as explained in section V.3.3.

V.3.3 Impact to conflict detection and resolution

The main issue with a bad intruder's trajectory prediction is that it adds a big deal of uncertainty to the detection of possible conflicts in the future. Figure V-6 shows the potential conflict geometry at different prediction times, assuming both aircraft start flying at $t = 0\,\text{s}$ and do not deviate from their own individually cost-optimal trajectory (i.e., without self-separation). For a full prediction at each replan, $\hat{S}_h$ represents the estimated minimum horizontal separation between aircraft, and $\hat{S}_v|_{\hat{S}_h<3\,\text{NM}}$ the estimated minimum vertical separation when the horizontal separation is not granted (in this case study less than 3 NM). The actual horizontal and vertical separation is represented respectively by S_h and $S_v|_{S_h<3\,\text{NM}}$.

Effectively, due to the big errors in the initial prediction, the ownship presumes that the vertical separation is maintained throughout the flight (even if the horizontal minimum separation is not). However, from the real situation (the reference truth) we know this is not so. In case A, soon after take-off a new prediction is generated, but the appreciation of the conflict from the ownship does not change much: the ownship is still oblivious to the future loss of separation (see figure V-6(a)). Effectively, this situation continues until the replan at $t = 200\,\text{s}$, when the ownship finally realises the situation. Dramatically, this is only $106\,\text{s}$ before entering into loss of separation with the intruder.

In comparison, when using a mass estimation process (figure V-6(b)), even if the initial prediction is equally erroneous, case B rapidly corrects for the mass inaccuracies and soon after take-off the ownship predicts that a loss of separation will occur (in the example, this happens at $t = 50\,\text{s}$, but with a higher replan rate this would have been noticed even before). Therefore, this leaves more room for efficient resolution of the conflict: more than $256\,\text{s}$.

Moreover, the impact on the conflict resolution is also huge. Figure V-7 repeats cases A and B but now, at each replan (in this simulation, every $50\,\text{s}$), the ownship generates a new trajectory

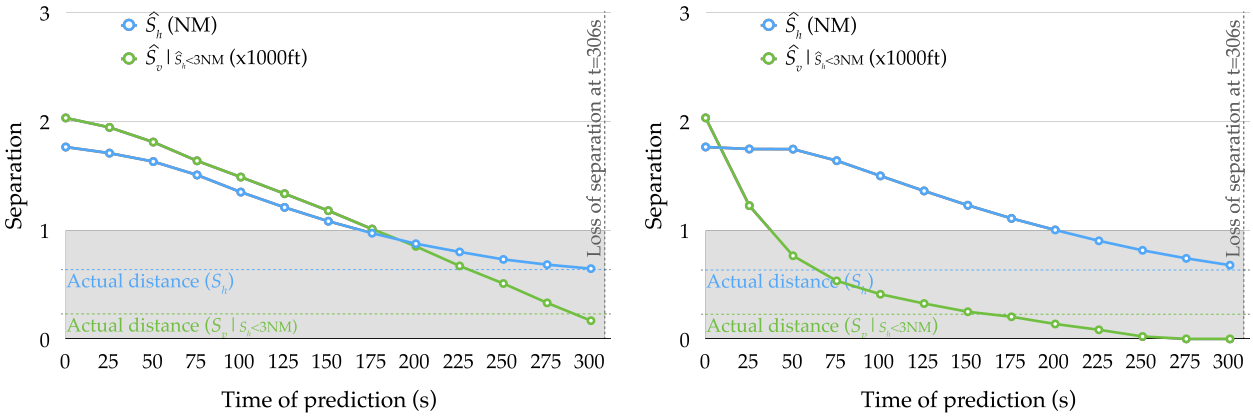

(a) Case A (b) Case B

Figure V-6: *Predicted minimum horizontal and vertical separation between the ownship (BCN) and the intruder (RES) at different predictions and the real situation.*

that resolves all conflicts from the predicted trajectories. Effectively, in case B, BCN starts deviating soon during the flight, resulting in an efficient resolution that only increments the total fuel burned with 5.4 kg. As expected, in case A the reaction comes very late and results in an unavoidable loss of separation.

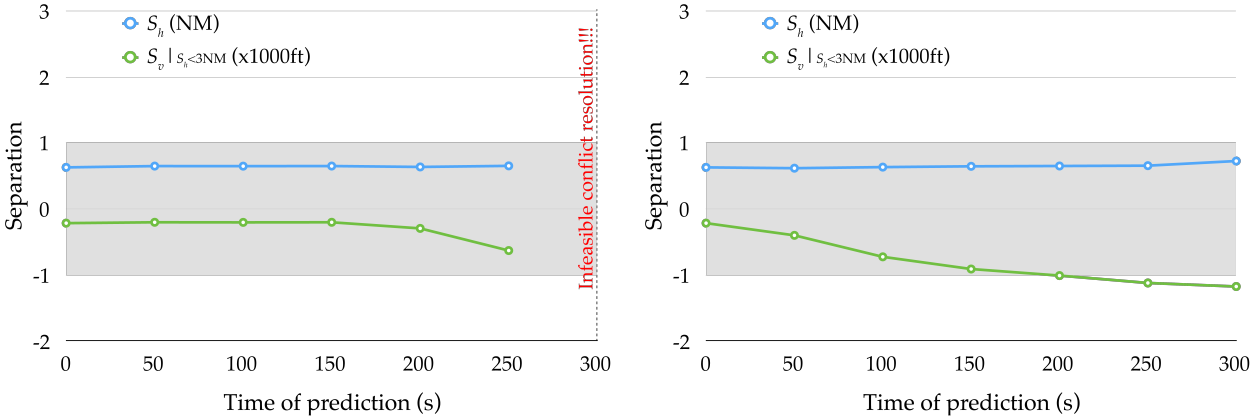

(a) Case A (b) Case B

Figure V-7: *Minimum horizontal and vertical separation between the ownship (BCN) and the intruder (RES) at different replans.*

V.3.4 Enhanced flight plan data

In section V.3.2 one of the conclusions is on the difficulty of enhancing horizontal predictability. To cope with this issue, in this section we propose two new cases (C and D) that provide different type of information in the shared flight intents, to help in the trajectory prediction. Such information is extracted from the Flight Management System (FMS) reference trajectory. At this moment, the uncertainty of such data has been deliberately kept out of the study to isolate the effectivity of the presented concept from other external factors. Additionally, each of these situations will test with

and without parameter estimation (cases A and B).

Case C: Flight Plan with ETA
The shared flight intents contain estimated time of arrival (ETA) at each fix.

Case D: Flight Plan with velocity estimates
The shared flight intents contain estimated velocities at each fix.

Figure V-8 shows the along track deviation error for cases C_A and C_B (vertical errors are similar in magnitude than those for cases A and B respectively, so these are ommited). These plots demonstrate that knowing the ETA at fixes reduces the uncertainty highly. Furthermore, with mass estimation, these are even smaller, and in the example, always lower than 0.1 NM.

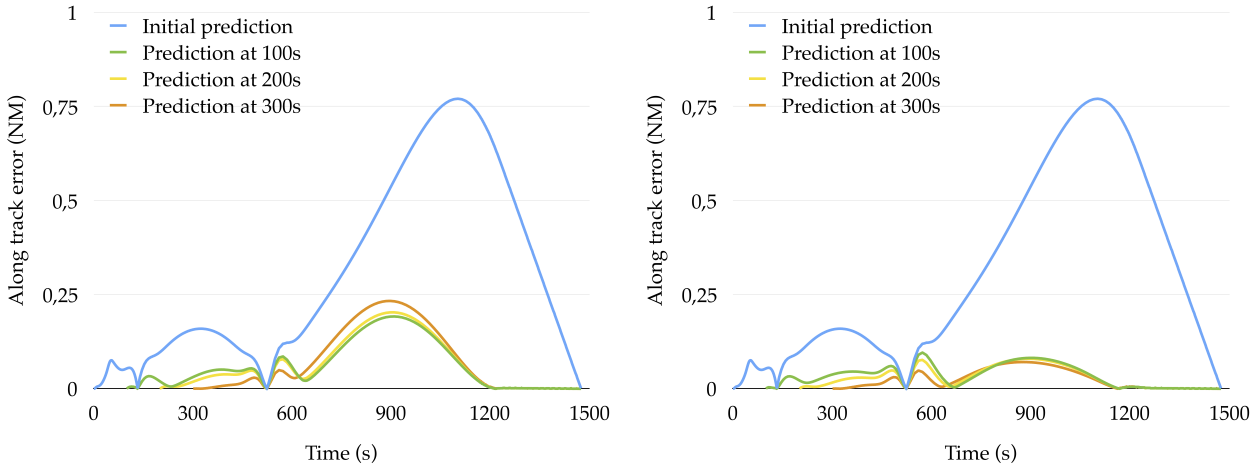

(a) Case C_A (b) Case C_B

Figure V-8: *Along track deviation between the intruder predicted trajectory and the reference truth after each replan for cases C_A and C_B.*

Finally, figure V-9 shows the along track deviation error for cases D_A and D_B. As for cases C_A and C_B, vertical error plots are ommited. In these cases, the along track error is higher when compared to cases C_A and C_B. Again, estimating the mass iteratively helps reducing the error to more than a half.

Conclusively, even if nowadays such information sharing is still far from operational implementation, we present results on the degree that these could help in improving air traffic predictability, more so in combination with the mass estimation model. Besides, similar degrees of information sharing are already contemplated in concepts such as TBO and SWIM and alike, fostered within SESAR and NextGen programmes.

V.4 Conclusion and further work

In a very secretive air traffic system, the application of efficient collaborative operations such as TBO and self separation remain a big challenge. For such concepts to be effective, an accurate awareness of surrounding traffic's future states is required. But such accuracy is impeded when basic aircraft parameters such as aircraft weight, performance data or airline strategies are not available at the time of prediction. In this chapter the authors have described a framework to compensate this hindrance by continuously integrating the state of the surounding traffic to improve the ownship knowledge of other aircraft's dynamics. We use direct collocation methods to

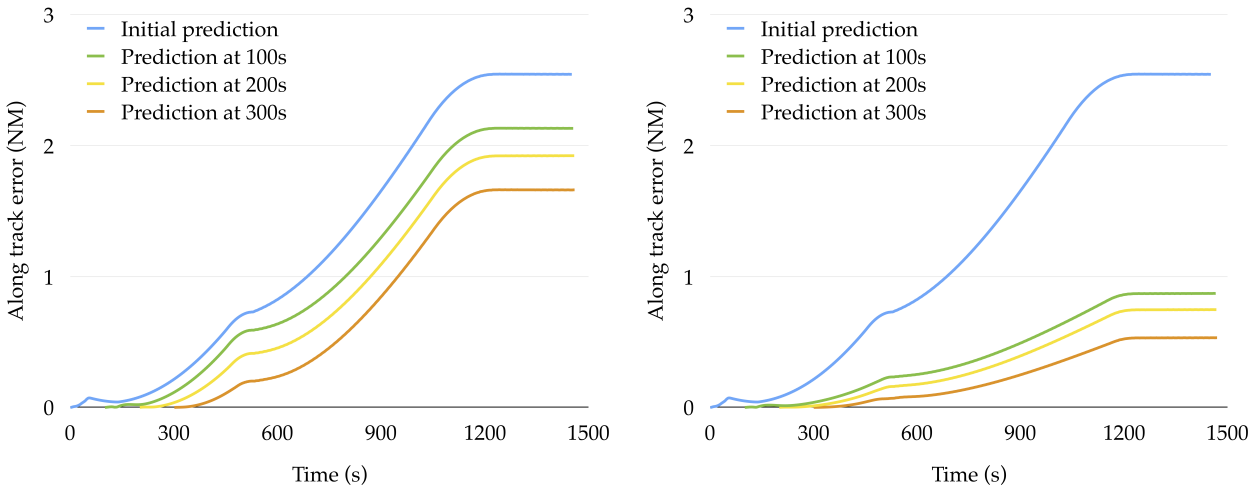

(a) Case D_A (b) Case D_B

Figure V-9: *Along track deviation between the intruder predicted trajectory and the reference truth after each replan for cases D_A and D_B.*

convert the complex problem into a continuous multiphase optimal control problem that is solved with NLP techniques. This same framework is used for conflict-free trajectory optimisation, prediction and parameter estimation.

The effectivity of the whole framework is demonstrated with a semi-cooperative scenario where aircraft current state and future intents are shared between airspace users (ADS-B). In it, two aircraft depart from close-by airports in the Catalonia region, in a configuration that soon leads to a loss of separation. It is shown how the prediction of the potential conflict is enhanced (i.e., is realised earlier by the affected aircraft) when a parameter estimation process is used in combination with the trajectory prediction. Specifically, the estimation of the other aircraft mass, which was previously unknown, is inferred, reaching estimation errors below 2% soon after take-off.

Furthermore, once the ownship has generated a more accurate prediction of the intruder (thanks to a better estimate of the take-off mass) it directly regenerates a cost-optimal conflict-free trajectory of its own, in a continuous iterative process. In the previous chapter, we monitor the conformance of the intruder's current state with respect to the predicted trajectory and relaunch the process when the residuals go over certain threshold, although for simplification and isolation of this chapter's objectives, the current chapter has set this iterations to happen on a timely basis. The fully integrated framework could be assessed in a numerical case study in the future.

Despite the higher vertical predictability, big lateral deviations still occur due to the inaccuracies of the performance model used in the trajectory prediction process. We show an example of how more informed flight intents in combination with the parameter estimation method reduces inacuracies greatly. However, without the will of cooperation and information sharing, this is probably very utopic. Therefore, future research should focus on adding the estimation of other performance parameters (i.e., drag and thrust corrections) and airline strategies (i.e., cost index). Besides, external factors such as meteorological events and ATCo advisories should also be taken into account, along with integrating state sensor errors.

VI

Optimisation of multiple conflicting trajectories in full cooperation

In this chapter we describe a very utopic scenario assuming a fully cooperative situation where **global trajectory optimisation** is possible due to full disclosure of aircraft performance data, cost index strategy and flight intents. Nowadays the strong commercial competition between airlines derive in these not providing such information to other airspace users, and thus such scenario is far from reality. However, the solution to a global optimisation problem should presumably result in the most cost-effective possible trajectories. This chapter explores this global solution and compares its results to the other strategies presented in this thesis.

To this extend, we provide a new mathematical formulation, very strongly based on the optimal control problem formulation for the single-aircraft problem presented in chapter II, but extended to cope with multiple aircraft in the same optimisation problem. It is true that other chapters in this thesis have studied the interference between two aircraft trajectories (an ownship and an intruder). However, this cannot be regarded as multi-aircraft since, even if two aircraft are indeed represented in the problem, only one aircraft is optimised: the ownship deviates from a pre-calculated intruder's optimal predicted trajectory (this strategy is further detailed in chapter IV).

The new problem formulation presented in this chapter allows for the **simultaneous optimisation of an arbitrary number of aircraft in a single optimisation problem**. Indeed, to enable such a global optimisation, the optimising engine has to be fully aware of the mathematical model, the performance coefficients, the cost index strategy, the route, and any other characteristic of relevance of all the aircraft in the scenario.

Even if multi-aircraft optimisation is already a challenge *per se*, with each aircraft having its own individual route, its own parameters, its own start time, its own vertical and speed profile,

etc., it is not an operationally interesting problem. Indeed, it does not make any sense to optimise multiple aircraft simultaneously if their trajectories are completely detached one another, in which case multiple single-aircraft optimisation would be simpler and most probably computationally faster. Such a complex problem only makes sense when all the aircraft in the study enter in conflict at some point during the flight. In this case, the multi-aircraft optimisation problem can alter all trajectories simultaneously to maintain separation at all times. The resolution of these multiple conflicting trajectories pose the two main contributions of this chapter:

- the reformulation of the mathematical approach from the single-aircraft to the **multi-aircraft problem**, allowing each aircraft to have its own specificities; and
- the implementation of a **separation assurance** strategy in the multi-aircraft optimal control problem with accurate **time synchronisation** between all trajectories.

This chapter presents the new formulation of the problem and presents some results for the generic *roundabout* situation of multiple aircraft converging to a same point, and for the specific airport interference scenario presented in previous chapters between Barcelona and Reus.

Please note that the term *global* in the context of this chapter relates to the fact that **all aircraft** are considered in the same optimisation problem, and not to the term used in mathematical optimisation to differentiate between *local* minima and *global* minima (which, in fact, cannot be guaranteed with the gradient based methods used in this PhD thesis).

The following sections are organised as follows:

- Section VI.1 lays out the particularities of the new problem formulation applied to the generic approach described in chapter II regarding the global optimisation of multiple conflicting aircraft in full cooperation.
- Section VI.2 describes the set-up of the optimisation framework described in II.3 for the demonstration of the chapter's objectives.
- Section VI.3 describes the scenarios and results that have been obtained.
- Finally, section VI.4 presents the author's conclusions.

VI.1 Problem formulation

The formulation of the problem laid out in section II.2.1 is multiplied by the number of aircraft (A). Effectively, we divide the multi-aircraft optimisation problem into A **non-consecutive stages**, each stage $a \in \{1, ..., A\}$ pertaining to one aircraft in the problem. Each stage is further divided into N_a **consecutive phases**, which relates to the route (a flight leg) of aircraft a (as described for one aircraft in section II.2.3). See figure VI-1 for a graphical representation of this formulation.

Let $\vec{x}^{(i_a)}(t) \in \mathbb{R}^{n_{x^{(i_a)}}}$ be the state vector describing the trajectory of the aircraft a at phase $i_a \in \{1, ..., N_a\}$ over time $t \in \mathbb{R}$ in the time period $[t_0^{(i_a)}, t_f^{(i_a)}] \subset \mathbb{R}$ and $\vec{u}^{(i_a)}(t) \in \mathbb{R}^{n_{u^{(i_a)}}}$ the control vector that leads to a specific trajectory in that particular phase. The goal of the multi-aircraft optimal control problem is to find the best control vector functions for each phase that minimise a given cost functional $J : \mathbb{R}^{n_{x^{(1_1)}}} \times \mathbb{R}^{n_{u^{(1_1)}}} \times \cdots \times \mathbb{R}^{n_{x^{(N_1)}}} \times \mathbb{R}^{n_{u^{(N_1)}}} \times \cdots \times \mathbb{R}^{n_{x^{(1_A)}}} \times \mathbb{R}^{n_{u^{(1_A)}}} \times \cdots \times \mathbb{R}^{n_{x^{(N_A)}}} \times \mathbb{R}^{n_{u^{(N_A)}}} \to \mathbb{R}$:

$$J\left(\vec{x}^{(1_1)}(t), \vec{u}^{(1_1)}(t), \ldots, \vec{x}^{(N_1)}(t), \vec{u}^{(N_1)}(t), \ldots, \vec{x}^{(1_A)}(t), \vec{u}^{(1_A)}(t), \ldots, \vec{x}^{(N_A)}(t), \vec{u}^{(N_A)}(t)\right). \quad \text{(VI.1)}$$

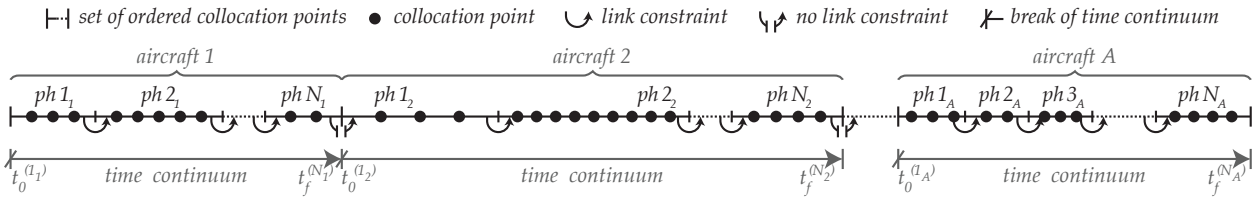

Figure VI-1: *Multi-aircraft problem divided into multiple stages (aircraft) and each stage further divided into phases (flight legs).*

The objective function J defines the problem functional that will be minimised by the algorithm. Notice that the cost functional may depend on quantities computed in each of the $N = \sum_{a=1}^{A} N_a$ phases. Moreover, for each stage a the value of $t_0^{(1_a)}$ is fixed by the scenario definition (i.e., each aircraft can start the trajectory at a different time) and the value of $t_f^{(i_a)}$ is a decision variable itself and will be fixed by the optimisation algorithm (i.e., the optimiser is free to find the best time to end each phase).

Equally to the problem described in section II.2.1, the state and control vectors for each phase remain as described in eq. (II.2) and (II.1), respectively. Also, the dynamics of the system (dynamics of the state vector) are expressed by the non-linear differential equations (II.3), but in this case depend on the aircraft a and are established by non-linear vector functions $\vec{f}^{(i_a)} : \mathbb{R}^{n_{x^{(i_a)}}} \times \mathbb{R}^{n_{u^{(i)}}} \to \mathbb{R}^{n_{x^{(i_a)}}}$ as:

$$\frac{\mathrm{d}\vec{x}^{(i_a)}}{\mathrm{d}t} = \dot{\vec{x}}^{(i_a)}(t) = \vec{f}^{(i_a)}\left(\vec{x}^{(i_a)}(t), \vec{u}^{(i_a)}(t)\right). \tag{VI.2}$$

In addition, the solution might satisfy some algebraic event constraints $\vec{e}^{(i_a)} : \mathbb{R}^{n_{x^{(i_a)}}} \times \mathbb{R}^{n_{u^{(i_a)}}} \times \mathbb{R}^{n_{x^{(i_a)}}} \times \mathbb{R}^{n_{u^{(i_a)}}} \to \mathbb{R}^{n_{e^{(i_a)}}}$ (i.e. initial and final conditions at the different phases of aircraft a), expressed in the general form with vector functions:

$$\vec{e}_L^{(i_a)} \leqslant \vec{e}^{(i_a)}\left(\vec{x}^{(i_a)}(t_0^{(i_a)}), \vec{x}^{(i_a)}(t_f^{(i_a)}), \vec{u}^{(i_a)}(t_0^{(i_a)}), \vec{u}^{(i_a)}(t_f^{(i_a)})\right) \leqslant \vec{e}_U^{(i_a)}. \tag{VI.3}$$

some algebraic path constraints $\vec{h}^{(i_a)} : \mathbb{R}^{n_{x^{(i_a)}}} \times \mathbb{R}^{n_{u^{(i_a)}}} \to \mathbb{R}^{n_{h^{(i_a)}}}$ such as

$$\vec{h}_L^{(i_a)} \leqslant \vec{h}^{(i_a)}\left(\vec{x}^{(i_a)}(t), \vec{u}^{(i_a)}(t)\right) \leqslant \vec{h}_U^{(i_a)}. \tag{VI.4}$$

and simple bounds on the state, control and time variables (box constraints):

$$\begin{aligned} \vec{x}_L^{(i_a)}(t) \leqslant \vec{x}^{(i_a)}(t) \leqslant \vec{x}_U^{(i_a)}(t), \qquad & t_{0_L}^{(i_a)} \leqslant t_0^{(i_a)} \leqslant t_{0_U}^{(i_a)}, \\ \vec{u}_L^{(i_a)}(t) \leqslant \vec{u}^{(i_a)}(t) \leqslant \vec{u}_U^{(i_a)}(t), \qquad & t_{f_L}^{(i_a)} \leqslant t_f^{(i_a)} \leqslant t_{f_U}^{(i_a)}. \end{aligned} \tag{VI.5}$$

In the previous notation, $(\cdot)_L \in \mathbb{R}^{n_{(\cdot)}}$ and $(\cdot)_U \in \mathbb{R}^{n_{(\cdot)}}$ are respectively the lower and upper bounds for these constraints. It should be noted that equality constraints can be defined by setting the lower bound equal to the upper bound, i.e. $(\cdot)_L = (\cdot)_U$.

Even if apparent in the mathematical notation, it is worth emphasising that eqs. (VI.2) to (VI.5) are defined for each aircraft a and each phase $i_a \in \{1, ..., N_a\}$. Therefore, this set of equations is effectively repeated N times, and the compilation of **all** the equations for **all** aircraft and **all** phases of each aircraft would be the full mathematical definition of the problem constraints. In other words, this allows the dynamics of the system, the event, path and box constraints to be different for each aircraft and for each phase of each aircraft.

To ensure that the consecutive phases of an aircraft are correctly linked one another in compliance with the dynamic models, and that they relate to the time continuum they represent, the following constraint applies to the state vector of each aircraft a:

$$\vec{x}^{(i_a+1)}(t^+) - \vec{x}^{(i_a+1)}(t^-) = 0;\ i_a = 0, \dots N_a - 2. \tag{VI.6}$$

Note that eq. (VI.6) does not link two phases corresponding to two different aircraft. As already mentioned, each aircraft is free to fly as many phases as its route requires, independently to other aircraft in the optimisation problem. Furthermore, each aircraft will start and end its route as desired, without having any dependency to the order or sequence in time of other phases of other aircraft.

VI.1.1 Optimisation objective

The goal of our multi-aircraft optimisation problem is to find the best trajectories for all aircraft that minimise the following cost functional:

$$J = \sum_{a=1}^{A} \sum_{i=1}^{N_a} \int_{t_0^{(i_a)}}^{t_f^{(i_a)}} FF_a(\vec{x}^{(i_a)}, \vec{u}^{(i_a)}) + CI_a \mathrm{d}t. \tag{VI.7}$$

See that the cost index (CI) depends of aircraft a. Effectively, each aircraft will have its own cost structure and its airline policy. Similarly, the fuel flow (FF) is also specified for each aircraft, given the differences in aircraft model, performance coefficients, etc. of each aircraft.

VI.1.2 Separation assurance

One of the main challenges when separating two trajectories is the perfect alignment in time of the position points so a fair comparison can be performed. In other words, aircraft separation is lost when two aircraft are at each other's protection volume **at the same time instant**. Hence, comparing two points in space that differ in the time dimension has no meaning for separation purposes.

As already mentioned in chapter II, the optimisation problem described in this thesis relies on discretisation techniques that convert the infinite-dimensional original problem into a finite-dimensional NLP problem in the time interval $[t_0^{(1)}, t_f^{(N)}]$. To do so, a collocation strategy is performed resulting in collocation points in the time dimension. Furthermore, these are placed in the time dimension at the optimiser's discretion to fulfil the problem constraints in an optimal trajectory.

In the previous chapters, the position of the ownship, directly available from the state vector at the discrete time instants over the N phases $\vec{t} = [t_0^{(1)}, t_1^{(1)}, \dots, t_f^{(1)}, t_0^{(2)}, t_1^{(2)}, \dots, t_f^{(2)}, \cdots, t_0^{(N)}, t_1^{(N)}, \dots, t_f^{(N)}]$, is compared to the intruder position, directly available from the continuous curves represented by Γ, as described in section IV.1.1.2. See how the *continuous* nature of Γ ensures that whatever discrete time instants in $\vec{t}$, the position of the intruder is always available. This is possible due to the *static* nature of the intruder prediction: during the optimisation problem resolution, Γ will remain unchanged (i.e., the ownship solely manoeuvres to resolve the conflict).

In this chapter, however, not only the ownship but also the intruder(s) are prone to deviate from their originally planned trajectory to resolve the conflict. Therefore, an intruder trajectory cannot be assumed *static* and the splines represented by Γ are no longer valid. The mathematical formulation of this statement has been presented above, where each aircraft a has a different set of

time samples $\vec{t}_a = [t_0^{(1_a)}, t_1^{(1_a)}, \ldots, t_f^{(1_a)}, t_0^{(2_a)}, t_1^{(2_a)}, \ldots, t_f^{(2_a)}, \cdots, t_0^{(N_a)}, t_1^{(N_a)}, \ldots, t_f^{(N_a)}]$, which result in incomparable collocation points between aircraft as depicted in figure VI-2.

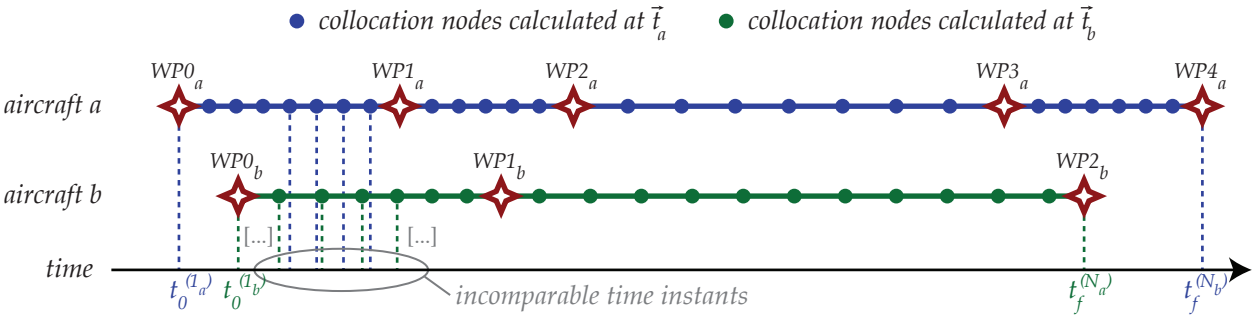

Figure VI-2: *Collocation nodes for two trajectories in relation to the time dimension.*

In the literature, many studies simplify the optimisation scenario and do not directly face this issue. Most of the times, constant speed, altitude or even fixed time intervals are assumed in a simplified one-phase scenario, removing thus such incompatibility problem (Hu *et al.*, 2002; Omer & Farges, 2012). Others, adjust the number of nodes and project them forwards or backwards to have smaller time differences when comparing the 4D collocation points (Soler *et al.*, 2012). In (Bittner *et al.*, 2014) the authors assume that all aircraft start at the same point in time and the collocation points are evenly spaced and introduce a fade-out condititon to aircraft.

For a bigger flexibility and more freedom to each individual flight, we present a novel approach where the dependency upon the exact location of the collocation points is removed. Instead of using the aircraft coordinates defined in the state vector (e, n, h) and compare them to these of the other aircraft (again, at uncomparable collocation points), we define a new set of auxiliary variables (e'_a, n'_a, h'_a) for each aircraft a that are calculated following the dynamics of its counterparts but are discretised equally for all aircraft (e.g., every 5s starting at t'_0). Hence, these allow for a fair spatial comparison between the trajectories as shown in figure VI-3.

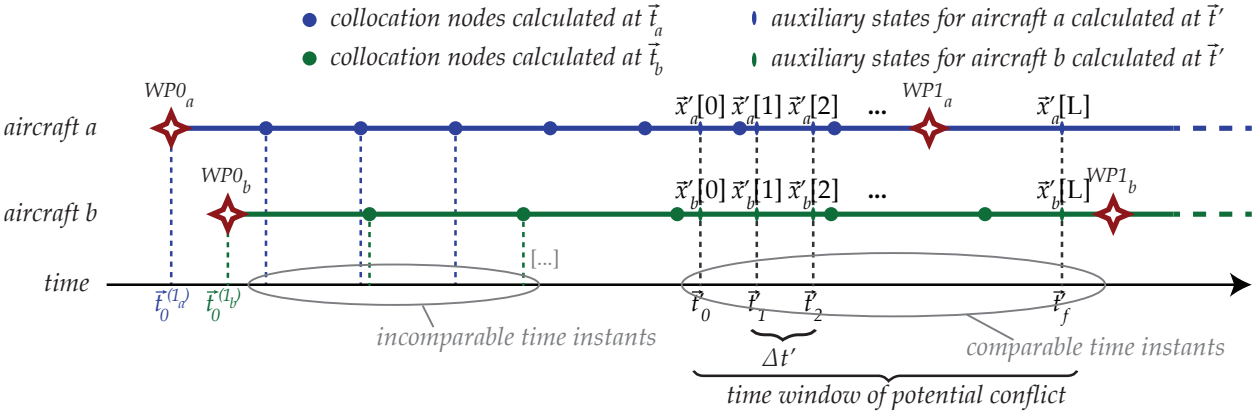

Figure VI-3: *Collocation nodes and comparable auxiliary variables for two trajectories in relation to the time dimension.*

Let $\vec{x}'_a(t) = [e'_a(t), n'_a(t), h'_a(t)]$ be the auxiliary state vector describing the trajectory of the aircraft a over time $t \in \mathbb{R}$ in the time period $[t'_0, t'_f] \subset \mathbb{R}$ (which can relate to the whole time period of the full scenario, or only a part of it if the conflicts in the scenario are known to be constrained in a specific time window). Let $\vec{t}' = [t'_0, \ldots, t'_f]$ be the discretised vector of L time instants equally spaced by the chosen interval $\Delta t'$ (referenced to as *comparable time instants* in figure VI-3). And recall $\vec{t}_a$ as the discretised vector of time instants at the M_a collocation points of aircraft a, spaced

at intervals at the optimiser's discretion (M_a relates to the aggregate number of collocation points for all phases of aircraft a). Even if $\vec{x}'_a(t)$ is continuous throughout its domain, it is calculated at the $\vec{t}'$ instants $[\varrho]$ as a function of $\vec{x}_a$ at the $\vec{t}$ instants $[\varsigma]$, as follows:

$$\vec{x}'_a[\varrho] = \sum_{\varsigma=0}^{M_a-1} \left(\vec{x}_a[\varsigma] + \dot{\vec{x}}_a[\varsigma](\vec{t}'[\varrho] - \vec{t}[\varsigma]) \right) \Upsilon(\varrho, \varsigma) \tag{VI.8}$$

where Υ is a piecewise switching function that depends on ς (the collocation index in $\vec{t}$), ϱ (the comparable collocation index in $\vec{t}'$), and k as the steepness coefficient of the switching function:

$$\Upsilon(\varrho,\varsigma) = \begin{cases} (1 - \left[\frac{1}{2} + \frac{1}{\pi}\arctan(k(\vec{t}'[\varrho] - \vec{t}[\varsigma]))\right]) & \text{if} \quad \varsigma = 0 \\ \left[\frac{1}{2} + \frac{1}{\pi}\arctan(k(\vec{t}'[\varrho] - \vec{t}[\varsigma]))\right] - \left[\frac{1}{2} + \frac{1}{\pi}\arctan(k(\vec{t}'[\varrho] - \vec{t}[\varsigma+1]))\right] & \text{if} \quad 0 < \varsigma < M_a - 1 \\ \left[\frac{1}{2} + \frac{1}{\pi}\arctan(k(\vec{t}'[\varrho] - \vec{t}[\varsigma+1]))\right] & \text{if} \quad \varsigma = M_a - 1 \end{cases} \tag{VI.9}$$

This formulation allows for a continuous and differentiable function (i.e., numerically friendly) that calculates the east, north and altitude coordinates of each of the aircraft in the study completely independent of the collocation strategy at the NLP. Furthermore, note how $\vec{x}'_a(t)$ is completely agnostic from aircraft phases. Therefore, in the previous notation, the $(\cdot)^{(i_a)}$ superscript denoting the phase has been removed and replaced directly by $(\cdot)_a$ (i.e., depending only of aircraft a). This is specially relevant for the state vector $\vec{x}$, which, in the problem formulation presented in this chapter depends of the phase i of aircraft a and is actually written as $\vec{x}^{(i_a)}$. Finally, even if the full state vector $\vec{x}$ is used in eq. (VI.8), only the east, north and altitude coordinates are relevant: even if all other state variables can also be calculated in the equally spaced instants of $\vec{t}'$, they are not relevant for the separation purposes for which this whole strategy is actually implemented. For a graphical example of eqs. (VI.8) and (VI.9), see figure VI-4.

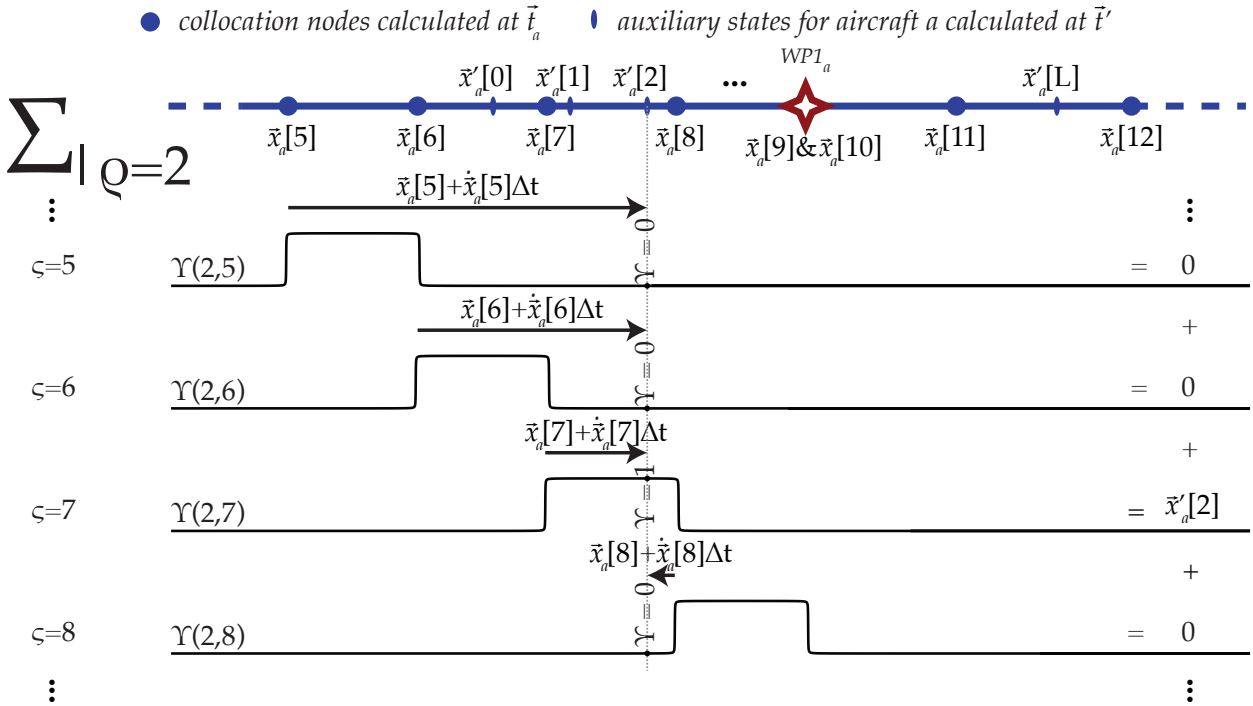

Figure VI-4: *Graphical example of the resampling strategy for $\varrho = 2$ and summatory iterations $\varsigma = \{5, ..., 8\}$.*

As already briefly mentioned, the initial and final times of comparison $[t'_0, t'_f]$ are known variables that represent the time window during which the conflict is expected. This can actually represent the whole time span from the start time of the first aircraft to a time after the estimated end of the last aircraft, or can be carefully selected to represent only the instants before, during, and after the conflicts in the scenario. Besides, the time interval between two instants in $\vec{t}'$ ($\Delta t'$) can be configured. The best combination of these parameters must be sought to bring enough accuracy to the solution, whilst not increasing too much the computational burden. Also, a good point of this strategy is that it decouples how disperse the collocation nodes are to the actual calculations of separation assurance. This would allow having the state nodes with big time intervals but still comparing aircraft positions at, for example, every second. The values of $[t'_0, t'_f]$ can be easily inferred after generating the optimal trajectory of each route independently and assessing the potential conflicts. This reference single-aircraft optimal trajectory is used as the initial guess for each aircraft in the multi-aircraft problem, which renders faster convergence to a feasible solution.

Conclusively, this whole strategy presented with eqs. (VI.8) and (VI.9) is effectively a resampling of e, n and h so that they can be used for a fair comparison between aircraft for separation assurance purposes. In other words: the state variables in $\vec{x}$ modulate the trajectories to fulfil the dynamic, spatial, time and velocity constraints defined in the scenario, whereas the auxiliary variables in $\vec{x}'$ are calculated for the sole purpose of keeping aircraft away from each other.

The constraint that maintains the separation between aircraft has been already presented in eq. (IV.5) for an ownship and an intruder. For the multi-aircraft problem tackled in this chapter, we define a set $\mathcal{A}$ that contains all the combinations of two different aircraft (a, b) in the scenario, and the separation constraint is reformulated with the following set of equations:

$$\underset{(a,b)\in\mathcal{A}|a\neq b}{\forall} \left(\frac{(e'_a(t) - e'_b(t))^2 + (n'_a(t) - n'_b(t))^2}{{d_h}^2} \right)^p + \left(\frac{(h'_a(t) - h'_b(t))^2}{{d_v}^2} \right)^p \geq 1 \tag{VI.10}$$

VI.2 Framework set-up

To demonstrate the methodology presented in this chapter, we use the same optimisation framework that has been described in chapter II, and used throughout the thesis. The theoretical background that lies behind this chapter does not require a real-time simulation environment, and therefore only DYNAMO is used.

The description of the scenario is, however, more complex than in all previous chapters, as we now define multiple aircraft, each with its own route, in the same problem definition (i.e., the same scenario file contains multiple routes).

No further intrication is found in the demonstration: after defining the scenario, we call DYNAMO directly on a static environment and when the results are available, we prepare them manually for presentation.

VI.3 Numerical results

This section presents two case studies: a very simple scenario for the typical *roundabout* problem of four aircraft converging to one central point, and another scenario which replicates the airport interference situation between Barcelona and Reus that has already been presented in the other chapters of this thesis. The aircraft of study for the two cases is the same Airbus A320 presented in the previous chapters with a $CI = 0$.

VI.3.1 The *roundabout* problem

The typical *roundabout* problem comprises four aircraft climbing to an altitude of 2500ft with free lateral, vertical and speed profiles. The simplicity in this scenario (single phase, same number of collocation nodes per each aircraft, identical aircraft type, same initial time instant, *allegedly*-same along path distance, etc.) would also allow a *semi*-fair comparison by directly comparing the state vector of each aircraft at the collocation nodes. However, since it is the optimiser's discression to place the collocation nodes along the time dimension (and $t_f^{(N_a)}$ is not fixed), the collocation nodes could still have (even if presumably small) time divergences between aircraft.

This *direct comparison* strategy is compared to the *resampling* strategy presented in section VI.1.2, and the results are shown in figure VI-5. Surprisingly enough they show differences in the resulting trajectories: the *direct comparison* strategy deviates only in the horizontal dimension (leaving identical vertical profiles for all trajectories) whereas the *resampling* strategy deviates both in the vertical and horizontal dimensions, allowing a shorter path (and a slightly shorter time).

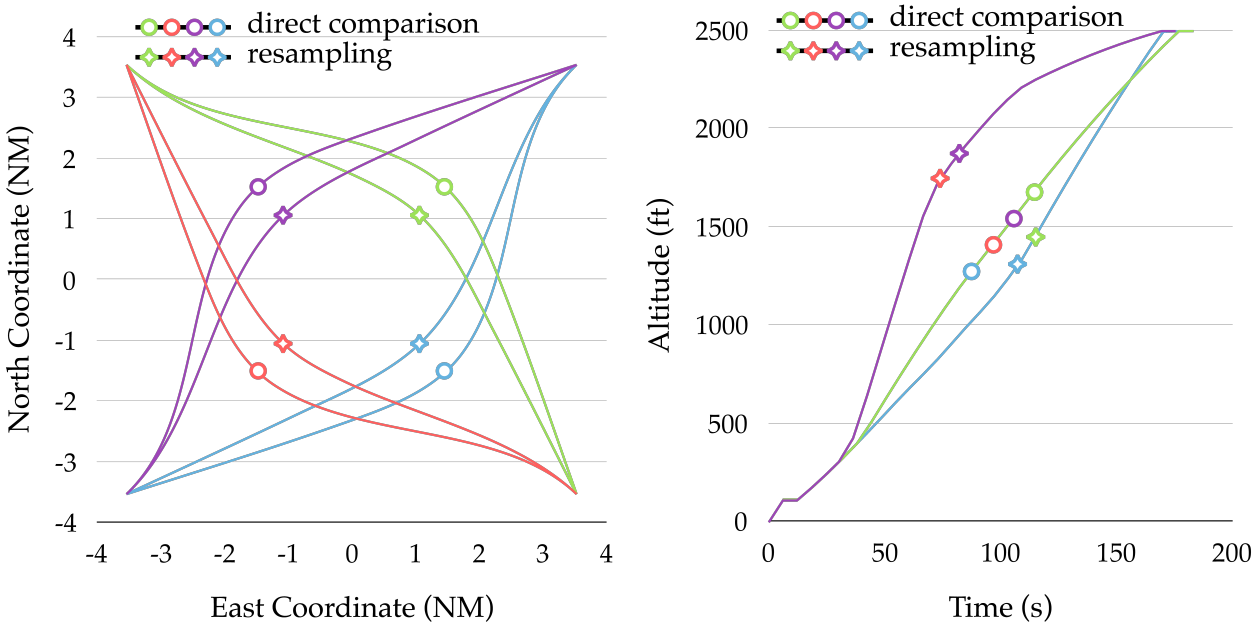

(a) Lateral profile

(b) Vertical profile

Figure VI-5: *Typical* roundabout *problem with complete lateral, vertical and speed freedom of four aircraft (purple, blue, red and green) converging in one central point.*

This simple non-realistic scenario demonstrates that the *resampling* strategy works: the four aircraft never violate the minimum separation requirement. Furthermore, when studying the deviation of the resampled collocation nodes from the original collocation nodes (compared in post-processing), the results show no difference at all, proving that even if the resampling is done using a very complex strategy using switching functions (described in section VI.1.2), no error is introduced.

Also, as expected, whereas the *direct comparison* strategy shows slight time differences between the time instants at the compared collocation nodes (not visible in the figures), the *resampling* strategy enforces exact time instances. This, even if not really rellevant in this simple scenario, becomes a real advantage for more complex scenarios, where *direct comparison* is not even a valid option. To better understand this issue, let's recall some concepts: the phases represent the different waypoints along the route; each phase can have a different number of collocation points; each phase is delimited in time by an initial and final time (none of which is fixed previous

to the optimisation execution, unless required times of arrival are enforced); the duration of each phase is unknown, and therefore the time interval between collocation points in the phase is also unknown. This complex architecture is the basis of the flexibility to configure all kinds of flights and routes in this thesis optimisation framework. And this same architecture has been maintained when solving the multi-aircraft problem (as already explained in section VI.1.2), keeping thus the same flexibility for each aircraft (same as when individually solving the single-aircraft problem). Given all these summarised statements, one can easily deduce why *direct comparing* the state vector at the collocation points of two different aircraft is not valid under this architecture.

The following section presents a more complex scenario where, indeed, only thanks to the *resampling* technique proposed in this thesis the two aircraft positions can be compared, and a valid conflict resolution is produced.

VI.3.2 Airport interference problem

This section presents a more complex and realistic situation, based on the scenario already described in previous chapters, with trajectories following standard instrumental departures for Reus and Barcelona (i.e., multiple phases, completely different routes, etc.). Figure VI-6 shows different results for this scenario, corresponding to the different optimisation and deconfliction strategies described in this thesis. First, the independently optimal trajectories (*baselines*) are presented for Barcelona (BCN) and Reus (RES), using the single-aircraft problem described in chapter II (i.e., no deconfliction). Then, a semi-cooperative scenario is presented where the ownship (RES) separates from the intruding trajectory (BCN), which effectively corresponds to the results of chapter IV. Finally, a global optimal solution is presented, corresponding to the multi-aircraft optimisation problem presented in this chapter.

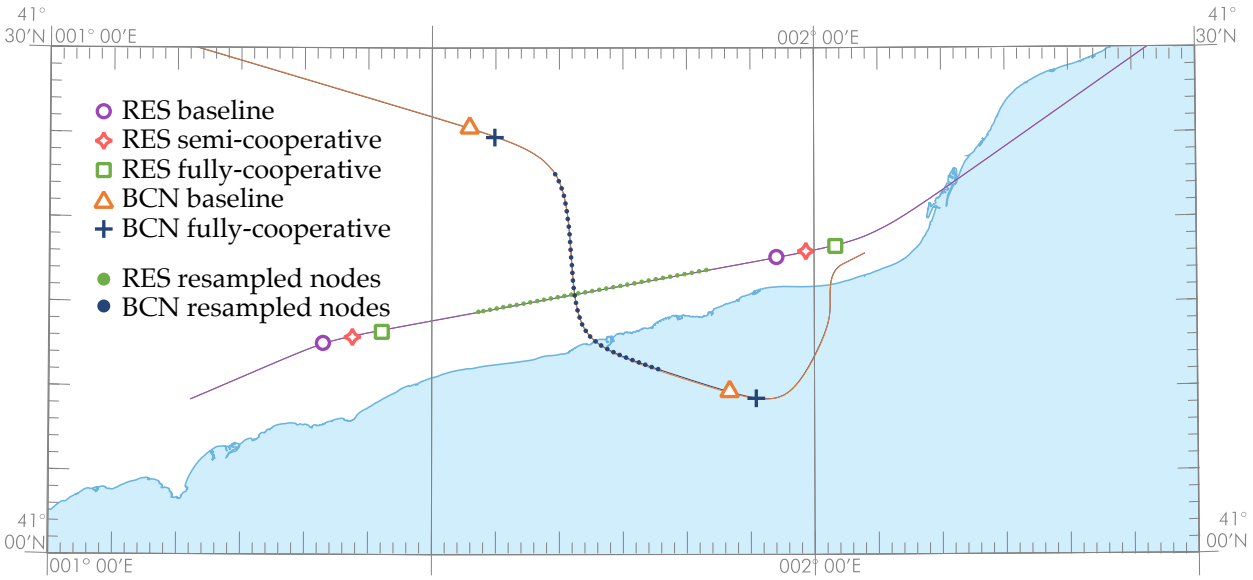

Figure VI-6: *Horizontal profile for RES and BCN departures in the different optimisation and deconfliction strategies.*

See how for the execution of the fully-cooperative solution, the separation assurance strategy has not been performed for the whole scenario duration: to reduce the computational complexity, this has been limited to the instants before, during and after the conflict. This can be seen in the figure, represented by solid circles, every circle corresponding to a *resampled* collocation node (the resampling interval $\Delta t'$ is 10s).

In this example, the conflict is resolved mostly on the vertical dimension, both for the semi-

cooperative and the fully-cooperative cases, leading to very similar horizontal profiles and therefore they all appear overlapped in the figure. Figure VI-7 shows the vertical deviations (when compared to the baseline) performed to maintain the required separation.

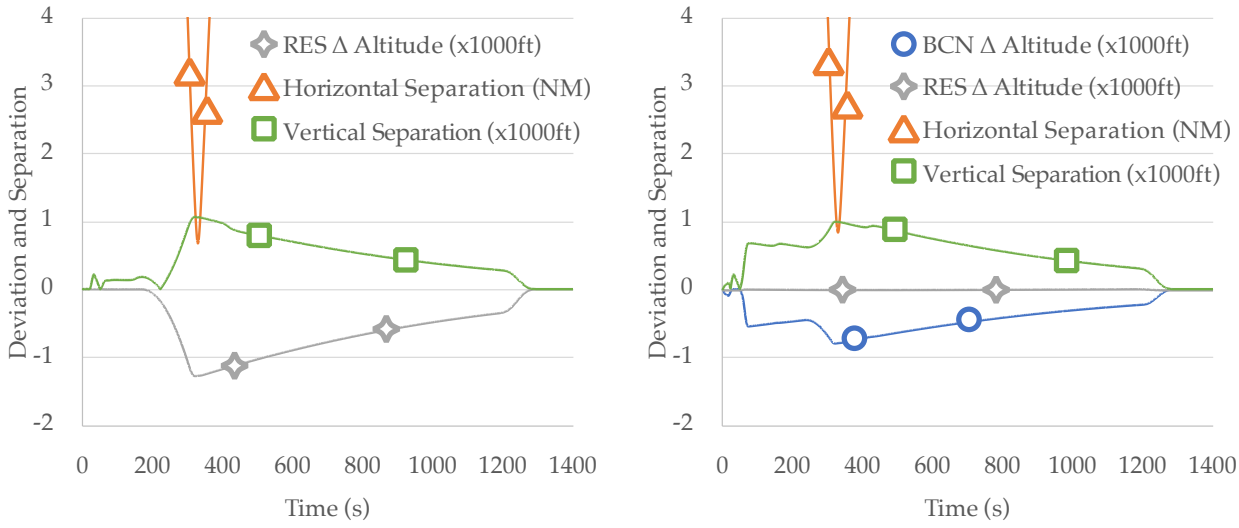

(a) Semi-Cooperative

(b) Fully-Cooperative

Figure VI-7: *Vertical deviations (from the reference) for RES and BCN departures to maintain separation between aircraft.*

Effectively, the conflict is mostly resolved by action taken on the vertical profile: both subfigures show how the vertical separation is the required minimum 1000ft at the moment of losing the horizontal separation. For the fully-cooperative case, the similitude of the curves for the vertical separation and the altitude deviation of BCN denotes that the conflict is mostly resolved by action taken by the aircraft coming from Barcelona. This is quite unexpected (both aircraft are free to take action), but corresponds to the decision of the optimiser for this very specific conflict resolution, and other conflict geometries would presumably have different results. This is even further evidenced when comparing the cost increase: the cost increase for RES is almost zero, whereas the cost increase for BCN is slightly bigger.

With the objective of showing what could happen in cases where separating on the vertical dimension is not an option, or a less favorable one, we provide another perspective of this same scenario. Actually, the exact same scenario is kept, with only one difference: we force the separation on the horizontal domain. This extends the results presented in the previous paragraphs by showing whether deviating laterally increases by much the total operational cost. The horizontal profile for this scenario is depicted in figure VI-8.

See in this case that the horizontal deviation is evident. As expected, the semi-cooperative case shows the highest deviation as only the ownship takes resolutive action. Indeed, the fully-cooperative case shares the horizontal deviation between BCN, and RES, summing up to a lesser increase in the traveled distance.

The results in terms of fuel are really similar between the semi-cooperative and the fully-cooperative cases. Indeed, only a few kilograms of burned fuel and a few seconds in the flight time separate the two strategies, negligible when compared to the total fuel burned and the total flight time (up by two to three orders of magnitude). Effectively, the objective function is very flat: different trajectories provide very similar results (in this case, separating horizontally or vertically is quite similar in terms of fuel burned). Nevertheless, when compared to the current air traffic control strategy, the results presented in this thesis are indeed very promising.

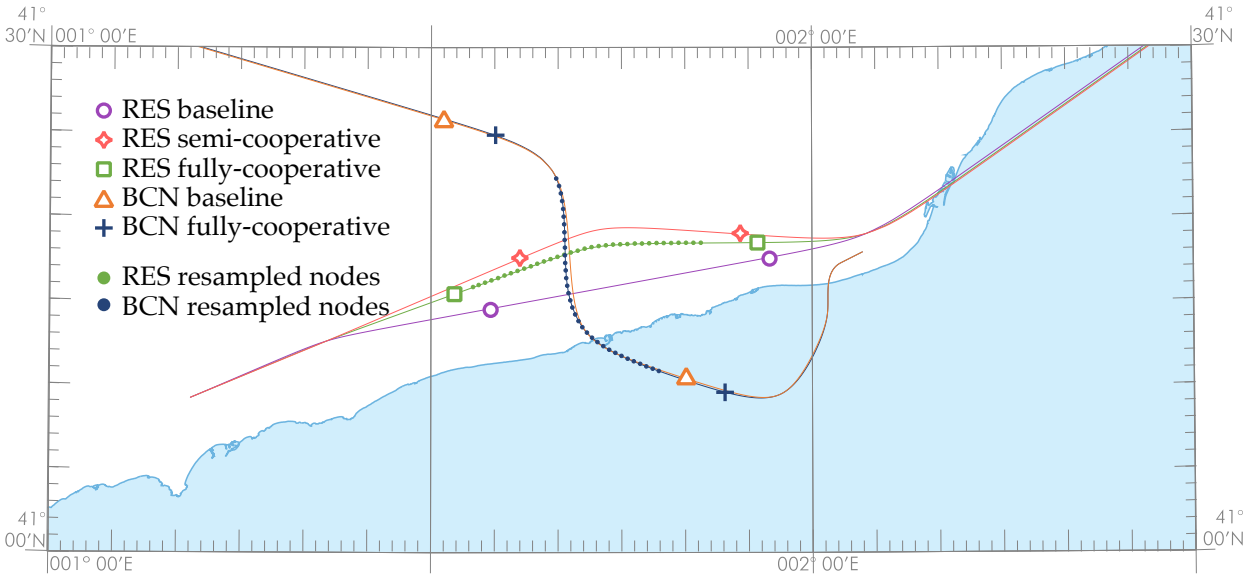

Figure VI-8: *Horizontal profile for RES and BCN departures in the different optimisation and deconfliction strategies, separating only on the horizontal dimension.*

VI.4 Conclusion and further work

This chapter resolves the airborne aircraft conflict in a single optimisation problem with separation assurance. This gives the overall cost-optimal trajectories that all involved aircraft could follow without violating the separation constraints. However, this requires full collaboration and a great amount of information sharing betweeen airspace users. Besides, the gains in operational cost of the fully-cooperative when compared to the semi-cooperative are negligible in the numerical example. This could be only intrinsic to this specific scenario, but even so it is an interesting outcome.

The operational implementation of this fully collaborative paradigm is very complex and presumably still far off in the future. Even if the results in this chapter show that for the presented scenario a semi-cooperative case if quite similar in cost, the fully-cooperative solution shares responsibility between all aircraft. This leads to a more balanced and commercially *fair* resolution of the conflict. Therefore, the tradeoff between added deployment complexity (for a similar global cost) versus the fairness of the conflict resolution to all actors is something to be further adressed.

Indeed, in future research more scenarios should be prepared to demonstrate the potential gains of this method in other conflict geometries. Besides, to reduce operational implementation complexity due to secretive airline strategies, the minimum required amount of information sharing between involved actors should be sought, as well as finding alternatives to securely share sensitive data among airspace users (e.g., *blockchain*, *smart-contracts*, business-to-business services, etc.).

Furthermore, the conformance monitoring and parameter estimation presented in previous chapters could be implemented in combination with the global optimisation presented here, which could bring interesting results. In it, the results presented in this chapter would only be the initial planning of the situation. When aircraft started flying, the conformance monitoring would detect deviations (either for a wrong piece of shared information, for inacuracies of the performance model, or for unknown weather along the route) and recalculate the whole situation (or part of it, to be studied) for a new global optimal. Models, methods and tools (plus the simulation environment) to support for this futuristic scenario have been proposed in this thesis, but the outcomes of it are, at this moment, out of the scope of this work.

VII

Concluding remarks

Air traffic globally is evolving towards higher efficiency in an effort to reduce the emission of noise and pollutants to the environment. Aircraft structures, engines, ground infrastructures, procedures and overall systems are gradually upgraded to reach this neverending goal. The work presented within this thesis seeks to contribute from an ATM perspective by presenting the problematic of poor aircraft predictability in dense traffic areas and providing methods and tools to improve capacity and efficiency in these. Part of this work is focussed on the definition and modelling of the problem, which poses the adequate issues to address, and the other part works on potential solutions to these. A complete and ultimate solution to all problems is (obviously) not provided, so some topics have been detected that remain for further research. The following sections list the main conclusions of the achieved results and hints the possible lines where further research should follow.

VII.1 Summary of contributions

The main contributions of this PhD thesis are summarised as follows:

Definition of an optimisation framework

- An **optimisation framework** is presented as the main support tool for the evaluation and resolution of the presented issues. This framework has been built in a modular way which allows for the resolution of diverse problems, including the **optimisation of a single aircraft** through a predefined route and the resolution of a **multi-aircraft deconfliction problem**. After presenting the lacks and virtues of other optimisation methods, an optimal control prob-

lem is described which offers good flexibility and performance and allows for high accuracy of the mathematical model (equations of motion, atmosphere, wind, splines, etc.). The continuous infinite-dimensional real-world problem is converted into a finite-dimensional non-linear programming (NLP) problem with a finite set of decision variables.

- The presented optimisation framework can be configured to resolve a good diversity of optimisation problems. Via a scenario definition mechanism, using configuration files, and the implemented modularity through the different C++ and GAMS software modules, the framework provides results for trajectory optimisation, trajectory prediction and parameter estimation problems of different kind and complexity. Together with a simulation environment, these serve the purpose of evaluating current ATM paradigm structure and procedures, along with proposing enhancements for a more sustainable future.

- As briefly mentioned, the same framework is presented to provide **trajectory prediction** functionality. Instead of the conventional numerical integration of aircraft dynamics with an iterative process to meet the published intents, *we propose to use an optimisation method for trajectory prediction*. The optimisation problem will modulate the controls as required in order to comply with the set of constraints, finding not only one of the possible solutions to the prediction problem (e.g., climb first vs. accelerate first), but the one that is most cost effective. The assumption of the objective function allows for more flexibility than the conventional assumptions taken for prediction methods (fixed throttle setting, vertical speed, flight path angle, etc.). This method allows for more complex predictions and can potentially provide more accurate results when many restrictions apply to a trajectory.

- Also, the same framework is presented to provide **parameter estimation** functionality. The idea behind this is based on exploiting the past known states of an intruder trajectory to better predict its future states. Using ADS-B messages, the ownship can generate a trailing trajectory that positions the intruding aircraft along the time (in the past). The longer this trailing trajectory, the more can be extracted from it. Then, the optimisation framework is configured to find the initial equivalent mass that would generate a trajectory as close as possible to this trailing path. In this case, the cost functional is set to the root mean square of the difference between trajectories.

Functional application and thesis results

- A sensitivity study has been developed to assess the potential (loss-of)gains of continuous vertical profile operations when implemented in dense traffic areas using RTAs to mitigate the negative impact to airspace capacity. Numbers show that **imposing RTA at fixes produce higher costs when compared to unrestricted continuous operations**. However, when compared to level-off phase (as current ATCo may impose for tactical separation), the gains are considerable, **reaching very low increases in cost when the RTAs are defined in collaboration** to all aircraft involved in a potential conflict. The study shows a comprehensive sweep of RTAs and CI values with the attributable cost impact and the resulting separation between aircraft. It is proposed that having such results in a *live* situation (and updated in real time for the traffic inside a TMA) could support an ATCo taking decisions when separating, aligning and merging traffic.

- Reaching beyond the current ATM paradigm, we then describe a **conflict-free optimisation and conformance monitoring** methodology to lay out the basis for an interactive all-autonomous self-separated air traffic management. In a future situation, we could assume that tactical coordination between aircraft (i.e., who should deviate?) will be in place. This could be seen as a functionality similar to the current TCAS but with a much higher anticipation, reacting at the tactical conflict aviodance level, as opposed to the collision avoidance

level. This would render much safer, less aggressive, and overall more efficient conflict-free trajectories. Chapter IV provides the tools to resolve the conflict from the ownship perspective.

- However, an accurate prediction of surrounding traffic's future states is impeded when basic aircraft parameters such as aircraft weight, performance data or airline strategies are not available at the time of prediction. Therefore, **techniques for target tracking and conformance monitoring have been introduced**. Thanks to these, the ownship replans a new trajectory when the tracker alerts of a deviation in the intruder trajectory (from the expected trajectory). In the depicted case, thanks to the conformance monitoring, the different replans reveal an initially unexpected conflict.

- Due to the latent errors in the prediction model the intruder quickly deviates from the predicted trajectory. In chapter V the authors describe a framework to **improve the ownship's knowledge of the intruder's aircraft dynamics** by continuously integrating its past states. A case study is depicted, showing how the prediction of the potential conflict is greatly enhanced when a parameter estimation process is used. Specifically, the estimation of the other aircraft mass, which was previously unknown, is inferred, reaching **estimation errors below** 2% **soon after take-off**. Conclusively, the evasive manoeuvre is started earlier during the flight, which results in higher effectiveness and lower operational and environmental costs.

- On a last study case, a fully-collaborative concept of operations has been assumed that **resolves the conflict in cooperation among all involved aircraft**. In the presented example, this global optimisation provides conflict-free trajectories with a negligible increase in cost. However, this scenario is still considered as utopic for its difficulty in operational implementation. The main complexity resides in the need for high accuracy TBO and self-separation concepts (to account for predictability errors), as well as the current lack of information sharing between airspace users.

Final Conclusions

- In a highly automated air traffic system the framework described in this study enhances the situational awareness of the airspace user by providing information of the ownship energy state in accordance to the separation with the surrounding traffic and the possibilities for efficient separation assurance. The methodology is well aligned with SESAR concepts and works towards the enablement of TBO and self-separation.

- The concepts and methods presented in this thesis are still far from operational implementation due to the difficulty of reaching real time conflict resolutions and the nature of the numerical complexity of the non-linear programming problem resolution. However, as more computational power becomes available in consumer's market computing, numerical approaches to this problem are not only a reality, but an effective solution. Besides, basic trajectory integration (as done nowadays) could be a default solution in an eventual case where no optimal trajectory is found.

- When comparing the different strategies that have been presented for optimal conflict resolution of aircraft, the increase in operational cost (with respect to the individual optimal trajectory) is negligible. Actually, compared to the current air traffic control separation paradigm the sole introduction of trajectory optimisation presents big gains. Whereas the ATCo cannot decrease safety margins in a fully human-controlled air traffic, higher automation levels in combination with trajectory optimisation would presumably result in a huge advance in air traffic management efficiency.

VII.2 Future research

During this thesis new questions and research lines arose. Taking advantage of the optimisation framework that has been developed and for the sake of completeness, the following work items are proposed for the future:

- The equations of motion presented in chapter II and used throughout the thesis take the wind into account. Furthermore, the optimisation framework presents a way to model the wind during problem resolution with splines approximation from GRIB files (forecast and historical data). However, for the sake of simplicity and unbiased results, all simulations have been performed assuming a winds-calm situation. Further studies could include different wind situations to demonstrate the performance of the presented algorithms and methods in the presence of wind. The variability of the wind and the errors in weather forecast will probably have an impact in the resolution of the presented problems that will be interesting to assess.

- Chapter III presents a methodology that could assist an ATCo in efficiently maintaining safe separation between aircraft in a dense traffic situation. The potential applicability of such support tool in an ATC environment should be further explored, by assessing in more depth the operational benefits this could bring to ATCo. Its adoption to departure and/or arrival support systems, as well as merging point and sequencing, could be studied.

- Results in chapters IV and V are based on the assumption that an aircraft either plays the role of an *ownship* or an *intruder*. This, even if applicable to current rules of the air (e.g., right-of-way) and ATC decisions (assigned priorities), does not cover the whole complexity of potential cases and scenarios. Further effort can be put in defining how this priority is given, prior to effectively resolving the conflict. Additionally, the fully-cooperative case, can also be further explored, even if it may be still considered as very-long-term research.

- The case where an uncooperative intruder is found is not covered in this thesis. Assuming that at least the position of the intruder is known (even if only from RADAR tracks), trajectory prediction could only rely on current and historical data to produce the immediate future states (project the estimated velocity vector to the future). As this would render very poor prediction results, it would be interesting to assess the performance of the algorithms and methods presented in this thesis. Even if this is not a desired case, many causes can lead to it (malfunctioning of on-board systems, violation of aispace volumes of non-equipped aircraft, intentional miss-behaviour, etc.), thus making such study relevant.

- Generally, only one conflict is assumed in the results. This serves well the purpose of describing the algorithms and methods of this thesis and showing their performance and applicability. As the implemented separation strategy is easily extrapolated to multiple conflicts, a separate study should address the resolution of multiple conflicts in line, providing results on the impact that resolving one conflict has to the other conflicts and measuring the potential network effect.

- The divergence between predicted and real trajectories in chapter IV are based on an induced wrong assumption of the *intruder's* aircraft mass. The replans happen thus repetitively on a quite regular pattern. Incorrect assumption of other *intruder's* aircraft performance parameters, as well as *in-air* fligh plan changes, weather forecast errors or even un/deliberate non-conformance to fligh plan (amongst other eventualities) could be addressed in an exhaustive set of tests to demonstrate the performance of the proposed methodology in a sensibility study.

- In chapter V we show how an equivalent mass can be accurately estimated with few seconds of track data. Further studies should show how this same method can be used to estimate other aircraft performance parameters (i.e. drag and thrust *corrections*) and airline strategies (i.e. cost index).
- In chapter VI we show results for a fully collaborative centralised optimisation. This case should be further explored by adding the conformance monitoring and parameter estimation presented in previous chapters and providing real-time results.
- Generally, the same scenario has been provided to show all the thesis results. Even if this depicts well the outcomes of the work, more scenarios with different routes and conflict geometries will have to be addressed in the future.

References

AIRBUS. 1998. *Getting to Grips With the Cost Index*. Tech. rept. II. Airbus. 33

AIRBUS. 2002. *Getting to Grips With Aircraft Performance Monitoring*. Tech. rept. Airbus. 33

ALLIGIER, RICHARD, GIANAZZA, DAVID, & DURAND, NICOLAS. 2012. Energy Rate Prediction Using an Equivalent Thrust Setting Profile. *In: International Conference for Research in Air Transportation (ICRAT)*. Berkeley (California): Federal Aviation Administration & Eurocontrol. 57

ALLIGIER, RICHARD, GIANAZZA, DAVID, GHASEMI HAMED, MOHAMMAD, & DURAND, NICOLAS. 2014. Comparison of Two Ground-based Mass Estimation Methods on Real Data. *In: International Conference for Research in Air Transportation (ICRAT)*. Istanbul (Turkey): Federal Aviation Administration & Eurocontrol. 57

BAKOLAS, EFSTATHIOS, ZHAO, YIYUAN, & TSIOTRAS, PANAGIOTIS. 2011. Initial Guess Generation for Aircraft Landing Trajectory Optimization. *In: Guidance, Navigation, and Control Conference and Exhibit*. Guidance, Navigation, and Control and Co-located Conferences. American Institute of Aeronautics and Astronautics. 14

BETTS, JOHN T. 2010. *Practical methods for optimal control and estimation using nonlinear programming*. 2nd edn. Advances in design and control, no. 19. Society for Industrial and Applied Mathematics. 19

BETTS, JOHN T, & CRAMER, EVIN J. 1995. Application of Direct Transcription to Commercial Aircraft Trajectory Optimization. *Journal of Guidance, Control, and Dynamics*, **18**(1), 151–159. 33

BEZAWADA, RAJESH, DUAN, PENGFEI, & UIJT DE HAAG, MAARTEN. 2011. Hazard tracking with integrity for surveillance applications. *In: Digital Avionics Systems Conference (DASC)*. Sydney (Australia): American Institute of Aeronautics and Astronautics & Institute of Electrical and Electronics Engineers. 6

BITTNER, MATTHIAS, FISCH, FLORIAN, & HOLZAPFEL, FLORIAN. 2012. A Multi-Model Gauss Pseudospectral Optimization Method for Aircraft Trajectories. *In: Atmospheric Flight Mechanics Conference*. Guidance, Navigation, and Control and Co-located Conferences. Reston, Virigina: American Institute of Aeronautics and Astronautics. 13

BITTNER, MATTHIAS, FLEISCHMANN, BENJAMIN, RICHTER, MAXIMILIAN, & HOLZAPFEL, FLORIAN. 2014. Optimization of ATM Scenarios Considering Overall and Single Costs. *In: International Conference for Research in Air Transportation (ICRAT)*. Istanbul (Turkey): Federal Aviation Administration & Eurocontrol. 73

BLOM, HENK, & BAKKER, G J BERT. 2011. Safety of advanced airborne self separation under very high en-route traffic demand. *In: SESAR Innovation Days (SID)*. Toulouse (France): SESAR. 5

BONAMI, PIERRE, OLIVARES, ALBERTO, SOLER, MANUEL, & STAFFETTI, ERNESTO. 2013. Multiphase Mixed-Integer Optimal Control Approach to Aircraft Trajectory Optimization. *Journal of Guidance, Control, and Dynamics*, **36**(5), 1267–1277. 22

BRONSVOORT, JESPER. 2014. *Contributions to Trajectory Prediction Theory and its application to arrival management for Air Traffic Control*. Ph.D. thesis, Universidad Politécnica de Madrid. 5, 39

BROWN, ROBRT GROVER, & HWANG, PATRICK Y. C. 2012. *Introduction to Random Signals and Applied Kalman Filtering*. New York: John Wiley & Sons. 50

BRYSON, ARTHUR E., & HO, YU-CHI. 1975. *Applied Optimal Control: Optimization, Estimation and Control*. New York: John Wiley & Sons. 19

CHALOULOS, GEORGIOS, ROUSSOS, GIANNIS, LYGEROS, JOHN, & KYRIAKOPOULOS, KOSTAS. 2008. Ground Assisted Conflict Resolution in Self-Separation Airspace. *In: Guidance, Navigation and Control Conference and Exhibit*. Guidance, Navigation, and Control and Co-located Conferences. American Institute of Aeronautics and Astronautics. 5

CHALOULOS, GEORGIOS, CRÜCK, EVA, & LYGEROS, JOHN. 2010. A simulation based study of subliminal control for air traffic management. *Transportation Research Part C: Emerging Technologies*, **18**(6), 963–974. 5

CLARKE, JOHN-PAUL, & PARK, SANG GYUN. 2012. Vertical Trajectory Optimization for Continuous Descent Arrival Procedure. *In: Guidance, Navigation, and Control Conference and Exhibit*. Guidance, Navigation, and Control and Co-located Conferences. American Institute of Aeronautics and Astronautics. 14

COPPENBARGER, RICHARD, MEAD, ROB, & SWEET, DOUGLAS. 2007. Field evaluation of the tailored arrivals concept for datalink-enabled continuous descent approach. *In: Aviation Technology, Integration and Operations Conference (ATIO)*. American Institute of Aeronautics and Astronautics. 5

DAHLBERG, JOEN, ANDERSSON GRANBERG, TOBIAS, POLISHCHUK, TATIANA, SCHMIDT, CHRISTIANE, & SEDOV, LEONID A. 2018. Capacity-Driven Automatic Design of Dynamic Aircraft Arrival Routes. *In: Digital Avionics Systems Conference (DASC)*. London (United Kingdom): American Institute of Aeronautics and Astronautics & Institute of Electrical and Electronics Engineers. 34

DALMAU, RAMON, & PRATS, XAVIER. 2015. Fuel and time savings by flying continuous cruise climbs: Estimating the benefit pools for maximum range operations. *Transportation Research Part D: Transport and Environment*, **35**, 62–71. 4

DALMAU, RAMON, & PRATS, XAVIER. 2017. Assessing the impact of relaxing cruise operations with a reduction of the minimum rate of climb and/or step climb heights. *Aerospace Science and Technology*, **70**, 461–470. 5

DE JONG, P M A. 2014. *Continuous Descent Operations using Energy Principles*. Ph.D. thesis, TU Delft. 5

ENAIRE. 2010. *Normalised Departure Chart. Standard Instrumental Procedure for Reus. RWY07. Aeronautical Information Publication (AIP). Part AD. LERS*. 34

ENAIRE. 2012. *Normalised Departure Chart. Standard Instrumental Procedure for Barcelona / El Prat. RWY25L / RWY20. Aeronautical Information Publication (AIP). Part AD. LEBL*. 34

ERAT CONSORTIUM. 2012. *Final Report*. Tech. rept. Environmentally Responsible for Air Transport (ERAT) Project, Sixth Framework Programme, E.C. 5

EUROCONTROL. 2002. *Review of ASAS Applications studied in Europe*. Tech. rept. CARE/ASAS Action. CARE/ASAS Activity 4. 4

EUROCONTROL. 2011. *User Manual for BADA Revision 3.9*. Tech. rept. Eurocontrol. 17

FRANCO, ANTONIO, & RIVAS, DAMIÁN. 2014. Analysis of optimal aircraft cruise with fixed arrival time including wind effects. *Aerospace Science and Technology*, **32**(1), 212–222. 19

FRANCO, ANTONIO, RIVAS, DAMIÁN, & VALENZUELA, ALFONSO. 2010. Minimum-Fuel Cruise at Constant Altitude with Fixed Arrival Time. *Journal of Guidance, Control, and Dynamics*, **33**(1), 280–285. 19

FRICKE, HARTMUT, SEISS, CHRISTIAN, & HERRMANN, ROBERT. 2017. Fuel and Energy Benchmark Analysis of Continuous Descent Operations. *Air Traffic Control Quarterly*, **23**(1), 83–108. 4

GALLO, EDUARDO, LÓPEZ-LEONÉS, JAVIER, VILAPLANA, MIGUEL ÁNGEL, NAVARRO, F.A., & NUIC, A. 2007. Trajectory computation Infrastructure based on BADA Aircraft Performance Model. *In: Digital Avionics Systems Conference (DASC)*. Columbia (Maryland): American Institute of Aeronautics and Astronautics & Institute of Electrical and Electronics Engineers. 6, 61

GAMS. 2019. *GAMS User Manual*. Tech. rept. GAMS Development Corporation. 27

GONG, CHESTER, & SADOVSKY, ALEXANDER. 2010. A Final Approach Trajectory Model for Current Operations. *In: Aviation Technology, Integration, and Operations (ATIO)*. Reston (Virigina): American Institute of Aeronautics and Astronautics. 33

HARTJES, SANDER, VISSER, HENDRIKUS G, & HEBLY, S. J. 2010. Optimisation of RNAV noise and emission abatement standard instrument departures. *The Aeronautical Journal*, **114**(1162), 757–767. 23

HARTJES, SANDER, VISSER, HENDRIKUS G, BRAAKENBURG, MENNO, & HEBLY, SANDER J. 2011. Development of a Multi-Event Trajectory Optimization Tool for Noise-Optimized Approach Route Design. *In: Aviation Technology, Integration, and Operations Conference (ATIO)*. Virginia Beach (Virginia): American Institute of Aeronautics and Astronautics. 13, 14

HOUACINE, M, & KHARDI, S. 2010. Gauss Pseudospectral Method for Less Noise and Fuel Consumption of Aircraft Operations. *Journal of Aircraft*, **47**(6), 2152–2158. 14

HU, JIANGHAI, PRANDINI, MARIA, & SASTRY, SHANKAR. 2002. Optimal Coordinated Maneuvers for Three-Dimensional Aircraft Conflict Resolution. *Journal of Guidance, Control, and Dynamics*, **25**(5), 888–900. 73

ICAO. 2001. *Procedures for Air Navigation Services. Air Traffic Management*. Tech. rept. International Civil Aviation Organization. 34

ICAO. 2006. *Aircraft Operations. Volume I - Flight Procedures*. Tech. rept. International Civil Aviation Organization. 7, 22, 24

ICAO. 2010. *DOC 9931 - Continuous Descent Operations (CDO) Manual*. Tech. rept. International Civil Aviation Organization. 4

ICAO. 2012. *Continuous Climb Operations (CCO) Manual Doc. 9993 AN/495*. Tech. rept. International Civil Aviation Organization. 4

ICAO. 2016. *North Atlantic Operations and Airspace Manual*. Tech. rept. International Civil Aviation Organization. 4

JACOBSON, IRA, & RUDRAPATNA, ASHOK. 1974. *Flight simulator experiments to determine human reaction to aircraft motion environments*. Tech. rept. National Aeronautics and Space Administration. 21

JOHNSON, CRAIG M. 2011. Analysis of Top of Descent (TOD) uncertainty. *In: Digital Avionics Systems Conference (DASC)*. Sydney (Australia): American Institute of Aeronautics and Astronautics & Institute of Electrical and Electronics Engineers. 4

KAISER, MICHAEL, SCHULTZ, MICHAEL, & FRICKE, HARTMUT. 2011. Enhanced jet performance model for high precision 4D flight path prediction. *In: International Conference on Application and Theory of Automation in Command and Control Systems (ATACCS)*. Barcelona (Spain): SESAR. 18

LÓPEZ-LEONÉS, JAVIER, VILAPLANA, MIGUEL ÁNGEL, GALLO, EDUARDO, NAVARRO, FRANCISCO A., & QUEREJETA, CARLOS. 2007. The aircraft intent description language: A key enabler for air-ground Synchronization in trajectory-based operations. *In: Digital Avionics Systems Conference (DASC)*. Columbia (Maryland): American Institute of Aeronautics and Astronautics & Institute of Electrical and Electronics Engineers. 57

MENON, PADMANABHAN, SWERIDUK, G D, & SRIDHAR, B. 1999. Optimal Strategies for Free-Flight Air Traffic Conflict Resolution. *Journal of Guidance, Control, and Dynamics*, **22**(2), 202–211. 48

MOHAN, KRITHIKA, PATTERSON, MA, & RAO, ANIL V. 2012. Optimal Trajectory and Control Generation for Landing of Multiple Aircraft in the Presence of Obstacles. *In: Guidance, Navigation, and Control Conference and Exhibit*. Guidance, Navigation, and Control and Co-located Conferences, no. August. Minneapolis (Minnesota): American Institute of Aeronautics and Astronautics. 14, 48

MUSIALEK, BEN, MUNAFO, CF, RYAN, H, & PAGLIONE, MIKE. 2010. *Literature Survey of Trajectory Predictor Technology*. Tech. rept. Federal Aviation Administration, William J. Hughes Technical Center. 11, 47, 57

MUTUEL, LAURENCE H, & NERI, PIERRE. 2013. Initial 4D Trajectory Management Concept Evaluation. *In: USA/Europe Air Traffic Management Research and Development Seminar*. Chicago (Illinois): Federal Aviation Administration & Eurocontrol. 5

OMER, JÉRÉMY, & FARGES, JEAN-LOUP. 2012. Automating air traffic control through nonlinear programming. *In: International Conference on Research in Air Transportation (ICRAT)*. Berkeley (California): Federal Aviation Administration & Eurocontrol. 73

PATEL, RUSHEN B, & GOULART, PAUL J. 2011. Trajectory Generation for Aircraft Avoidance Maneuvers Using Online Optimization. *Journal of Guidance, Control, and Dynamics*, **34**(1), 218–230. 14

PÉREZ CASTÁN, JAVIER, VALDÉS, ROSA, GOMEZ COMENDADOR, VICTOR, & GUEVARA MARTÍNEZ, SERGIO. 2015. Continuous climb operations: The following step. *In: International Conference on Application and Theory of Automation in Command and Control Systems (ATACCS)*. Toulouse (France): SESAR. 4

PRATS, XAVIER. 2010. *Contributions to the optimisation of aircraft noise abatement procedures*. Ph.D. thesis, Universitat Politècnica de Catalunya. 14, 17

PRATS, XAVIER, PUIG, VICENÇ, & QUEVEDO, JOSEBA. 2011. A multi-objective optimization strategy for designing aircraft noise abatement procedures. Case study at Girona airport. *Transportation Research Part D: Transport and Environment*, **16**(1), 31–41. 12

PRATS, XAVIER, BUSSINK, FRANK, VERHOEVEN, RONALD, & MARSMAN, ADRI. 2015. Evaluation of in-flight trajectory optimisation with time constraints in a moving base flight simulator. *In: Digital Avionics Systems Conference (DASC)*. Prague (Czech Republic): American Institute of Aeronautics and Astronautics & Institute of Electrical and Electronics Engineers. 12

PRATS, XAVIER, DALMAU, RAMON, VERHOEVEN, RONALD, & BUSSINK, FRANK. 2017. Human-in-the-loop performance assessment of optimized descents with time constraints. *In: USA/Europe Air Traffic Management Research and Development Seminar*. Seattle (Washington): Federal Aviation Administration & Eurocontrol. 5

RAGHUNATHAN, ARVIND U., GOPAL, VIPIN, SUBRAMANIAN, DHARMASHANKAR, BIEGLER, LORENZ T., & SAMAD, TARIQ. 2004. Dynamic optimization strategies for three-dimensional conflict resolution of multiple aircraft. *Journal of guidance, control, and dynamics*, **27**(4), 586–594. 14, 48

ROBERSON, BILL. 2007. *Fuel Conservation Strategies: Cost Index Explained*. Tech. rept. AeroMagazine. Boeing. 33

ROY, KAUSHIK, LEVY, BENJAMIN, & TOMLIN, CJ. 2006. Target tracking and estimated time of arrival (ETA) prediction for arrival aircraft. Guidance, Navigation, and Control and Co-located Conferences. Keystone (Colorado): American Institute of Aeronautics and Astronautics. 5

RTCA SC-181. 2003a. *Minimum Aviation System Performance Standards: Required Navigation Performance for Area Navigation*. Tech. rept. 52

RTCA SC-181. 2003b. *Minimum Operational Performance Standards for Required Navigation Performance for Area Navigation*. Tech. rept. 52

RTCA SC-186. 2002. *Minimum Aviation System Performance Standards for Automatic Dependent Surveillance-Broadcast (ADS-B)*. Tech. rept. 52

RTCA SC-186. 2009. *Minimum Operational Performance Standards (MOPS) for 1090 MHz Extended Squitter Automatic Dependent Surveillance-Broadcast (ADS-B) and Traffic Information Services-Broadcast (TIS-B)*. Tech. rept. 9, 47

SCHULTZ, CHARLES A., THIPPHAVONG, DAVID, & ERZBERGER, HEINZ. 2012. Adaptive Trajectory Prediction Algorithm for Climbing Flights. *In: Guidance, Navigation, and Control Conference and Exhibit*. Guidance, Navigation, and Control and Co-located Conferences. Minneapolis (Minnesota): American Institute of Aeronautics and Astronautics. 57

SESAR. 2017. *ATM Information Reference Model Primer*. Tech. rept. SESAR. 6, 57, 61

SOLER, MANUEL, OLIVARES, ALBERTO, STAFFETTI, ERNESTO, & BONAMI, PIERRE. 2011. En-Route Optimal Flight Planning Constrained to Pass Through Waypoints using MINLP. *In: USA/Europe Air Traffic Management Research and Development Seminar*. Berlin (Germany): Federal Aviation Administration & Eurocontrol. 13

SOLER, MANUEL, KAMGARPOUR, MARYAM, TOMLIN, CLAIRE, & STAFFETTI, ERNESTO. 2012. Multiphase mixed-integer optimal control framework for aircraft conflict avoidance. *In: Conference on Decision and Control (CDC)*. Maui (Hawaii): Ieee. 73

SOLER, MANUEL, KAMGARPOUR, MARYAM, & LYGEROS, JOHN. 2014a. A Numerical Framework and Benchmark Case study for Muti-modal Fuel Efficient Aircraft Conflict Avoidance. *In: International Conference on Research in Air Transportation (ICRAT)*. Istanbul (Turkey): Federal Aviation Administration & Eurocontrol. 5, 6

SOLER, MANUEL, ZOU, BO, & HANSEN, MARK. 2014b. Flight trajectory design in the presence of contrails: Application of a multiphase mixed-integer optimal control approach. *Transportation Research Part C: Emerging Technologies*, **48**, 172–194. 12

TADEMA, JOCHUM, THEUNISSEN, ERIK, RADEMAKER, RICHARD, & UIJT DE HAAG, MAARTEN. 2010. Evaluating the impact of sensor data uncertainty and maneuver uncertainty in a conflict probe. *In: Digital Avionics Systems Conference (DASC)*, vol. 6. Salt Lake City (Utah): American Institute of Aeronautics and Astronautics & Institute of Electrical and Electronics Engineers. 5

THOMPSON, TERRY, MILLER, BRUNO, MURPHY, CHARLES, AUGUSTINE, STEPHEN, WHITE, TYLER, & SOUIHI, SOFIA. 2013. Environmental Impacts of Continuous-descent Operations in Paris and New York Regions. *In: USA/Europe Air Traffic Management Research and Development Seminar*. Chicago (Illinois): Federal Aviation Administration & Eurocontrol. 35

VISSER, HENDRIKUS G, & HARTJES, SANDER. 2014. Economic and environmental optimization of flight trajectories connecting a city-pair. *Proceedings of the Institution of Mechanical Engineers, Part G: Journal of Aerospace Engineering*, **228**(6), 980–993. 12

WARREN, A W, & EBRAHIMI, YAGHOOB S. 1998. Vertical path trajectory prediction for next generation ATM. *In: Digital Avionics Systems Conference (DASC)*. Seattle (Washington): American Institute of Aeronautics and Astronautics & Institute of Electrical and Electronics Engineers. 57

WU, DI, & ZHAO, YIYUAN. 2009. Performances and Sensitivities of Optimal Trajectory Generation for Air Traffic Control Automation. *In: Guidance, Navigation, and Control Conference and Exhibit*. Guidance, Navigation, and Control and Co-located Conferences. American Institute of Aeronautics and Astronautics. 13

YAN, SU, & CAI, KAIQUAN. 2017. A multi-objective multi-memetic algorithm for network-wide conflict-free 4D flight trajectories planning. *Chinese Journal of Aeronautics*, **30**(3), 1161–1173. 11

YANG, LIANG, QI, JUNTONG, XIAO, JIZHONG, & YONG, XIA. 2014. A literature review of UAV 3D path planning. *In: World Congress on Intelligent Control and Automation (WCICA)*. Shenyang (China): Institute of Electrical and Electronics Engineers. 11